AD-A204 615

AD _____

DEVELOPMENT OF IN VITRO ISOLATED PERFUSED PORCINE SKIN FLAPS FOR STUDY OF PERCUTANEOUS ABSORPTION OF XENOBIOTICS

ANNUAL/FINAL REPORT

J.E. RIVIERE
N. A. MONTEIRO-RIVIERE
K. F. BOWMAN

JUNE 30, 1987

Supported by

U.S. ARMY MEDICAL RESEARCH AND DEVELOPMENT COMMAND
Fort Detrick, Frederick, Maryland 21701-5012

Contract No. DAMD17-84-C-4103

College of Veterinary Medicine
North Carolina State University
Raleigh, North Carolina 27606

Approved for public release; distribution unlimited

The findings in this report are not to be construed as an official Department of the Army position unless so designated by other authorized documents.

89   1   18   093

REPORT DOCUMENTATION PAGE

Form Approved
OMB No. 0704-0188

1a. REPORT SECURITY CLASSIFICATION	1b RESTRICTIVE MARKINGS
Unclassified	

2a. SECURITY CLASSIFICATION AUTHORITY	3. DISTRIBUTION/AVAILABILITY OF REPORT
	Approved for public release;
2b. DECLASSIFICATION/DOWNGRADING SCHEDULE	distribution unlimited

4 PERFORMING ORGANIZATION REPORT NUMBER(S)	5. MONITORING ORGANIZATION REPORT NUMBER(S)

6a. NAME OF PERFORMING ORGANIZATION	6b. OFFICE SYMBOL (If applicable)	7a. NAME OF MONITORING ORGANIZATION
College of Veterinary Medicine North Carolina State University		

6c. ADDRESS (City, State, and ZIP Code)	7b. ADDRESS (City, State, and ZIP Code)
Raleigh, North Carolina 27606	

8a. NAME OF FUNDING/SPONSORING ORGANIZATION U.S. Army Medical Research & Development Command	8b. OFFICE SYMBOL (If applicable)	9. PROCUREMENT INSTRUMENT IDENTIFICATION NUMBER
		DAMD17-84-C-4103

8c. ADDRESS (City, State, and ZIP Code)	10. SOURCE OF FUNDING NUMBERS			
Fort Detrick Frederick, Maryland 21701-5012	PROGRAM ELEMENT NO. 61102A	PROJECT NO. 3M1-61102BS11	TASK NO. AA	WORK UNIT ACCESSION NO. 002

11. TITLE (Include Security Classification) (U) Development of In-Vitro Isolated Perfused Porcine Skin Flaps for Study of Percutaneous Absorption of Xenobiotics

12. PERSONAL AUTHOR(S)
J.E. Riviere, N.A. Monteiro-Riviere, and K.F. Bowman

13a. TYPE OF REPORT	13b. TIME COVERED	14. DATE OF REPORT (Year, Month, Day)	15. PAGE COUNT
Annual/Final	FROM 9/30/84 TO 6/30/87	1987 June 30	126

16. SUPPLEMENTARY NOTATION

Annual report covers period of time September 30, 1986 - June 30, 1987

17. COSATI CODES			18. SUBJECT TERMS (Continue on reverse if necessary and identify by block number)
FIELD	GROUP	SUB-GROUP	Pig, Skin, Flap, Porcine, Integument, Surgery, Absorption, Pharmacology, Microscopy, Histology, Toxicology, RA 5
06	15		
06	04		

19. ABSTRACT (Continue on reverse if necessary and identify by block number)

20. DISTRIBUTION/AVAILABILITY OF ABSTRACT	21. ABSTRACT SECURITY CLASSIFICATION
☐ UNCLASSIFIED/UNLIMITED ☒ SAME AS RPT ☐ DTIC USERS	Unclassified

22a. NAME OF RESPONSIBLE INDIVIDUAL	22b TELEPHONE (Include Area Code)	22c. OFFICE SYMBOL
Mary Frances Bostian	301-663-7325	SGRD-RMI-S

DD Form 1473, JUN 86   Previous editions are obsolete.   SECURITY CLASSIFICATION OF THIS PAGE

19. ABSTRACT

This report describes the development of a novel in vitro alternative animal model for use in dermatology and cutaneous toxicology. A single pedicle, axial pattern, island-tubed skin flap was created in crossbred Yorkshire weanling pigs in one surgical procedure and then transferred 2 or 6 days later to a computer-controlled temperature-regulated perfusion chamber for 10 to 12 hr studies. The development of this two-stage surgical procedure is fully described. Perfusate consisted of Krebs-Ringer bicarbonate buffer (pH=7.4) containing albumin and glucose. Viability was assessed by glucose utilization, lactate production, and an absence of significant concentrations of the intracellular enzyme lactate dehydrogenase in the perfusate. Light and electron microscopy was used to develop a morphological viability index and to differentiate degenerative lesions from normal surgery or perfusion changes or lesions from exogenously applied toxins (NaF). A mean lactate to glucose ratio of 1.7 suggested primarily anaerobic glycolysis. This model was validated for xenobiotic percutaneous absorption studies by assessing under identical experimental conditions (40 $\mu g/cm^2$; ethanol vehicle), in vivo and in the isolated perfused porcine skin flap (IPPSF) the percutaneous absorption of radiolabeled benzoic acid (B), caffeine (C), diisopropylfluorophosphidate (D), parathion (P), malathion (M), progesterone (R), testosterone (T), and triamcinolone (A). The in vivo bioavailability was estimated by collecting excreta for 6 days and administering an intravenous dose of compound to correct for systemic disposition. These studies demonstrated a route-dependent change in urine/fecal excretion ratio for four compounds. The IPPSF bioavailability was assessed by fitting a pharmacokinetic model to the venous efflux profiles and extrapolating to infinity. Modifications were needed in the basic three-compartment model to account for an unknown, saturable diffusion process for benzoic acid and for flux-dependent perfusate flow increases seen with caffeine. The resulting linear correlation coefficient (R) for in vivo to IPPSF bioavailability for all compounds was 0.94 ($p < 0.002$). Thin layer chromatographic (TLC) separation of perfusate contents from IPPSF's given parathion revealed a significant first-pass bioactivation (70%) to paraoxon during percutaneous absorption, a process which was decreased when pretreatment with a mixed function oxidase inhibitor occurred. Occlusion of the parathion application site increased parent compound flux and altered the metabolic profile. Because the skin of weanling Yorkshire swine has similar anatomy, biochemistry, and permeability to topical agents, the impact of these findings on human dermal risk assessment studies in cutaneous toxicology and on the development of transdermal drug delivery systems may be substantial. This preparation would be a humane alternative animal model for studies in cutaneous toxicology, physiology, oncology, and percutaneous drug absorption and metabolism.
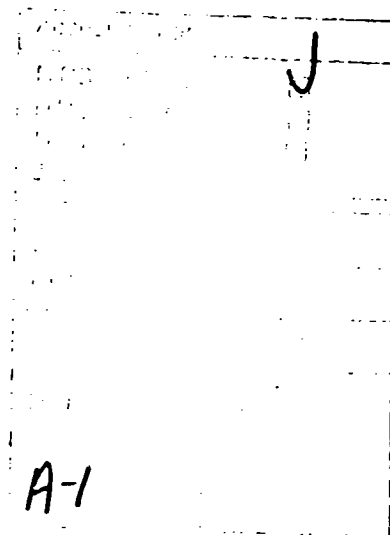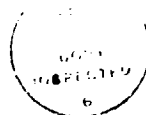
FOREWORD

In conducting the research described in this report, the investigators adhered to the "Guide for the Care and Use of Laboratory Animals," prepared by the Committee on Care and Use of Laboratory Animals of the Institute of Laboratory Animal Resources, National Resource Council (DHEW Publication No. (NIH) 86-23, Revised 1985).

Citations of commercial organizations and trade names in this report do not constitute an official Department of the Army endorsement or approval of the products or services of these organizations.

A-1

TABLE OF CONTENTS

Tables

TABLE OF CONTENTS continued

TABLE OF CONTENTS continued

<u>Figures</u>

TABLE OF CONTENTS continued

<u>Figures</u>

INTRODUCTION

One of the most promising areas for pharmacological and toxicological investigation involves the transport of chemical substances through skin, or percutaneous absorption. It is universally accepted that skin is a major portal of entry into the body for drugs and environmental agents, thus skin must be considered a target organ for both drugs and toxins. Therapeutic strategies are available in which drugs applied topically may penetrate in sufficient amounts to treat problems localized to the skin and, more recently, transdermal drug delivery systems have been developed to provide a convenient, noninvasive method for infusing drugs systemically.

In order to fully characterize the interaction of skin with topical agents, a better understanding of the mechanisms of percutaneous absorption is necessary, particularly with regard to the animals used as surrogates for human percutaneous absorption studies. Comparative anatomy of animal and human skin suggests that certain pink-skinned porcine species are more dermatologically similar to humans than most other animals studied. Similarities between human and pig skin in pelage density and thickness of the various dermal layers (1-3), cutaneous vasculature and microcirculation (4-6), biochemistry and cellular metabolism (7-9), histochemistry and enzyme distribution (10,11), epidermal and surface lipid content (1,10,12-15), and ultrastructure (16,17) lend support to this hypothesis.

Interspecies comparisons of percutaneous absorption rates and penetration characteristics for a wide range of compounds in vivo (18-26) all suggest that weanling or miniature pig and human skin are equivalent when studied under identical conditions. Although the rhesus monkey may represent an even better model for human skin than weanling pigs (27-31), these animals are much more expensive and difficult to handle and animal rights legislation may eventually outlaw their use in research projects altogether.

Studies on the function of skin have been limited by a lack of in vitro models for investigating cutaneous physiology in an anatomically and physiologically intact preparation. This limitation is especially evident when those studies require measuring arterial-venous concentration differences of endogenous compounds metabolized or produced by the skin. Current techniques assessing the percutaneous absorption of drugs and chemicals are severely limited if the absorbed compounds are extensively metabolized by the skin or form cutaneous depots (32). An anatomically intact, viable, isolated, perfused tubed skin preparation would overcome many of these limitations because perfusate composition could be controlled rigidly, allowing comparison of the arterial and venous compositions of perfusate during assessment of cutaneous metabolism and function. Pigs were selected because their skin is functionally and structurally

similar to that of humans (17,19,26,33-36). Earlier studies utilized flat skin flaps in dogs (37,38), which, as described, were not amenable to long-term computer-controlled experiments with skin exposed in an ambient environment. Skin in the caudolateral epigastric region of the pig has direct cutaneous vasculature, the caudal superficial epigastric artery (CSEa), and its paired venae comitantes, which is compatible with closed isolated organ perfusion techniques.

This project has five primary phases: 1) develop a surgical technique for creating and harvesting tubed skin flaps amenable for isolated perfusion; 2) develop a technique for isolated perfusion of these flaps; 3) identify morphological and biochemical criteria for viability; 4) create a data base of xenobiotic percutaneous absorption data in vivo to be used to validate isolated perfused porcine skin flap (IPPSF) absorption results; and 5) assess xenobiotic percutaneous absorption in the IPPSF, correlate these results to the in vivo data, and derive a pharmacokinetic model applicable to describe absorption data in this model.

Overview of Surgical Procedure:

The arterial blood supply to the dermal-subdermal plexi of skin will traverse three types of vasculature: 1) the segmental, 2) the perforators, and 3) the cutaneous. In general, the venous return parallels the arterial supply. Segmental vessels arise from the aorta, lay deep to the muscle mass, and usually follow the course of a peripheral nerve. Perforating vasculature functions by supplying blood to the muscles through which it passes and serves as a conduit from the segmented vasculature to the cutaneous circulation. The cutaneous arterial supply is subdivided into two types: 1) the musculocutaneous arteries and 2) the direct cutaneous arteries. In humans and pig, the main blood supply to the skin is via many musculocutaneous arteries which penetrate directly from muscle through the subcutaneous tissues and into the overlying skin. Musculocutaneous arteries supply relatively small areas of skin. The musculocutaneous arterial system is supplemented by limited numbers of anatomically variable, direct, cutaneous arteries which course parallel, instead of perpendicular, to the skin at a level above the muscle and fascia. Direct cutaneous arteries supply much greater areas of skin. Unlike humans and pig, the dog and other loose-skinned animals do not have a musculocutaneous arterial system; their primary vascular supply to the skin is from direct cutaneous arteries.

A skin flap consists of skin and subcutaneous tissue that is moved from one part of the body to another with a vascular ccpedicle or attachment to the body being maintained for nourishment. Skin flaps are classified based upon their blood supply, or by the location to which they are moved (i.e., local or distant). Pedicles of random pattern flaps are usually supplied by musculocutaneous arteries, which in turn perfuse the dermal-subdermal plexi of the skin flap. The surviving length of

random pattern flaps is related to the arterial perfusion pressure and venous drainage; however, these skin flaps can be made larger (50-100 %) if they are "delayed." When a skin flap is designed to include a direct cutaneous artery within its longitudinal axis, it is called an axial pattern flap. Axial pattern flaps are further subclassified as 1) peninsular flaps, having direct cutaneous vasculature with an intact skin/subcutaneous tissue bridge; 2) island flaps, lacking a skin/subcutaneous tissue bridge, but attached to a vascular supply; and 3) free flaps, which are transplanted to distant sites and connected to recipient vasculature by microvascular anastomosis.

The surviving length of an axial pattern flap is determined by the extent of the direct cutaneous artery in the flap plus that distal skin which is perfused through its dermal-subdermal plexus. Island flaps survive to at least the same length as peninsular flaps when both are made under similar conditions. Axial pattern flaps often survive to 50% greater length than "delayed" random flaps, and axial pattern flaps can be made longer by delay procedures.

Among the several types of distant skin flaps is the tubed flap. A tube flap is bipedicled (i.e., attached at both ends), which has been raised in an area of abundant skin and its parallel edges sewn together to form a tube resembling a suitcase handle. The skin beneath the tubed flap (i.e., the donor site) is either undermined and closed by primary suture or grafted. Thereafter, the tubed flap can be detached one end at a time and "tumbled," "waltzed," or "caterpillared" to the distant, recipient site. After a tubed flap is raised, vascular transformation occurs; however, the change in random pattern tubed flaps and axial pattern tubed flaps is different.

The objectives of the surgical phase of this study were 1) to identify and establish the normal vasculature to proposed skin flap donor sites, and 2) to develop a single pedicle, axial pattern tubed flap which can 1) be raised in one operation, 2) survive to its entire length, 3) be characterized regarding its physiological characteristics during healing, and 4) be harvested for transfer to the in vitro percutaneous absorption studies.

Development of Isolated Perfusion Protocols

The objective of this phase of the project was to develop a reproducible technique for isolated perfusion of the tubed skin flaps harvested from the live pig. Additionally, biochemical indices of viability useful for real-time monitoring of IPPSF experiments during absorption studies must be identified.

Morphological Viability Studies:

The objective of this phase of the study was to assess and quantitate over time the changes that occur in skin 1) as a result of normal cell death, 2) as a function of the surgical procedure used in creating the flap, 3) as a result of isolated

perfusion, and 4) to determine changes which occur secondarily to chemically induced toxicity. A classification of these structural changes is essential for the proper application of morphological criteria as a discriminator between cell death, surgery, perfusion, and chemically induced toxicity in the IPPSF.

In Vivo Percutaneous Absorption

Recently, there has been some concern that the underlying assumptions inherent in the protocol used to assess percutaneous absorption in vivo, which was standardized over 20 years ago (39), may not always be valid. In particular, the exclusive use of urinary excretion of radiolabel following intravenous (IV) and topical administration may not provide accurate estimates of percutaneous absorption for some compounds. In addition to the obvious need to identify the penetrating species, given the known capacity of skin for biotransformation reactions (40-42), there is a growing body of evidence that topical and IV excretion profiles or, more specifically, the urine/fecal excretion ratios may differ (43-47). These two phenomena may be related, since an analogous and well known "first-pass effect" occurs after oral administration and the route of xenobiotic excretion often differs from that which is observed following a parenteral dose.

The present investigation of percutaneous absorption in weanling Yorkshire pigs was undertaken for several reasons. First, a data base for topical absorption of several chemical classes is needed to validate use of the IPPSF for examining cutaneous pharmacology and toxicology in vitro (7,48,49). Compounds chosen for this study represent a wide range of lipid-water partition coefficients (50) and have been examined previously in pigs at other sites and applied surface concentrations (19,20,22,23,25,50). Urine and fecal clearances after both intravenous and topical routes of administration will be compared to determine whether it is necessary to collect total excrement for accurate measurements of percutaneous absorption in vivo.

Percutaneous Absorption in the Isolated Perfused Porcine Skin Flap (IPPSF)

The purpose of this final phase, and arguably the most important, is to compare the extent of topical bioavailability in the IPPSF with the results obtained from the in vivo studies described above. In order to make a valid comparison, it is important that both experimental protocols be as close as possible (applied dose, vehicle, area, body site). These variables were fixed in both the in vivo and IPPSF studies. Finally, a pharmacokinetic model is required to quantitatively describe percutaneous flux of compounds in the IPPSF so that extrapolations can be made to the in vivo situation and so that mechanisms of absorption can be explored. Finally, preliminary studies were conducted on the cutaneous biotransformation of topically applied parathion in the IPPSF.

MATERIALS AND METHODS

Development of Surgical Procedure:

Experiment 1: Two weanling female pigs weighing approximately 40 kg were anesthetized, exsanguinated, and embalmed with injectable latex. Prosection of the pelt was done to elucidate the pattern of cutaneous vasculature in three prospective skin flap donor sites (i.e., buttock, lateral thoracic, and caudal abdominal regions) (51-55) and to provide reference anatomical preparations.

Experiment 2: Two female pigs were anesthetized. Stainless steel staples were applied to the skin bilaterally, defining the limits (4 x 12 cm) of the proposed skin flap donor site. Incision and blunt dissection exposed the femoral and CSE arteries. The arteries, in order, were cannulated to allow infusion of 60% meglumine iothalamate for _in vivo_ angiography of the cutaneous vasculature. Following completion of these studies, the pig was heparinized and exsanguinated, its thoracic aorta was cannulated, and 2-3 L of micropulverized barium sulfate-gelatin solution was infused under controlled constant pressure. The pig was skinned after the gelatin had solidified and the abdominal pelt was contact-radiographed to determine the architecture of the normal cutaneous vasculature.

Experiment 3: Six female pigs were anesthetized and prepared for aseptic surgery. Random (CSEa-ligated, n=2) and axial pattern (n=10) skin flaps (two flaps/pig) of dimensions based on the above studies and recommendations for design of tubed flaps were raised, based on the CSEa. Fluorescein was infused and the line demarcating perfused/nonperfused portions ("surviving length") of the skin flaps, if any, was marked with stainless steel skin staples. The pigs were recovered from anesthesia. Two to seven days later, each pig was anesthetized and heparinized. Fluorescein angiography was repeated and the surviving length of each skin flap was recorded. Thereafter, the pig was exsanguinated and either the aorta (random pattern skin flaps) or CSEa (axial pattern skin flaps) was cannulated to allow barium sulfate-gelatin infusion under controlled constant pressure. The skin flaps were resected, pinned to original size, and contact-radiographed to allow comparison with fluorescein angiography and surviving length data.

Experiment 4: This experiment comprised a two-stage surgical procedure for routine preparation (stage 1 procedure) of single pedicle, axial pattern tubed flaps (Figure 1). In the stage 1 procedure, each female pig was premedicated with atropine sulfate (0.04 mg/kg IM) and xylazine hydrochloride (0.2 mg/kg IM) and maintained with halothane delivered by endotracheal tube. Each female pig was prepared for routine aseptic surgery in the caudal abdominal and inguinal regions. The proposed skin incisions and reference marks for wound margin alignment and skin flap retraction/expansion studies were outlined in the
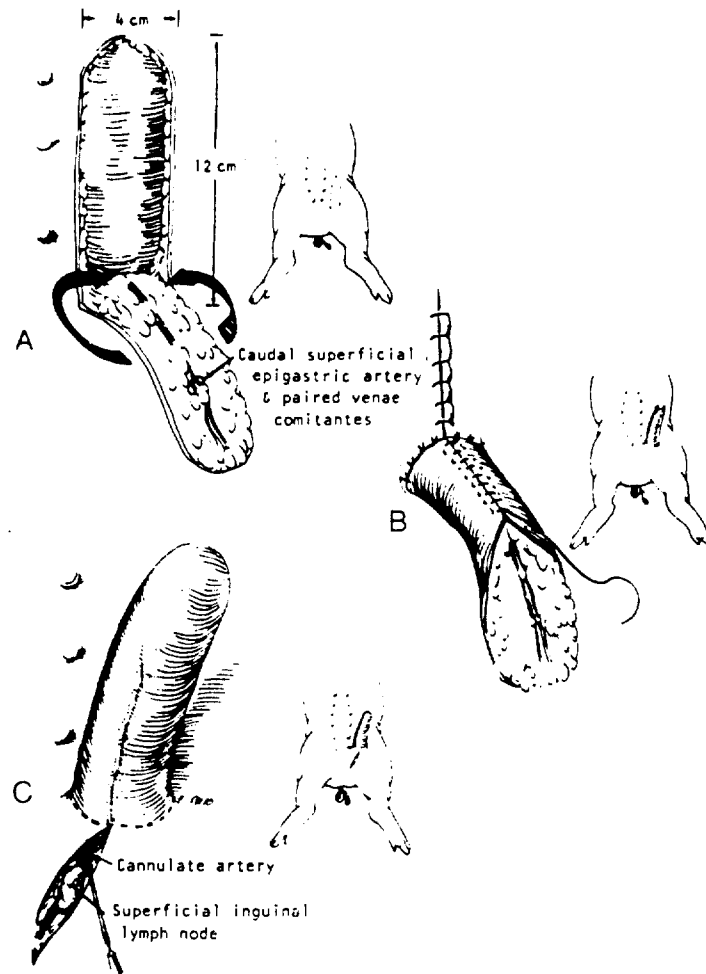
Figure 1. Surgical procedures for preparations of <u>in vitro</u>
isolated perfused porcine skin flaps. A, Stage 1
procedure: Single pedicle, axial pattern tubed flap,
supplied by the caudal superficial epigastric artery
and its paired venae comitantes, is raised on weanling
female Yorkshire pigs. B, The donor sight and tubed
flap are closed primarily, secured to the surrounding
abdominal skin via one or two sutures, and bandaged.
C, Stage 2 procedure: Two to 6 days later, the tubed
flap is harvested following cannulation of the caudal
superficial artery and one of the venae comitantes
(when possible) and transferred to the isolated organ
perfusion appartatus.

caudolateral epigastric region using a sterile marking pen. The skin incisions were made in order (medial, cranial, and lateral [peninsular stage 1 procedure, n=6] and caudal [island stage 1 procedure, n=6]) with a No. 10 scalpel blade and extended to the level of the muscular fascia. Craniomedial branches of the CSEa that supplied the caudal mammae were ligated and divided. Using skin hooks, the wound margins of the medial incision were retracted for direct visualization of the CSEa, allowing scalpel dissection of the subcutaneous tissue and skin flap elevation without vascular damage. In island stage 1 tube flaps, the caudal incision was realigned and sutured with a size 3-0 polypropylene suture, using modified three-point sutures to anchor the corners and a simple continuous pattern for the remaining wound. The tubed flap was formed and trimmed minimally of fat at its edges, if necessary. The tubed flap skin edges were closed using size 3-0 polypropylene in a simple continuous pattern. Starting 2.5 cm cranial to the base of the tubed flap, the subcutaneous tissues were apposed with five to seven vertically oriented, interrupted retention sutures using size 2-0 chromic gut. The superficial subcutaneous tissue was closed with 2-0 chromic gut in a simple continuous pattern. The skin incisions at the donor site and base of the flap were closed using size 2-0 nylon in simple continuous and simple interrupted patterns, respectively.

Fluorescein angiograms were evaluated 12 min after infusion of 5 ml of 10% fluorescein to predict surviving length of all tubed flaps. Thereafter, the surgical site and tubed flaps were bandaged using a self-adherent wound dressing that had been affixed to the skin using size 3-0 nylon in a continuous cruciate pattern. The pigs were recovered from anesthesia and housed individually.

The healing of axial pattern tubed flaps was evaluated by visual inspection, fluorescein angiography, and determination of tissue shrinkage during the postoperative period. This experiment was considered to be successful when it was determined that a single pedicle, axial pattern tubed flap could be raised and survive the entire length for an appropriate postoperative period.

In the stage 2 procedure, each female pig was preanesthetized, induced and maintained on anesthesia as described above. Visual inspection or fluorescein angiography was performed as described above to ascertain that the skin flap in each island stage 1 procedure had survived to its entire length. Each pig was prepared for routine aseptic surgery in the caudal abdominal and inguinal regions. A skin incision measuring 6 cm was made in the inguinal region, which extends caudally from the base of the tubed flap (Figure 1C). Using blunt dissection, the incision was deepened to the level of the superficial inguinal lymph node, thereby exposing the CSEa, which emerged from its deep surface. At this time, the pig was heparinized (3,000 IU IV) and the exposed vasculature bathed with 1-2 ml of 2% lidocaine hydrochloride to minimize vasospasm during subsequent manipulations. Aided by 3X microsurgical lenses, the CSEa was

isolated between two stay sutures of size 3-0 polypropylene. An opening in the wall of the CSEa was established and extended, using delicate 45 Potts cardiovascular scissors. The CSEa was cannulated with PE20 tubing, which was secured by the stay sutures. The patient side of the pedicle containing the caudal superficial epigastric vasculature was cross-clamped and the tubed flap resected. Heparinized, balanced polyionic saline solution (approximately 20 ml) was infused via the arterial cannula to clear the tubed flap of blood and establish that patency of the venae comitantes existed. The tubed flap was transferred to an assistant for transport in a clean tray to the isolated organ perfusion laboratory. The surgeon returned to the operative site on the pig and the vascular pedicle was double ligated with size 0 chromic gut. The wound was flushed and inspected to ensure adequate hemostasis and ventral drainage. The pig was recovered from anesthesia and the wound allowed to heal by second intention.

This experiment was considered to be completed successfully when the results of vascular transformation in the tubed flap, in conjunction with other findings (detailed below), allowed determination of the appropriate postoperative time for tubed flap harvest, which will allow satisfactory percutaneous absorption studies.

Isolated Perfusion Protocol:

Single pedicle, axial pattern, tubed flaps supplied by the CSEa were raised on female weanling Yorkshire pigs, weighing approximately 20 kg (stage 1 surgical procedure). Based on the experiments above, landmarks for a caudolateral epigastric flap (measuring 4 cm x 12 cm) were utilized. Venous drainage was provided by the paired venae comitantes associated with the artery. Two or 6 days later, the tubed flap was harvested (stage 2 surgical procedure) and transferred to the perfusion apparatus following cannulation of the artery. After the tube flap was harvested and the donor site healed completely, the pig was returned to the animal housing facility for later resale.

Perfusion media consisted of a Krebs-Ringer bicarbonate buffer solution (pH=7.4) containing the following in grams per liter (millimolar): NaCl, 6.89(117.9); KCl, 0.36(4.8); $CaCl_2$, 0.28(2.5); KH_2PO_4, 0.16(1.2); $MgSO_4-7H_2O$, 0.30(1.2); $NaHCO_3$, 2.75(32.7); glucose, 0.9(5.0); bovine serum albumin (Cohn fraction V), 45(0.7); gentamicin sulfate, 0.02(0.04); amphotericin B, 0.001(0.001); penicillin G, 10,000 IU; and sodium heparin, 5,000 USP. The perfusion apparatus (Figure 2) was a closed, recirculating system regulated for the relatively low perfusate flow rates (0.3-5.5 ml/min) seen in skin flaps. The apparatus was enclosed in a humidified plexiglass chamber maintained at $37^{\circ}C$. Medium was gassed with a mixture of 95% oxygen and 5% carbon dioxide using a silastic tube oxygenator (56). A variable rate peristaltic pump circulated 250 ml of medium to the cannulated artery of the skin flap. The perfusate was recirculated at a higher flow rate in an arterial-venous
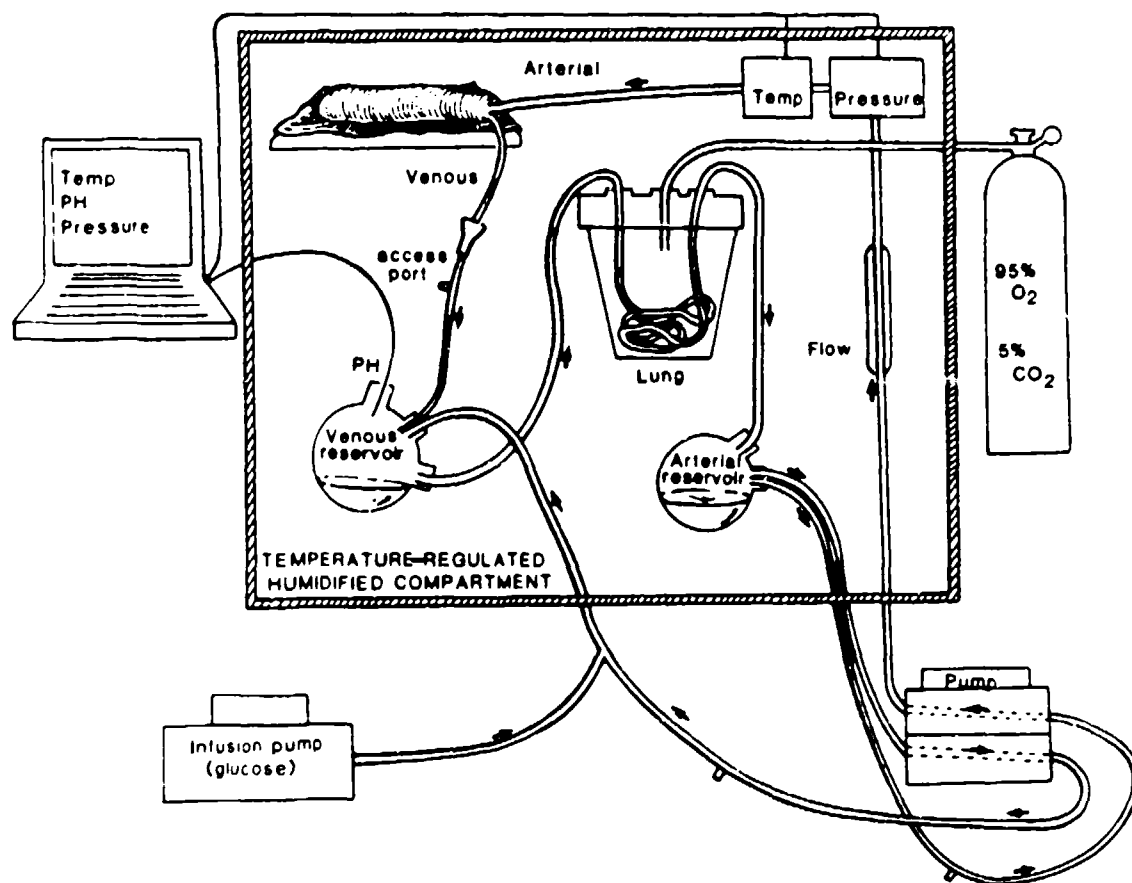
Figure 2. Schematic of the isolated perfused skin flap apparatus.

shunt line to provide adequate mixing of the medium. Glucose and sodium bicarbonate were infused into this shunt line to maintain arterial glucose concentrations between 80 and 120 mg/dl and stable perfusate pH (7.4).

Arterial perfusate pressure and temperature were constantly displayed and stored on a microcomputer. Arterial (2.5 ml) and venous (0.7 ml) perfusate samples were collected hourly for the determination of glucose concentrations (milligrams per deciliter), using an automated assay system (Glucose Analyzer 2; Beckman, Brea, CA), and osmolality (milli-osmoles per kilogram; Osmette A; Precision Systems, Sudbury, MA). Glucose utilization (mg/hr) was calculated from the product of glucose extraction (mg/dl) and the flow rate (ml/min) at each observation time. Cumulative glucose consumption was estimated from the area under the glucose clearance vs time curve using the trapezoidal rule. Arterial pH, lactate, and lactate dehydrogenase (LD) activity were also monitored to biochemically assess the flaps' viability. Lactate was assayed using Sigma Method 826-UV (Sigma Chemical Co., St. Louis, MO). LD, an intracellular enzyme, was used as a marker for cell membrane integrity (57) and was determined using a multistat centrifugal analyzer (MCA III$^+$; Instrumentation Laboratories, Lexington, MA).

Initial experiments (n=3) were not terminated at a specific time in order to determine markers of flap death. Subsequent flaps were terminated at 10-12 hr. Sodium fluoride (NaF), an inhibitor of glycolysis (58), was administered after 5 or 11 hr of perfusion (n=4) in order to assess the flap's sensitivity to metabolic inhibition. At the termination of each IPPSF experiment, skin samples were collected and processed for both light microscopy (LM) and transmission electron microscopy (TEM).

Morphological Viability Assessments by Light and Transmission Electron Microscopy:

If a morphological viability index was to be developed for the IPPSF, viability must first be defined. Viability in an IPPSF has a different connotation from that employed in cell culture work. In the flap, the majority of cells must be metabolically active, while in cell culture, only a small percentage of cells must be capable of subsequent growth on culture medium and cells may be in various dormant phases. Therefore, our criteria for viability, both morphological and biochemical, were more stringent than others. Morphological changes due to cell death, surgery, toxicity, isolated perfusion, or chemically induced toxicity must be differentiated before a meaningful index could be constructed.

In order to define changes due to cell death, a piece of skin (4 cm x 12 cm) was harvested from the normal site. Samples of skin were pinned to dental wax in a dissecting tray and floated on a 37°C water bath. The samples were kept moist only on the dermal side by bathing with lactated Ringer's in which antimicrobials were added (10 ug/ml gentamicin and 0.2 ug/ml

amphotericin B). Six-millimeter biopsy samples were taken from different locations on the flap based on a random digit table at 0, 15, 30, and 45 min and 1, 2, 3, 4, 8, 12, 24, 48, and 72 hr in three pigs. In two additional pigs, samples were taken at 1, 2, 4, 5, 6, 8, 9, 10, 12, 18, and 24 hr. The 6-mm biopsy was further divided in half for LM and the other half was divided between TEM and frozen samples. LM sections for each time period were independently scored by two investigators. Quantitative measurements were first based on basal dark nuclei, pyknotic basal cells, basal vacuoles, stratum spinosum dark nuclei, pyknotic stratum spinosum, and stratum spinosum on a scale from 1=(0-5 cells), 2=(5-10), 3=(10-20), 4=(20-40), to 5=(diffuse). The second assessment was a subjective rating on the overall appearance of a section, scored as 1 (no change-normal), 2 (mild changes), and 3 (obviously necrotic). This rating was then correlated to the individual assessment. In order to improve the discriminatory ability of the information collected, the total number of epidermal cells were counted for each slide. The percent of each cell type observed in the above evaluation was calculated using the midpoint of each range as the cell count. Three alternative scales were also evaluated: percentage (%), square roots (% + 0.5) and logarithm (log(%+1)). Each of the latter scales resulted in the misclassification of three to four more slides than the original scales and were not considered further.

In order to define changes that occur in _in situ_ flaps post-surgically, a biopsy study was performed _in situ_ for 7 days after creating the flap in the stage 1 procedure. Morphometric analyses of LM samples were performed on three _in situ_ skin flaps to help determine the optimal time of harvest following stage 1 surgery. Sections were collected daily on the flaps, from 0 (30 min after stage 1 surgery) to 7 days, at random sites along the length of the skin flap whose free end was sutured to the body wall to prevent traumatic injury. Pigs were immobilized with 0.2 cc of Rompun and 3 cc of ketamine. During these sampling procedures, the pig felt no pain, since cutaneous innervation was severed during the formation of the tubed flap. Paraffin-embedded sections, stained with hematoxylin and eosin, were examined with a 40X objective attached to an Olympus PM-10ADS (Olympus Corp., Washington, D.C.) automatic photomicrographic system, using a calibrated eyepiece reticle. Each section was evaluated at four points, two each at thin epidermal areas and two at the thickest areas, coinciding with rete pegs. Thickness of the stratum corneum was constant at all times and was not analyzed. Data in the tables and figures are reported as mean ± SE.

In order to define changes specifically related to isolated perfusion, IPPSF tissue samples were taken after 12 hr of perfusion. Finally, in order to determine whether the IPPSF was responsive to chemically induced toxicity, 10 mg/ml of NaF was administered to four flaps after 5 and 12 hr of stable perfusion. Glucose extraction ceased 40-90 min later.

Tissue processing techniques for LM, TEM, and histochemistry are routinely used in our laboratory. Specimens for LM are fixed overnight in half-strength Karnovsky fixative at $35^\circ C$ (2% paraformaldehyde and 2.5% glutaraldehyde <976 mOSM> in 0.1 M cacodylate buffer), routinely processed, embedded in paraffin, and stained with H&E or periodic acid Schiff (PAS). For enzyme histochemistry, small tissue pieces are quenched in an isopentane well in a Dewar flask filled with liquid nitrogen and stored at $-70^\circ C$ until studied. Tissue is then mounted on a stub with OCT compound and sectioned on an AO cryostat. Histochemical techniques presently being utilized in our laboratory on frozen sections include LD (59), acid phosphatase (60,61), ATPase (62), and nonspecific esterase (63). These should be useful for characterizing cell death and toxicity in IPPSF studies.

For TEM, tissue samples (1 mm^3) were fixed overnight in half-strength Karnovsky's ($4^\circ C$, pH 7.4, 976 mOSM), postfixed in 1% osmium tetroxide for 1 hr, dehydrated through graded ethanol solutions and infiltrated and embedded in Spurr's resin, placed in flat embedding molds and polymerized in a $70^\circ C$ oven overnight. Thick sections approximately 1 u were stained with toluidine blue for orientation. Ultrathin sections approximately 600 » were sectioned with a diamond knife cn a Reichert Ultracut E microtome (AO Reichert, Buffalo, NY). Sections were picked up on 300-mesh copper grids and stained with uranyl acetate and lead citrate and sections were then examined on a Philips 410LS transmission electron microscope (Phillips, Mahwey, NJ) at an accelerating voltage of 60 or 80 kv.

In Vivo Percutaneous Absorption

[1-methyl-^{14}C]Caffeine (specific activity = 47.5 mCi/mmol) and [7-^{14}C]benzoic acid (specific activity = 19.3 mCi/mmol) were purchased from New England Nuclear (Boston, MA). [2,3-^{14}C]Malathion (specific activity = 37 mCi/mmol), [ring 2,6-^{14}C]parathion (sp. act. = 21 mCi/mmol), [ring 4-^{14}C]progesterone (specific activity = 56 mCi/mmol), and [ring 4-^{14}C]testosterone (specific activity = 56.9 mCi/mmol) were purchased from Amersham (Arlington Heights, IL). Unlabeled (cold) caffeine (C), benzoic acid (B), testosterone (T), and progesterone (R) were purchased from Sigma (St. Louis, MO). Cold malathion (M) and parathion (P) were purchased from Chem Service, Inc. (West Chester, PA). The radiochemical purity of all ^{14}C compounds was certified by manufacturer's thin layer chromatographic (TLC) analyses to be >97%. Female weanling Yorkshire swine, weighing approximately 20 kg each (17.8 ± 0.4, N=64), were obtained for use in all studies. Pigs were acclimated for at least 1 week before entering into the study, housed at standard temperature $72^\circ F$.) and light-dark cycle (12:12 hr), and were fed 15% pig and sow pellets, 2 lbs/day (Wayne Feed Division, Chicago, IL), and approximately 2 L water/day.

Dosing solutions were prepared for intravenous injection by addition of cold compound in ethanol solution to the radiolabeled

material. This was further diluted in sterile physiolog(pH=7.4) saline to a final concentration of 0.02 mg/ml and a radioactive concentration of 1 uCi/ml. All IV solutions were prepared within 1 week of use. Pigs were weighed and anesthetized by intramuscular injection of 4 mg/kg xylazine (Rompun; Miles/Bayvet, Shawnee, KS) and 16 mg/kg ketamine (Ketaset; Bristol Laboratories, Syracuse, NY). Ten milliliters of the IV dosing solution was administered to each pig by bolus injection into an ear vein. Pigs were immediately placed into metabolism cages, constructed so that total urine and feces could be collected separately. Urine was collected at 6, 12 (where available), and 24 hr and daily thereafter for a total of 6 days. The volume of each collection was measured and a small sample was stored at $-20^{\circ}C$ until analysis. Feces were collected daily for 6 days and the total sample, placed in plastic bags, was also stored at $-20^{\circ}C$. At the end of the study, pigs were euthanized with 60-80 mg/kg (IV) pentobarbital solution (Uthol, Butler, Columbus, OH). Liver, both kidneys, and spleen were removed and weighed. Small samples of each, along with samples of lung, colon, skeletal muscle, and skin were stored as described above. For two pigs, one receiving benzoic acid and another dosed with malathion, a cannula was inserted through a 12 gauge-needle into the jugular vein and blood samples (1-ml each) were taken at 15, 30, 45, 60, and 90 min and at 2, 3, 4, 6, 8, 12, 24, and 48 hr for pharmacokinetic disposition studies.

For topical administration, dosing solutions were prepared by diluting cold and radiolabeled compound in 100% ethanol, to a final concentration of 1 mg/ml and 50 uCi/ml. Pigs were weighed and anesthetized as described for the IV studies and a topical application procedure similar to that described previously (23) was followed. The abdominal area on each pig was lightly shaved with electric clippers, taking care not to damage the skin surface (29,30). The intended area to be dosed (5 cm x 1 cm) was marked and a small foam rubber patch (10 cm x 5 cm x 2 cm) with the center cut out was glued to the skin immediately adjacent to this area. Neither the glue nor the patch touched the area to be dosed. Using a micropipettor (Hamilton, Reno, NV), 200 ul of the ethanolic dosing solution was applied to the site, to provide an applied surface concentration of 40 ug cm^{-2}. A nylon screen and nonocclusive gauze pad were used to cover the foam patch and were held in place by wrapping the pig's midsection with elastic tape (Elasticon; Johnson & Johnson, New Brunswick, NJ). Pigs were then placed in the metabolism cage. Excrement collections and tissue samples at termination of the study were the same as for the IV pigs, except that the foam patch, dosed site, and adjacent skin were also collected and stored separately.

Because the coefficient of variation in the radiolabel concentration determined from a single fecal collection chosen at random was 53% (n=5 replicates) without prior preparation, it was deemed necessary to homogenize all feces to provide a well mixed sample for accurate radiolabel determination. Each total daily fecal collection from both IV and topically dosed pigs was individually weighed and ground into a paste in a Waring

commercial blender, with addition of 100-300 ml physiological saline (pH=7.4) to facilitate grinding. A small amount of the homogenate was collected in a plastic vial and stored until assay. Coefficients of variation checked in two randomly selected samples were significantly lower, averaging 8-11% (n=5).

Aliquots of urine (500-800 μl), plasma (500 μl), red blood cells (200 μl), tissue samples from the internal organs (0.3-0.8 g), and fecal homogenate samples (0.6-0.8 g) were oxidized without further preparation in an open-flame tissue oxidizer (Model 306; Packard Instrument Co., Downers Grove, IL). The trapped radiolabel was measured using a liquid scintillation counter (LSC) equipped with automatic external standard quench and color correction (1219 Rackbeta; LBK Wallac, Turku, Finland). Each skin sample was weighed and immersed in a flask containing tissue solubilizer (BTS-450; Beckman Instruments, Fullerton, CA), in amounts of 5-10 ml/g wet tissue weight. The flask was placed in a water bath overnight and maintained at 42°C with shaking (80 oscil'ations/min). Aliquots of the solubilized skin (100 μl) were added to 10 ml scintillation cocktail (Scintiverse Bio-HP; Fisher Scientific, Fair Lawn, NJ) and counted by LSC as described above. Several samples of the application sites and patch skin were also directly oxidized and counted to assure that solubilization did not affect total recoveries. No significant differences were observed between the two procedures. Foam rubber patches were extracted in an 80:20 (v/v) ethanol methanol mixture. Samples of the extract (500 μl) were added to 10 ml of scintillation cocktail and counted as before.

Whole body residues and excretion recoveries were calculated by multiplying radiolabel concentrations by measured urine volumes and fecal and organ weights (liver, kidneys, spleen), or by the estimated organ weights for lung, colon, skin, and muscle (64). Skin samples and patch extract recoveries were calculated separately. A two-compartment pharmacokinetic model was fitted to the blood and plasma concentrations and clearance (Cl), volume of distribution (Vc and Vss), and half-life ($T_{1/2}$) were calculated according to standard formulas (65) . Percutaneous absorption, expressed as a percent of total dose, was corrected for incomplete excretion using the following formula (39):

$$\text{Corrected absorption} = \frac{\text{Topical excretion}}{\text{IV excretion}} \times 100\%$$

Percutaneous absorption estimates based on urine alone or urine + feces for each route were determined to compare the two methods for calculating fractional absorption (47). Elimination rates (K) for IV and topical excretion were estimated from simple linear regression of a sigma-minus plot of log [amount remaining to be excreted] vs time (65). All data in the tables and figures are reported as means $\pm$ SE and inferences were based on Student's t-statistic.

IPPSF Percutaneous Absorption

IPPSF's were removed from the apparatus after the trial period and fitted with a patch (8 cm x 3 cm) made of a flexible plastic (Stomahesive; ConvaTec, Princeton, NJ), from which the center area (5 cm X 1 cm) surrounding the intended topical dosing area was cut out. The patch was glued in place with nontoxic adhesive (Skin Bond; Pfizer Hospital Products, Largo, FL). Topical solutions prepared and applied exactly as described above for _in vivo_ experiments, containing either B (n=8), C (n=8), D (n=7), M (n=5), P (n=6), R (n=8), T (n=7), or A (n=5), were dosed onto each flap. After the ethanol vehicle evaporated a foil bridge was glued onto the patch, the flap was wrapped lightly in gauze in a nonocclusive fashion, and it was returned to the perfusion apparatus. The total amount of time for which the flap was not being perfused during this application procedure was not longer than 10 min. Samples from both the arterial reservoir and the venous drainage were then collected every half-hour for the first 4 hr after and every hour thereafter, for a total of 8-10 hr. Some of the IPPSF's dosed subsequently died, with sustained glucose utilizations <10 mg/hr (6.9 $\pm$ 0.9, n=9), or became very leaky (n=5) from tears in the epidermis caused by the glue drying under the patch. Absorption data and flux rates from these flaps, where available, were handled separately. The difference in mean hourly glucose utilizations in these nonviable flaps and the nonviable flaps terminated prior to dosing was not statistically significant when compared using Student's t-test. Overall mean hourly glucose utilization was significantly greater in the remaining 40 viable flaps (22.3 $\pm$ 1.0, p<0.0001). In experiments designed to examine _in vitro_ fluxes at time points greater than 8 hr, flaps dosed _in situ_ with either malathion [ISM (_in situ_ malathion), n=2] or parathion [ISP (_in situ_ parathion), n=1] were harvested 16-17 hr after dosing and perfused as before, with samples taken hourly throughout an 8-hr perfusion. At the termination of every IPPSF experiment, the flap was removed from the apparatus and weighed after removing the patch. The patch, dosed area (5 cm^2), and skin directly below the patch were removed and stored frozen until assay. In addition, the terminal volume of perfusate was measured and a large sample was stored, along with the remainder of the flap which was placed in a plastic bag.

Metabolite profiles for IPPSF studies of P penetration were determined following ethyl acetate (EtAc) extraction (see below) of terminal perfusate samples from two of the flaps dosed _in vitro_ and the flap dosed _in situ_ (ISP). A schematic diagram outlining the most important metabolic pathways for P, which are known to occur in the liver, lungs, kidneys, brain, and suprarenal glands (66), is shown in Figure 3. The primary pathways in liver are designated steps 1 and 2 and the initial step is considered to represent bioactivation, since the product, paraoxon (P=O), is more toxic _in vivo_ and a more potent cholinesterase inhibitor _in vitro_ (67-72). The initial reaction along each pathway (steps 1,3, and 4) is catalyzed by mixed-function oxidases, generally known as cytochrome P-450 monooxygenase in the liver, and is dependent on the presence of
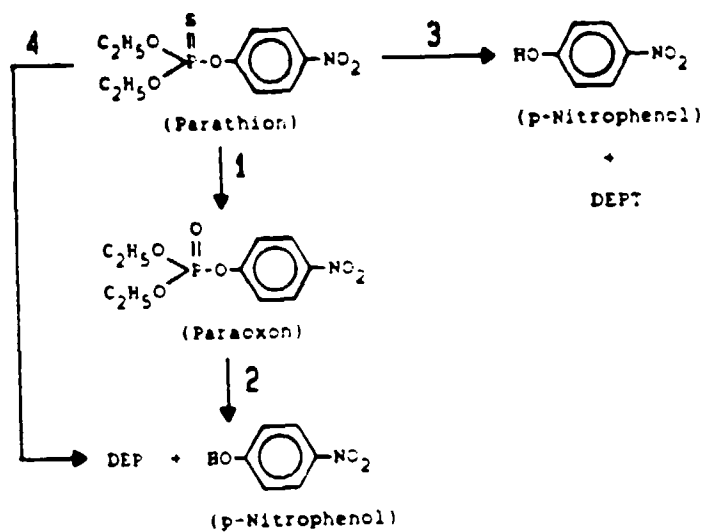
Figure 3. Biotransformation of parathion in the liver. Reactions 1, 3, and 4 are catalyzed by cytochrome P-450 mixed-function oxidase and reaction 2 is catalyzed by A-esterases.

NADPH and molecular oxygen, although the km (substrate concentration at half-maximal reaction velocity) for the latter is so low that the reaction will take place even after the system is flushed with nitrogen (66,67,73,74). These three reactions are not independent, as shown in the diagram, but proceed through the csame putative phosphooxythirane intermediate. Although P=O is formed in many extrahepatic tissues, complete degradation of P to para-nitrophenol (PNP) usually occurs only in the liver. The second reaction (step 2), catalyzed by A-esterases, takes place in most body organs and tissues studied (74-77). The contribution of each alternative pathway (steps 3 and 4) in vivo is not certain. The majority of PNP and diethylphosphate (DEP) formed is due to P=O metabolism, but a significant fraction results from water attack on the phosphooxythirane molecule (66). Direct hydrolysis to PNP + diethylphosphorothioate (DEPT, step 4) is a minor pathway for P metabolism. Since the [^{14}C]-atoms were components of the phenol ring, it was assumed that the radiolabel would be found only in ringed structures shown in Figure 4. Therefore, the DEP and DEPT, found mostly in the aqueous residue after extraction, are not labeled and were not measured in this study.

Further experiments were performed in which: (1) the application site was occluded with Saran wrap (n=2), or (2) the flap was dosed with 1-aminobenzotriazole (ABT, n=2) by injecting a saline solution of this nonspecific cytochrome monooxygenase inhibitor (78) at a dose of 50 μg/g (79) 1 hr prior to P application. In order to determine the extent of nonenzymatic P degradation during the perfusion period, dilute [^{14}C]-P solutions were injected directly into the recirculating perfusate, in the absence of a skin flap, in amounts equivalent to typical 8-hr absorption totals for P in the IPPSF. Terminal (8-hr) perfusate was then analyzed for degradation products as described below. Approximately 86% (90.6, 81.0) of this extract co-migrated with P, 9% (5.5, 12.2) with paraoxon, and 5% (3.8, 6.8) with PNP, indicating a very small component of nonenzymatic P metabolism in the IPPSF studies. The original topical dosing solution was also checked for degradation products and was shown to have radiochemical purity >99%.

Assay Methods and Calculations

Assay methods were as described for the in vivo topical studies. Five hundred - microliter perfusate samples were oxidized. Application sites and patch skin samples from each of the eight compounds tested were directly oxidized and counted to assure that the solubilization procedure did not affect total recoveries. No significant differences were observed between the two assay methods. Because total recovery was less than 85% in some flaps, particularly those dosed with strongly lipophilic penetrants (R, T), a portion of all flap remainders was also solubilized and counted. Cross-sections of this subcutaneous tissue (approximately 1 cm thick) were taken from the center of the application site, cut in half and treated in similar fashion as the skin samples. Foam rubber patches from the in vivo pigs
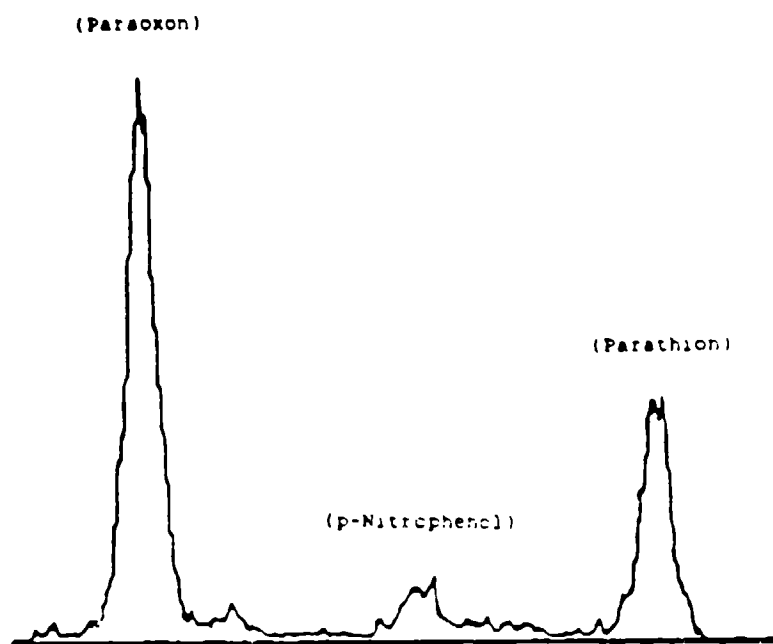
Figure 4. Radiochromatogram of an IPPSF perfusate sample. The primary EtAc-extractable metabolites are shown along with the parent compound (P).

and Stomahesive, gauze, and foil patches from IPPSF experiments were extracted in an 80:20 (v/v) ethanol methanol mixture. Samples of the extract (500 ul) were added to 10 ml of scintillation cocktail and counted as before.

For P metabolite separation and identification, each perfusate sample was adjusted to slightly acidic pH (5.5-6.5) with 1 N hydrochloric acid and extracted twice with 6 ml of EtAc. Extracts were pooled and evaporated under 100% nitrogen (N_2), resuspended in 100 μl EtAc, and spotted along with co-standards for P, paraoxon, and p-nitrophenol on silica gel TLC plates (HLF; Analtech, Newark, DE). Each plate was developed in a benzene-EtAc solution (4:1, v/v) and counted using a Berthold TLC linear analyzer connected to an Apple II+ computer. A typical radiochromatogram is presented in Figure 4, taken from an untreated IPPSF dosed with P. Relative amounts of the parent and metabolites were determined from the areas under each peak, expressed as a percentage of total radioactivity. LSC determinations of radiolabel quantities in the aqueous residue from each extraction revealed amounts only slightly greater than background radiation levels, accounting for less than 1-2% of total sample radioactivity in any experiment.

A multicompartment model describing the pharmacokinetics of percutaneous absorption in the IPPSF was developed for each compound using the computer program CONSAM, which is the interactive version of the simulation, analysis, and modeling (SAAM) language (80-82). Compartments and mass transfer constants were initially chosen based on the four-compartment model used to simulate _in vivo_ percutaneous absorption kinetics by others (83-86). Rate constants were estimated using an iterative method to provide a curvilinear function mapped onto the model's perfusate compartment until the best approximation of the IPPSF data (absorption rates) was obtained. The model itself was also simplified to the least number of compartments necessary to resolve absorption rate-time plots for all compounds in an equivalent fashion. Thus, the initial goal was to find a model which adequately predicted _in vitro_ percutaneous absorption pharmacokinetics in the IPPSF for any compound tested, without attempting to tailor the model to individual compounds. Where significant departures from the data points existed for a particular compound, a secondary, modified model was developed in an attempt to improve the "fits." All data in the tables and figures are reported as means ± SE. Statistical inferences were based on Student's t-test or using correlation coefficients derived from simple linear regression, and $p < 0.05$ was considered a significant difference.

RESULTS

Development of Surgical Procedure

Experiment 1: Prosection of the "omnipotential pig buttock flap" as a proximally based island arterial flap (sic) (54,55) based on the deep circumflex iliac artery (DCIa) was done and it was found that the caudal 8-10 cm of this flap was vascularized by musculocutaneous perforators. Although the DCIa provided a direct cutaneous arterial system to the cranial portions of that flap, it was judged difficult to isolate and cannulate surgically without dissection of the medial thigh region of the pig. During dissection, it was found that muscle adhered to the skin in those regions in which the cutaneous vascular supply was musculocutaneous in nature. Because the skin flap was thick, it would be hard to tube, and primary closure of the donor site would not be possible. Therefore, further development of the "omnipotential pig buttock flap" as a donor skin flap was abandoned.

Inspection of the ventrally based "trunk flaps" (sic) (51,52) indicated that development of an axial pattern tubed flap based on this donor site should be discontinued for lack of a well-developed direct cutaneous arterial system and the presence of thick cutaneous trunci (paniculus carnosus) muscles.

In the caudolateral abdominal region, it was found that both the left and right CSEa's followed similar distribution patterns: 1) origin, 2) caudomedial branches, and 3) cranial extension, which divides into a lateral portion supplying skin lateral to the line of mammae and craniomedial branches supplying each of the caudal mammae and median skin. Two venous systems were observed in the caudal abdominal skin region: 1) paired venae comitantes in association with the CSEa, and 2) a cranial superficial epigastric venous system with an anastomotic branch to the deep circumflex iliac vein and an ill-defined caudal extent that terminates in the region of the caudal mammae. Approximately 14-16 cm cranial to the caudalmost teat, i.e., at the level of the caudal extent of the cutaneous trunci muscle, the abdominal skin becomes nourished by musculocutaneous vasculature.

Based on the assessment of these results, an axial pattern tubed flap (10 x 4 cm) incorporating the skin perfused by the CSEa was considered feasible.

Experiment 2: Both angiography and contact radiography of the abdominal pelt confirmed the observations in experiment 1. Nonselective aortic angiography readily identified the pudendoepigastric arterial trunk and its subsequent distribution, including the CSEa, to the flank and abdominal skin. Using either nonselective aortic or selective CSEa angiography, CSEa branches coursed the entire length of the proposed skin flap. Communication between the two venous systems was observed; subsequent experience has indicated that enlargement of the venae

comitantes is obvious between days 2 and 29 in response to separation of the raised skin flap from the large venous system associated with the mammae.

Experiment 3: All caudolateral epigastric skin flaps survived to a level at least 13 cm cranial to the caudalmost teat (Table 1); however, filling of an axial vessel was seen in peninsular or island flaps only. Although additional replicates would be needed to correct the data for variability between pigs, e.g., weight and skin flap retraction, and to establish standard deviations for all measured parameters, certain trends have become apparent. The surviving lengths of island flaps $\geq$ penisular flaps > random flaps. One could expect approximately 10-15% greater surviving length of any flap 2-7 days later, compared to predicted survival at time 0, using our method of fluorescein angiography. Fluorescein angiography at 2-7 days postoperatively correlated consistently with surviving length of the skin flap. Vasculature was observed in the surviving portions of all skin flaps, but did not correlate as closely with surviving length as did fluorescein angiography. The microangiographic studies in this experiment did not allow us to elucidate clearly the venous drainage from the base of island vs peninsular skin flaps. Based on these studies, it was concluded that a single pedicle, axial pattern (either island or peninsular) tubed flap measuring 4 x 12 cm would probably survive to its entire length.

Experiment 4: In the initial experiments, nine female pigs (n=12 tubed flaps) weighing 22-50 kg were used for development of the stage 1 procedure. It was found that all stage 1 tubed flaps survived to their entire length for periods ranging from 5 -29 days. However, some degree of epidermal necrosis followed by secondary intentional healing occurred if excessive subcutaneous tissue was included within the tubed flap; therefore, female pigs weighing in excess of approximately 35 kg are not suitable for preparation of single pedicle, axial pattern tubed flaps as described above. Although six tubed flaps in this series were prepared on three female pigs, it was found that delay between procedures (approximately 60 days) to allow, ostensibly, intussusceptive growth and release of skin tension at the first donor site, thereby allowing primary closure of the second donor site, was complicated by weight gain in the female pigs, which made tubed flap closure without tension difficult, even with maximal subcutaneous tissue debulking.

Based on measurements of tubed skin flaps at time 0, 2 days, and 6 days after stage 1 procedure, estimations of tubed flap skin surface area retraction/expansion can be made (Table 2).

The Standard Operating Procedure (SOP) complete with detailed surgical diagrams is included in the Appendix to the this report. As of the completion of this report, our procedure is to lift two skin flaps on either side of the ventral abdominal midline. Minimal problems are encountered with this procedure. After the Stage 2 procedure is complete, primary closure of the

Table 1. Comparison of fluorescein angiography, surviving lengths, and microangiography data in various abdominal skin flaps

Flap Type	Size*	Initial Retraction (in length)	Fluorescein Angiography†				Later Retraction (in length)	Surviving Length†			Vessels Seen in Radiographs†
			0	48h	72h	7d		48h	72h	7d	
Peninsular Flap ("ventral type", n=1)	12x32		17.5	21.7			~12%	21.7			19.0
Peninsular (n=8)	8x32	~6%	17.0	23.0‡	17.7‡	19.8§	~18%	23.0‡	17.7‡	19.8§	17.8
Island (n=8)	8x32	~6%	18.7		19.7‡	22.5§	~12%		19.7‡	22.5§	20.5
Random (n=2)	8x32	~6%	8.8			13.2	~17%			13.2	12.8
Island (denervated, n=1)	8x32		19.7			21.2	~18%			20.2	16.0

*Dimensions in cm.
†Distance in cm (x) from base of flap.
‡n=1
§n=2
||n=3

Table 2. Measurements of stage 1 tubed flaps for determination of tubed flap skin surface retraction/expansion

Parameter	Postoperative Time (days)		
	$0^\dagger$	$2^\ddagger$	$6^\S$
Length*	7.2 ± 0.1	7.4 ± 0.1	7.5 ± 0.2
Diameter*			
Base	1.4 ± 0.03	1.7 ± 0.03	1.6 ± 0.09
Tip	1.4 ± 0.03	1.8 ± 0.05	1.7 ± 0.09
Calculated area[∥]	31.7 cm^2	40.7 cm^2	38.9 cm^2
Percentage of original area[¶]		128%	123%

* Dimensions in centimeters ($\bullet \pm$ SE).

∥ Based on formula: $\left(\dfrac{D_{base} + D_{tip}}{2} \right) \pi \times$ length = calculated area in cm^2.

¶ Percentage of original in situ dimensions (30.0 cm^2).

† n=38.

‡ n=27.

§ n= 6.

wound is not attempted since this procedure is now conducted using a "clean" and not "aseptic" protocol. Both Stage I and Stage 2 procedures are routinely performed by trained technical personnel.

Isolated Perfusion

Skin flaps harvested 2 or 6 days after stage 1 surgery remained viable for periods of 10-16 hr as assessed by glucose utilization, lactate production, absence of significant LD concentrations in the perfusate, a stable perfusate flow rate, and by LM and TEM. In two flaps perfused immediately after stage 1 surgery, vascular leakage occurred and criteria of viability were significantly poorer than in other flaps. Bacterial overgrowth occurred in two flaps, resulting in rapidly declining arterial pH, increased glucose utilization and the inability to maintain normal arterial oxygen tension. These indicators were succesfully used to predict overgrowth in later flaps prior to confirmation by standard clinical microbiological procedures. Bacterial isolates included <u>Klebsiella oxytoca</u> and <u>Aeromonas hydrophila</u>.

Data from 18 IPPSF's, which were harvested either 2 days (n=12) or 6 days (n=6) following stage 1 surgery, are summarized in Table 3. No major differences between 2-day and 6-day flaps were seen for any of the viability parameters listed in Table 3. Although statistically significant differences in terminal vs initial osmolality were found for both types of IPPSF (p<0.01), the increases were small (<10%) and were probably a result of lactate accumulation in the perfusate. Both 2-day and 6-day flaps showed a significant weight gain over the course of a 10-12 hr study (p<0.01), with 2-day IPPSF weight increasing approximately 25% and 6 day IPPSF weight increasing almost 42%. The exact nature of these increases is unknown; however, morphological evidence of mild dermal edema and hypertrophic growth was seen in most IPPSF's.

During the first 10-12 hr in all 18 preparations, the cumulative glucose consumption was linear, with squared correlation coefficients (R^2) between 0.97 and 0.999, indicating uniform glucose consumption with time (Figure 5). Further evidence of the viability of the IPPSF can be appreciated when glucose extraction is plotted against perfusate flow (Figure 6). In order for the IPPSF to maintain uniform glucose consumption over time, glucose extraction increased in direct proportion to decreased flow. In four earlier flaps in which constant arterial glucose concentrations greater than 80 mg/dl were not maintained by glucose infusion, glucose extraction was linearly correlated with arterial glucose concentration.

Flap death, first evident by 16 hr of perfusion in experiments not deliberately terminated at 10-12 hr (IPPSF's 1-3), was marked by a drop of glucose utilization and a plateau in the cumulative glucose consumption curve, concurrent with a rise in LD values. Terminal LD values during a viable period were

Table 3. Estimates[a] of biochemical function in perfused skin
flaps harvested either 2 or 6 days after stage 1 surgery

	Days After Stage 1 Surgery	
Variable	2 (n=12)	6 (n=6)
Arterial glucose concentration (mg.dl)[b]	114.6 ± 4.6	96.3 ± 5.6
Glucose utilization (mg/hr)[b]	25.1 ± 2.7	26.2 ± 5.4
Flow (ml/min)[b]	1.9 ± 0.2	1.7 ± 0.4
Cumulative glucose consumption (mg)[c]	241.0 ± 24.2	199.9 ± 18.6
Terminal lactate concentration (mM)[c]	2.2 ± 0.1	2.5 ± 0.3
Terminal LD (IU/L)[c]	7.6 ± 2.5	16.9 ± 4.6
Initial osmolality (mOsm/kg)	347 ± 18	331 ± 23
Terminal osmolality (mOsm/kg)[c]	374 ± 24	387 ± 17
Initial weight (g)	30.5 ± 1.1	30.3 ± 1.2
Terminal weight (g)[c]	38.3 ± 1.8	42.9 ± 7.5

[a]Mean ± SE.

[b]Individual values represent the average of 8-12 observations per
IPPSF.

[c]After 10-11 hr of infusion.
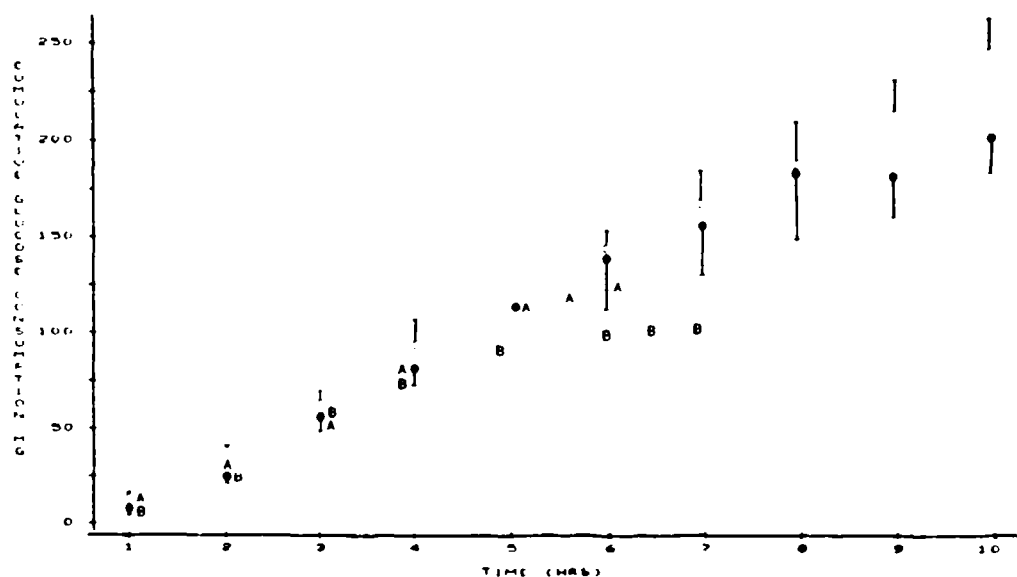
Figure 5. Plot of mean cumulative glucose consumption vs time for flaps harvested 2 days (open circles, n=12) and 6 days (closed circles, n=6) after stage 1 surgery. The bars represent one SE. Two preparations receiving NaF at 5 hr are plotted individually (A,B).
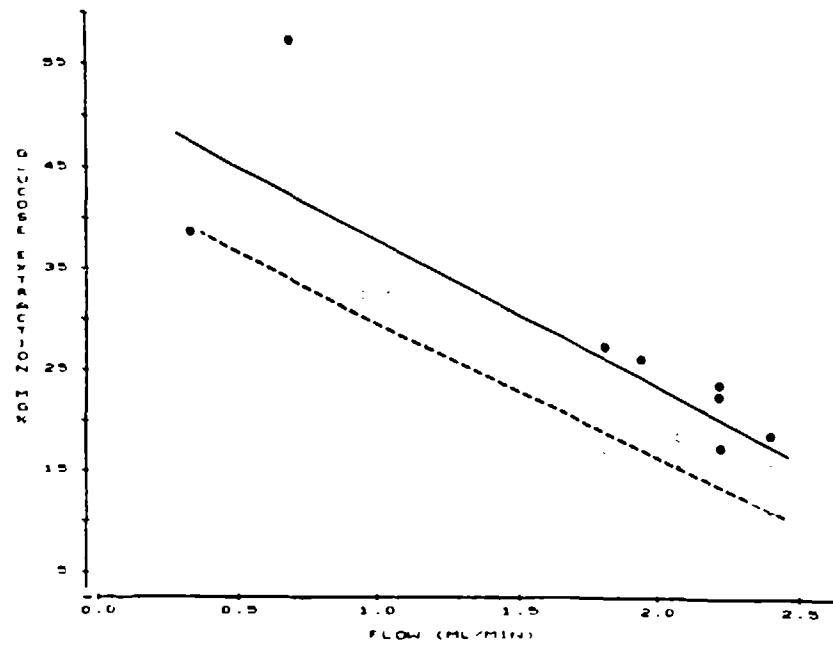
Figure 6. Plot of glucose extraction vs perfusate flow rate for an IPPSF harvested 2 days after stage 1 surgery (open circles) and 6 days after stage 1 surgery (closed circles).

relatively insignificant at 10.3 ± 2.4 Iu/L (range = 0-30 Iu/L), while 8- to 100-fold increases usually coincided with flap death. In four flaps, sodium fluoride (10 mg/ml) was administered after 5 (n=2) or 11 (n=2) hr of perfusion. Approximatel₃ 40-90 min later, glucose utilization abruptly ceased, evidenced by a plateau in cumulative glucose consumption at the termination of these experiments (Figure 5).

Arterial lactate concentrations increased progressively throughout each IPPSF experiment and had linear correlations greater than 0.97 with the cumulative glucose utilization (Figure 7). Based on the regression of millimoles of lactate produced vs millimoles of glucose consumed, the mean lactate/glucose ratio was 1.6 ± 0.2 for 2-day preparations (n=12) and 1.8 ± 0.2 for 6- day preparations (n=6). When arterial pH was not regulated by sodium bicarbonate infusions (five flaps), pH decreased over the course of a 12 hour experiment.

Morphological Studies:

LM evaluation on H&E sections collected from dying skin revealed noticeable changes occurring over time. A discriminant analysis revealed that the scores based on the counts of pyknotic basal cells, basal vacuoles, and pyknotic stratum spinosum contained information sufficient to correctly classify cell death. Including all six scores resulted in the correct classification of only two additional slides. Hence the sum of these three scores was used as an appropriate morphological viability index, a decrease in viability being reflected as an increase in the index. The decline in viability was significantly different ($p<0.05$) between the first three and the last two pigs. The best line fit through the data from pigs 1-3 had a slope of 0.45 as compared with a slope of 0.40 from pigs 4 and 5 (data not plotted). This difference, although small, is supported by examination of the change in subjective rating across time for the two groups. The shift from 1 to 2 (normal to transition) occurred between 2 and 3 hr for group 1 and between 5 and 12 hr for group 2. Similarly, the shift from 2 to 3 (transition to necrotic) occurred between 12 and 24 hr in group 1 and between 18 and 24 hr for group 2. Obvious abnormal LM changes occurred at 12 hr, consisting of dark basal nuclei, pyknotic basal cells, basal vacuoles, dark stratum spinosum cells, pyknotic stratum spinosum cells, and stratum spinosum vacuoles. By 24 hr, some pyknosis and degenerative changes occurred within the epidermal cell layers. At 48 hr, the dermis was abnormal, being granular in appearance, and almost all the epidermal cells were pyknotic and epidermal-dermal separation occurred. TEM observations showed normal morphological integrity until 8 hr. At 8 hr, morphological alterations consisted of large single vacuoles, disruption of mitochondrial membranes, chromatin clumping with nucleolar segregation, and nucleolar pleomorphism occurring within the stratum basale ana stratum spinosum layers. At 12 hr (Figure 8), nuclear envelope separation, single vacuoles, separation of desmosomes, and de-generative organelles and debris were in the intercellular space, yet the stratum corneum remained
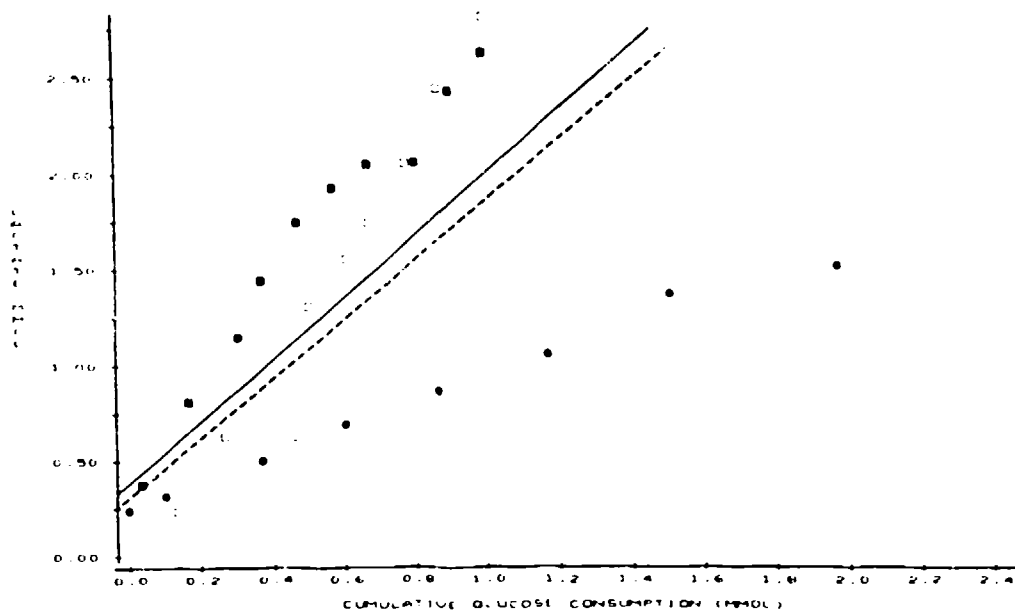
Figure 7. Plot of glucose consumption vs lactate production for four IPPSF's which form an envelope for the remaining 14 IPPSF's. The flap represented by closed squares had the maximum slope and the one represented by closed circles had the minimum slope of all flaps harvested 6 days after stage 1 surgery. The solid line has slope and intercept equal to the mean slope and intercept for 6-day IPPSF's. The 2-day harvests' maximum (open squares), minimum (open circles), and regression line (broken line) are similarly defined.

Figure 8. Electron micrograph of detached skin at 12 hr. Note
nuclear envelope separation and single vacuoles. X8,800.

intact. By 24 hr, classical pyknosis occurred with shrinkage of the nucleus and condensation of chromatin. Other changes associated with necrosis such as karyorrhexis, larger vacuoles, and at times lipid droplets near the mitochondrion were also observed.

In the <u>in situ</u> study, LM at day 0 after surgery demonstrated that the epidermis and dermis were normal. At day 1, edema was present in the superficial and deep dermis and chromatin clumping was seen. At day 2, edema was present in both superficial and papillary layers of the dermis and lymphatic vessels were dilated. Slight intracellular edema and chromatin clumping were present in the epidermal cell layers. Perivascular to diffuse eosinophilic mononuclear infiltrate occurred in the dermis. On day 3, similar changes were noted but dark stratum basale cells were also seen. Days 4, 5, and 6 were similar. By day 7, very slight intracellular edema of the epidermal cells was seen, perivascular and diffuse eosinophilic mononuclear infiltrates were present, but the superficial and deep dermis appeared normal.

From the morphometric analyses (Table 4), it is clear that the major difference attributable to the time between stage 1 and stage 2 surgeries is a thickened epidermal layer. By 7 days after stage I surgery, epidermal thickness had approximately doubled in both thin areas and at rete pegs, in addition to having greater variability over time, suggesting that the 2-day preparation may be more appropriate for percutaneous absorption studies. These data are also consistent with the hypertrophy seen in most 6-day IPPSF's. Ultrastructural observations at day 0 and day 1 were normal. On day 2, redistribution of nucleolar components into fibrillar and granular ribonucleoprotein filaments occurred. Several cells in mitosis were present in the stratum basale and spinosum layers. Some cells possessed a reticular nucleolonema with light granular and dense filamentous components and rounded pars amorpha areas or fibrous centers (Figure 9). On day 3, the ultrastructure of the nucleolus resembled that on day 2 but tended to have an increase in the dense filamentous component. On day 4, irregularities developed within the nucleolus, that is, the irregular shape, a compact appearance and nucleolar margination. On day 5, the nucleolus was enlarged and consisted of dense filamentous components. On day 6, nucleolar margination was prominent and nucleolus was very much enlarged. Several cells of the stratum basale and spinosum were characterized by a compact appearance without a developed nucleolonema and uniform distribution of structures containing RNA. Other nucleoli of some cells consisted of a dense fibrillar center with a periphery of granular components. On day 7, the nucleoli of both the stratum basale and stratum spinosum cells resembled that of day 6. No nucleolar caps, microsegregation, or macrosegregation was noted.

LM of the epidermis in IPPSF's terminated after 12 hr of perfusion demonstrated normal intact epidermis (Figure 10). To assess individual cellular morphology, TEM was also employed. Nucleolar pleomorphism was present in the stratum basale and

Table 4. Morphometric analyses of epidermal thickness[a,b] in situ skin flaps (n=3) at various times between stage 1 and stage 2 surgery

Day	Epidermis (um)	Rete Pegs (um)
0	37.1 ± 2.8	65.8 ± 16.9
1	43.5 ± 2.8	80.0 ± 13.0
2	68.1 ± 6.8	102.3 ± 4.4
3	82.9 ± 15.6	141.3 ± 12.0
4	67.4 ± 12.7	178.4 ± 13.8
5	96.4 ± 7.2	165.4 ± 11.8
6	86.2 ± 16.0	169.1 ± 23.5
7	68.1 ± 11.0	152.9 ± 38.3

[a]Mean ± SE in three in situ flaps.

[b]See Materials and Methods for a description of techniques used. Stratum corneum thickness did not vary and is not included in epidermal measurements reported here.
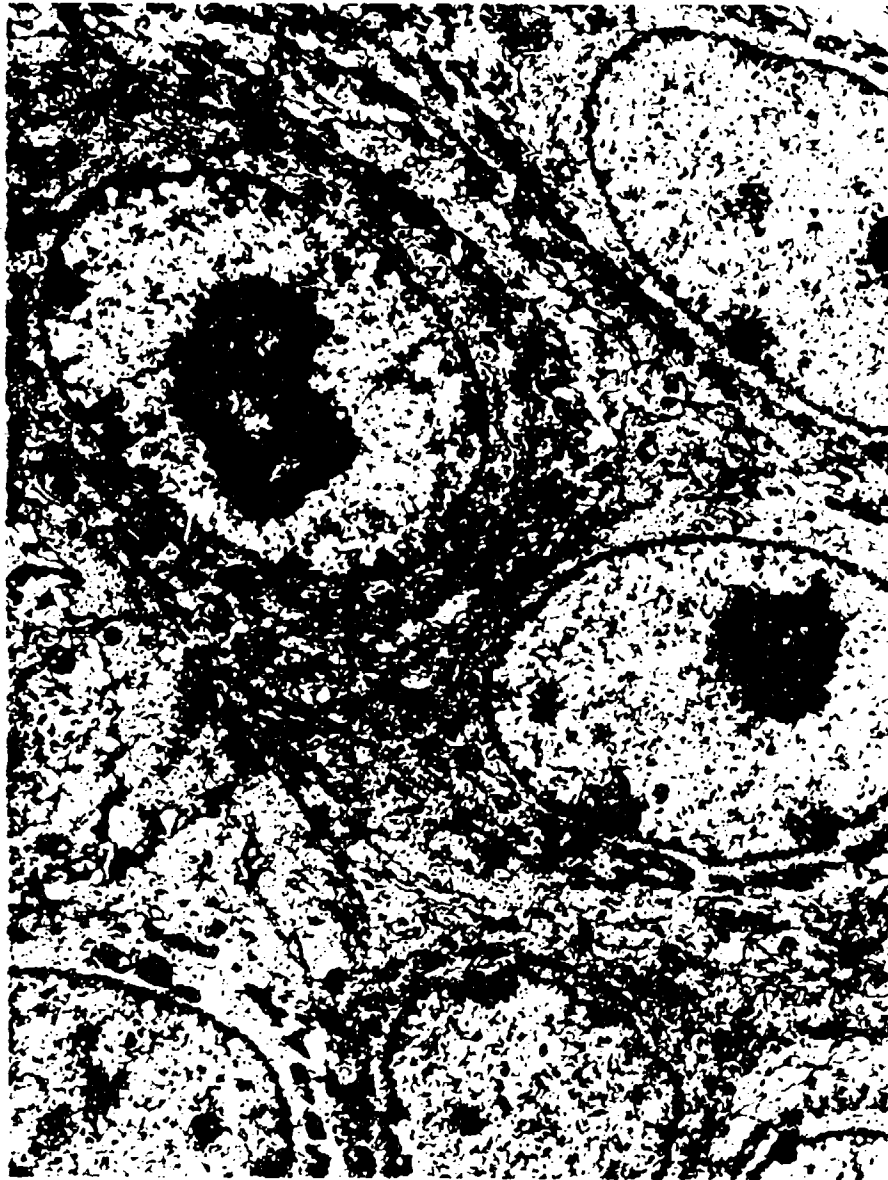
Figure 9. Electron micrograph of a 2-day _in situ_ flap after surgery.
Note the nuclear redistribution. X8,000.
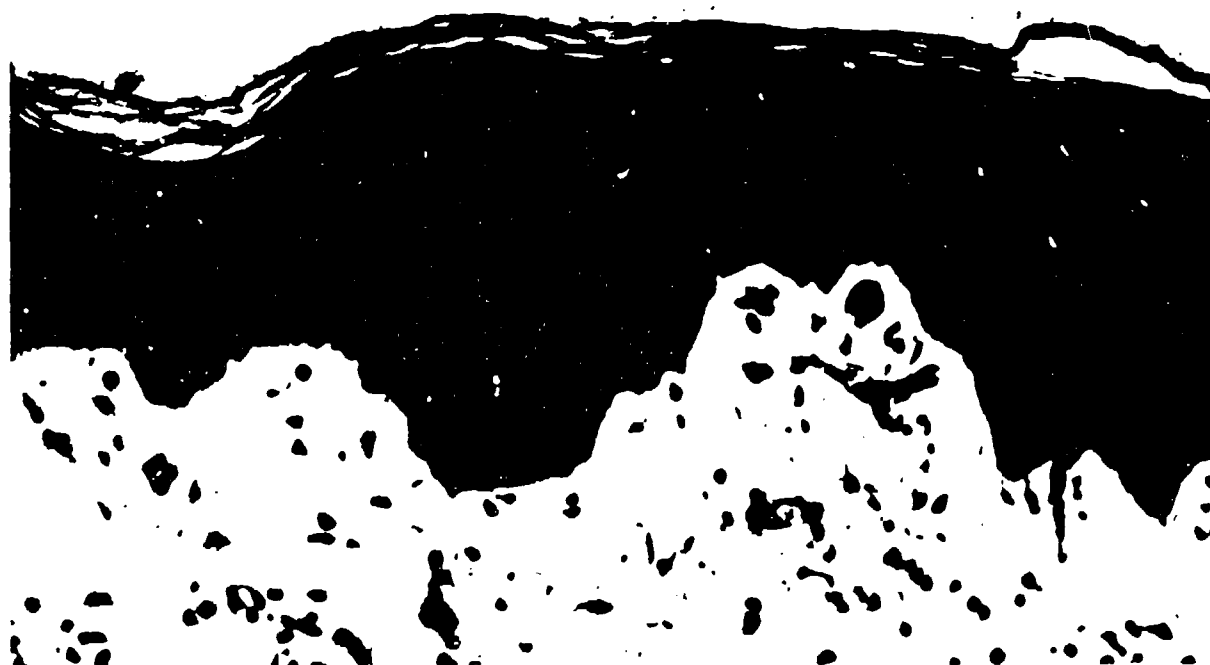
Figure 10.   Light micrograph showing viable epidermis and dermis in an
             IPPSF harvested 2 days after stage 2 surgery. H&E, X100.

spinosum layers (Figure 11). Some vacuolization was also observed, depending on the location of the sample on the IPPSF. However, degenerative changes such as those associated with cell death in the control study were not seen.

Finally, TEM on IPPSF's receiving NaF revealed normal epidermis except for the presence of large multiple vacuoles, often membrane-bound, and at times showed an amorphous substance in the stratum basale and spinosum layers (Figure 12). These changes seen in the NaF flaps should be considered acute toxic lesions rather than degenerative changes secondary to loss of viability.

In Vivo Percutaneous Absorption

Although hematocrits (PCV), measured in 15 randomly selected pigs, increased an average of 16% (initial PCV = 30.9 ± 0.5, terminal PCV = 36.0 ± 1.0), indicating a slight dehydration due to restricted water intake, this was not considered clinically significant and was independent of the route of administration. Other than a slight and transient erythema which occurred in the skin of all pigs given T topically, no toxicological or pharmacological reactions to the compounds used were noted and internal organs examined at necropsy all appeared normal.

The overall disposition of the radiolabel for the two routes of administration is shown in Tables 5 and 6. Total recoveries following the IV doses were high for B and C (near 90%), somewhat lower for the steroids (60-80%), and lowest for the more volatile organophosphates (50-60%). Since fat residues were not measured, the lower recoveries of steroids may be due to storage in body fat. In addition, it is impractical to collect expired air in pigs, which may account for the failure to retrieve a larger fraction of the injected organophosphates. As can be seen in Table 5, carcass totals, obtained by summing the individual organs assayed, were negligible for all but the organophosphates. Individual organ levels were near the lower limits of detection in most cases, although small amounts of C were found in the liver (0.3%), P in the skin (0.7%), and R in the lungs (0.2%). Significant residues of M were found in all organs assayed, particularly the skeletal muscle which contained over 11% of the injected M. For the nonsteroidal compounds, urinary excretion was much greater than fecal excretion, averaging over 80% of the total amounts excreted during the 6 day collection period. On the other hand, 25-70% of the total steroid excretion occurred by the fecal route.

For the topical route of administration, a different pattern emerged. As expected, most (50-95%) of the recovered radiolabel was found in the patch surrounding the application site and in the skin sample comprising the site itself. A small percentage of the dose was occasionally found in the skin surrounding this site. As demonstrated in the low carcass totals, individual organs retained levels which were barely detectable for any of the compounds. Although urinary excretion again predominated for
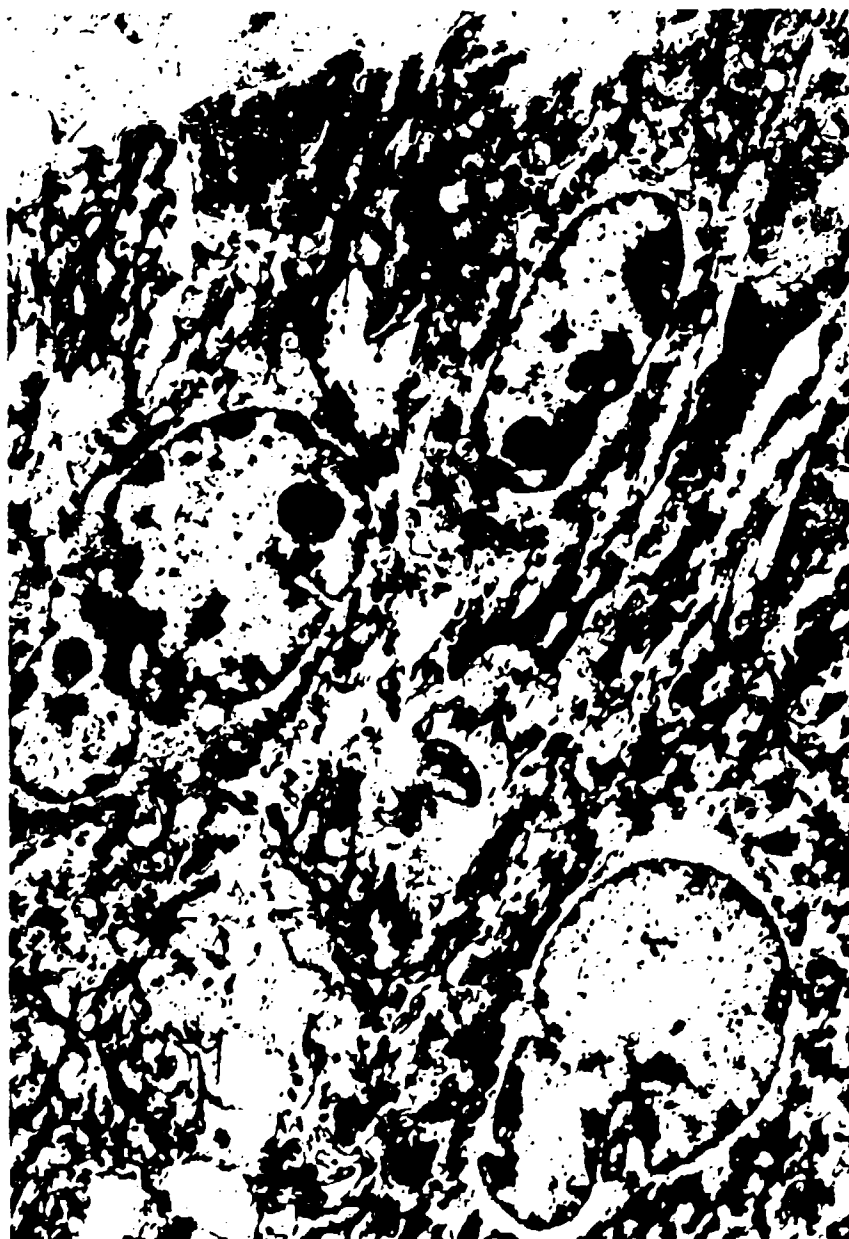
Figure 11. Transmission electron micrograph of a viable IPPSF after 12 hr
            of isolated perfusion. Note the nucleolar pleomorphism in the
            stratum basale layer. X5,400.
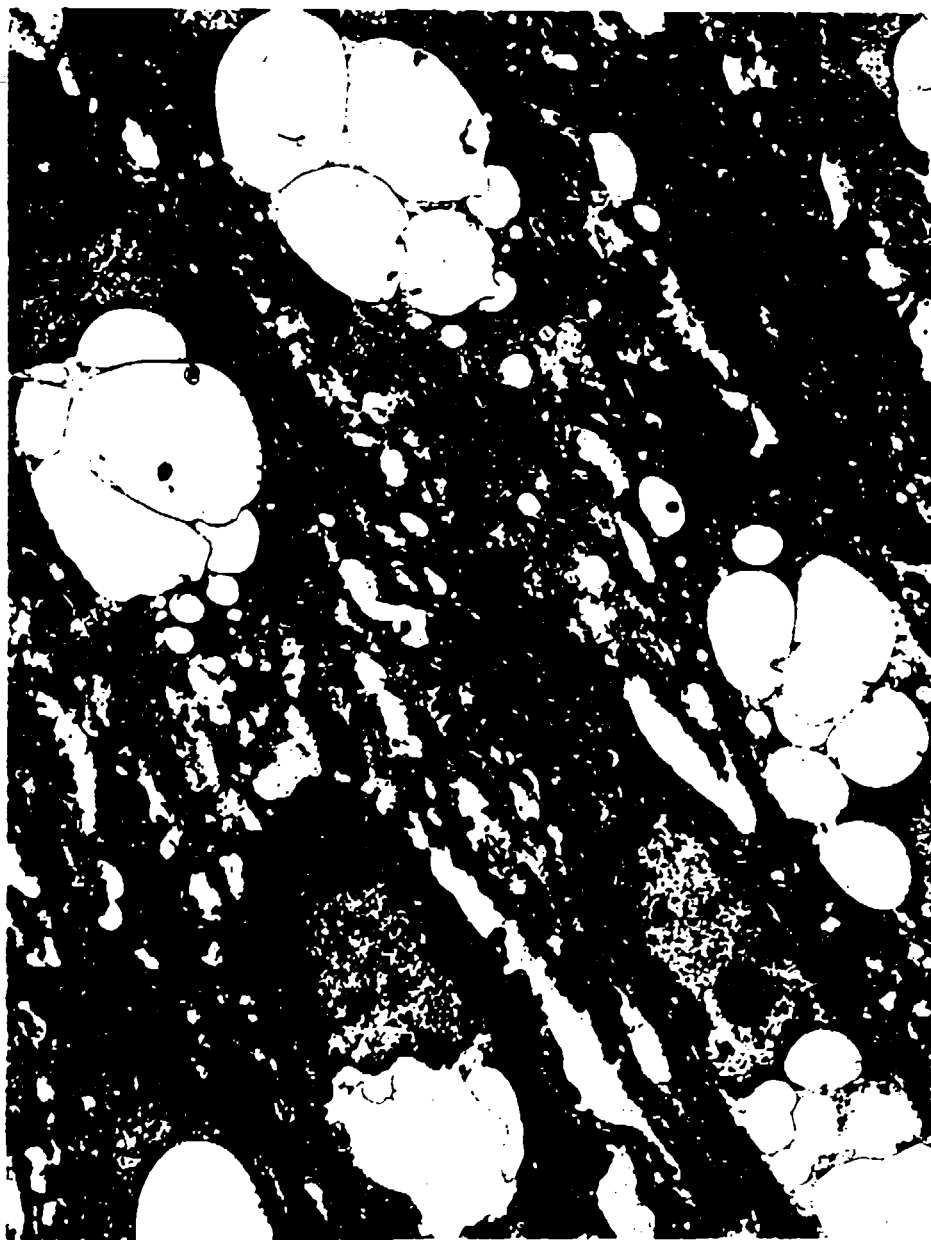
Figure 12.   Electron micrograph of an IPPSF administered sodium fluoride. Note the multiple vacuoles. X4,800.

Table 5. Radiolabel recovery (% dose) following IV administration of ^{14}C-labeled compounds to pigs[a,b]

Compound	Urine	Feces	Carcass	Total Recovery
B	84.5 ± 9.0	4.6 ± 1.2	0.1 ± 0.05	89.3 ± 9.3
C	68.2 ± 2.9	16.6 ± 4.1	1.5 ± 0.5	86.3 ± 3.2
D	44.3 ± 1.7	5.7 ± 0.9	7.6 ± 3.6	57.6 ± 4.9
M[c]	32.2 ± 3.3	4.9 ± 0.7	13.1 ± 2.7	50.2 ± 3.5
P	57.8 ± 2.3	2.0 ± 0.4	1.2 ± 0.6	61.1 ± 2.0
R	22.1 ± 4.0	40.0 ± 4.2	0.6 ± 0.1	62.7 ± 4.4
T	54.4 ± 3.6	21.2 ± 2.7	0.7 ± 0.3	76.3 ± 2.4
A	28.4 ± 8.9	53.2 ± 7.5	1.0 ± 0.3	82.6 ± 16.3

[a]Total dose = 200 μg, 10 μCi/pig (n=4).

[b]Mean ± SE.

[c]N=3.

Table 6. Radiolabel recovery (% dose) following topical administration of ^{14}C-labeled compounds to pigs[a,b]

Compound	Urine	Feces	Carcass	Patch	Dosed Skin	Patch Skin[c]	Total Recovery
B[d]	20.0 ± 2.3	2.9 ±0.3	0.8 ± 0.4	40.2 ± 0.3	12.2 ± 1.0	9.1 ± 2.1	85.4 ± 4.2
C	5.8 ± 0.4	4.2 ±1.0	2.7 ±1.0	75.3 ± 4.9	2.8 ± 0.8	1.9 ± 0.2	92.7 ± 3.3
D	0.3 ± 0.1	0.2 ±0.1	0.1 ±0.1	9.7 ± 2.5	0.5 ± 0.1	0.5 ± 0.1	11.3 ± 5.0
M[d]	1.7 ± 0.3	0.2 ±0.1	0 0	86.2 ± 7.6	2.1 ± 0.1	2.0 ± 1.2	92.2 ± 8.6
P	3.1 ± 0.6	0.9 ±0.2	1.3 ±1.0	77.2 ± 1.8	0.6 ±0.1	0.6 ± 0.3	83.6 ± 1.2
R[d]	2.6 ± 0.6	7.4 ±1.3	0.3 ±0.1	58.2 ± 0.8	8.6 ± 1.0	7.2 ± 0.2	94.5 ± 11.9
T	3.8 ± 1.7	2.8 ±0.8	0.7 ±0.2	81.2 ± 9.0	17.6 ± 4.9	4.7 ± 1.7	111.0 ± 4.5
A	0.3 ± 0.05	0.6 ±0.2	1.6 ±0.5	47.0 ± 4.7	14.1 ± 0.2	20.2 ± 2.2	83.8 ± 2.6

[a]Total dose = 200 μg, 10 μCi/pig (n=4).

[b]Mean ± SE.

[c]Skin taken from area immediately adjacent to dosed site out to patch boundaries.

[d]N=3.

all except the steroids, fecal clearance represented a greater fraction of total elimination in most pigs by the topical route of administration.

This latter finding is illustrated in Figure 13, in which the fecal clearances, expressed as a percentage of total for each route, are compared. As can be seen, for four out of six compounds studied (B, C, P, and T), the fraction of total radiolabel excreted by the fecal route was greater after topical administration than by IV dosage (p<0.05). Only M, for which the fecal clearance declined slightly following topical application, had almost identical elimination patterns for both routes. The rank order of corrected skin absorption was as follows: B (25.7%) > R (16.2%) > C (11.8%) > T (8.8%) > P (6.7%) > M (5.2%). With the exception of the reversal of C and R, the rank order can also be approximately expressed in terms of the classes as: well absorbed organic acid/base compounds > steroid hormones > organophosphate insecticides.

The calculated excretion rates are presented in Table 7. As expected, these rates were generally greater following IV administration, with statistically significant differences (P<0.05) seen for four out of the six compounds. Elimination half-lives $(T_{1/2})$, calculated using the mean elimination rates in Table 3, ranged from 15-20 hr following IV administration. The bulk of the radiolabel appeared in the urine and feces during the first 24 hr after dosing, with the highest rates during the first collection interval (0-6 hr, urine alone) for all compounds. IV elimination was generally biphasic, as exemplified by B, with a rapid elimination during the first day $(T_{1/2}=2.5$ hr) and a much slower rate over the next 5 days $(T_{1/2}=19.6$ hr). Pharmacokinetic parameters calculated from the blood data from a single pig are in agreement, with Cl = 7.35 ml/min/kg, Vss = 0.373 L/kg, Vc = 0.329 L/kg, and $T_{1/2}$ = 2.43 hr. The corresponding values for the serum available from one pig given M by the same route are: Cl = 0.90 ml/min/kg, Vss = 2.60 L/kg, Vc = 0.309 L/kg, and $T_{1/2}$ = 41.35 hr. Whereas B distributes almost entirely within the central compartment, M has a much greater apparent volume of distribution, which may be the reason for the difference in tissue residues seen in Table 1. Biphasic elimination patterns were not seen in the sigma-minus plots of topical excretion data, indicating that the elimination rates are masked kinetically by the much slower absorption rate processes. The period of peak absorption occurred during the second collection interval (6-24 hr) for all compounds except R (48-72 hr), and $T_{1/2}$ values ranged from 18-35 hr.

Finally, because the finding of an altered excretion profile has a potential impact on the interpretation of percutaneous absorption estimates derived from excretion methodology, a comparison of estimates using urine alone with those obtained from combined excrement is shown in Figure 14. Although the difference in percutaneous absorption totals given by the two methods is only statistically significant for C (p<0.05), the small number of pigs used for each route and compound and the

Figure 13. Comparison of fractional fecal excretion after IV (unfilled bars) and topical (hatched bars) administration. Error bars represent 1 SE and the asterisks denote significant differences between routes (p<0.05).
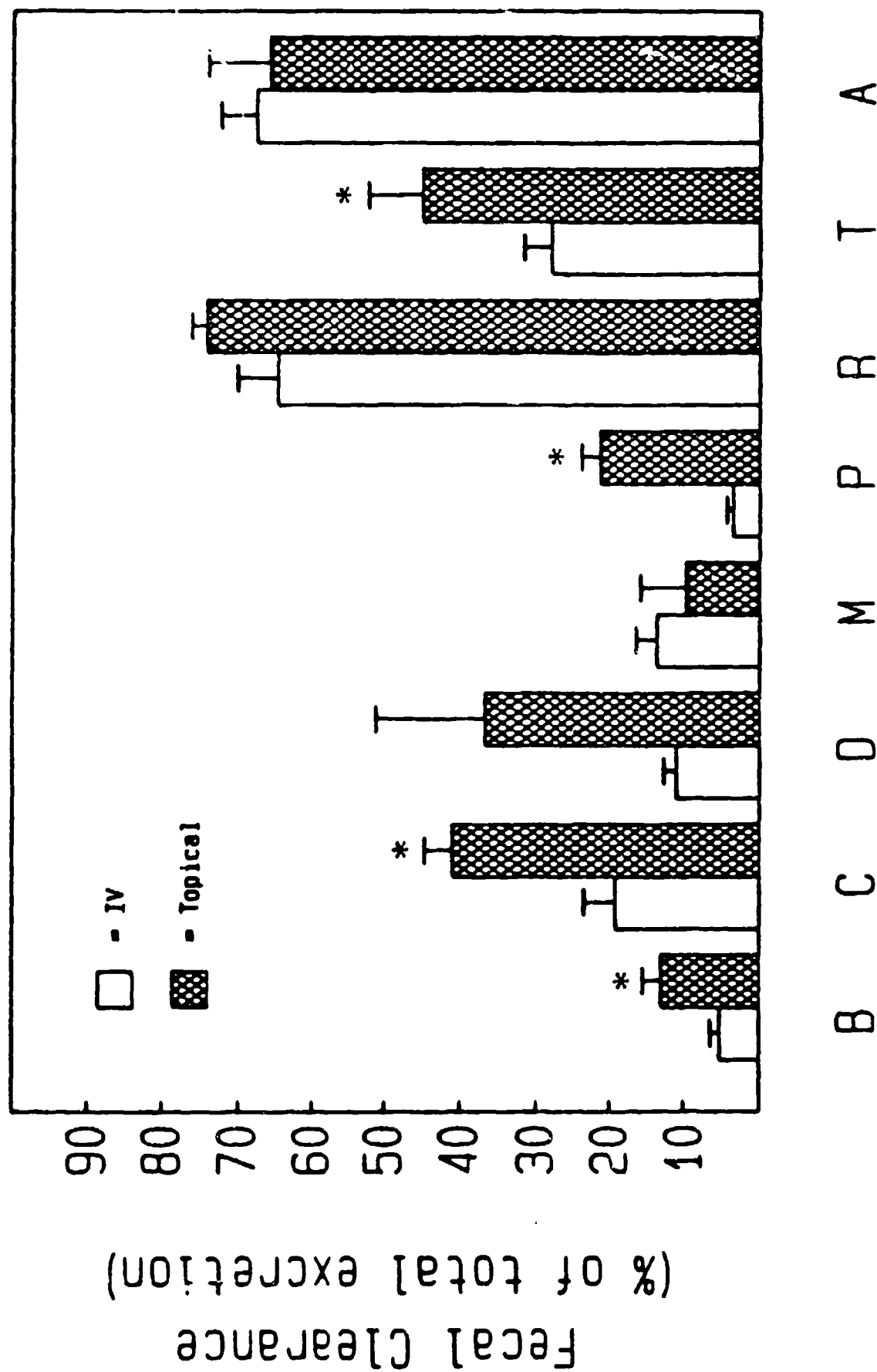
Table 7. Elimination rates (K) and half-lives ($T_{1/2}$) obtained from total radiolabel excretion after IV and topical administration[a,b]

Compound	IV		Topical	
	K	$T_{1/2}$	K	$T_{1/2}$
B	0.0354 ±0.0048 (4)	19.6	0.0289 ±0.0024 (3)	24.0
C	0.0467 ±0.0035 (4)	14.8	0.0240[c] ±0.0015 (4)	28.9
D	0.0363 ±0.0032 (4)	19.1	0.0295[c] ±0.0014 (4)	23.5
M	0.0377 ±0.0017 (3)	18.4	0.0381 ±0.0082 (3)	18.2
P	0.0386 ±0.0032 (4)	18.0	0.0276[c] ±0.0029 (4)	25.1
R	0.0368 ±0.0013 (4)	18.8	0.0200[c] ±0.0003 (3)	34.7
T	0.0414 ±0.0061 (4)	16.7	0.0223[c] ±0.0024 (4)	31.1
A	0.0420 ±0.0032 (4)	16.5	0.0206[c] ±0.0053 (4)	33.6

[a]Total dose for both routes = 200 µg, 10 µCi.

[b]Mean ± SE (n).

[c]Significantly lower than IV K ($p < 0.05$).

Figure 14. Corrected percutaneous absorption estimates calculated by two different methods: using urinary excretion alone (unfilled bars) or using both urine and fecal excretion (hatched bars). Error bars represent 1 SE and an asterisk denotes significant differences between the two methods (p<0.05).
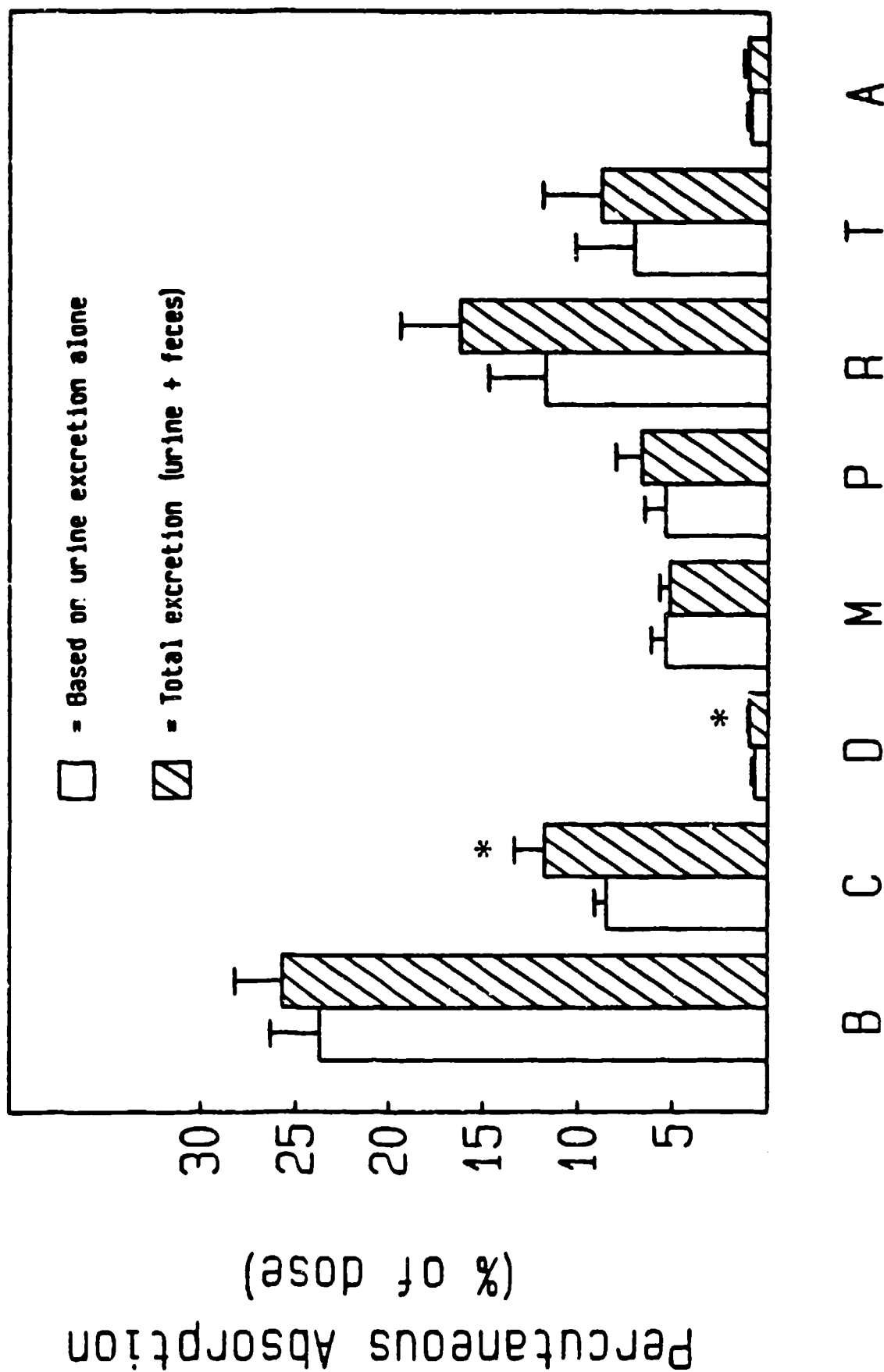
relatively high variability in the data obscure the overall significance of this finding. In the present study, percutaneous absorption totals obtained using urinary excretion alone underestimated the "true" value, assuming clearance by routes other than urine and feces is negligible, by approximately 8-30%.

IPPSF Percutaneous Absorption Studies

Glucose utilizations measured hourly were used exclusively to assess viability in the dosed IPPSF's and are shown in Table 8. These are in good agreement with the earlier validity studies in Table 3. Values for this viability index were well within normal ranges for all flaps to which chemicals were applied topically. There was a slight tendency for glucose utilization to increase during the 8-hr time frame of these experiments (p<0.05), but there was no evidence that any of the compounds affected viability while penetrating into the perfusate (post-vs pre-dosing comparisons). The initial weight of all IPPSF's was 27.4 $\pm$ 0.5 g (n=67), increasing by approximately 37% in viable skin flaps and over 48% in nonviable flaps (p<0.05). Perfusate flow rates were comparable across compounds, averaging about 2.5 ml/min, and were also typically somewhat higher at the end of the experiments. The only significant correlation between penetration rate and flow occurred for C (p<0.005). In some of the flaps dosed with C, flow increased by over 100%, primarily during the last few hours of the experiment. Because flow increased only in the flaps with the greatest C penetration rates, this increase was not reflected in the comparison of post-vs predosing flow seen in Table 8 (p>0.05). However, the difference between these two mean flows was 40% which was by far the largest increase observed.

Radiolabel recoveries are shown in Table 9. As with _in vivo_ studies in whole pigs, much of the [^{14}C] was found in the patch, along with a large fraction in the application site and smaller amounts in the skin immediately beneath the patch. Total recoveries were also similar, except for C and R, which were recovered better _in vivo_ (see Table 6). Differences may be due to irreversible binding of these compounds to the patch placed on the IPPSF, since patches were not made of the same materials _in vivo_ (foam rubber). The application site was not contacted _in vivo_ either, in contrast to the situation _in vitro_.

Total absorption _in vitro_ was calculated from the area under the absorption rate-time curve (AUC), using the trapezoidal method, from 0-8 hr for each compound. As can be seen in Table 9, most compounds penetrated into the perfusate to a similar extent during this period of time, except for B, which was very rapidly absorbed, and A, which was absorbed very poorly, if at all. Total flux across nonviable IPPSF's which were dosed (n=7) was almost undetectable, averaging 0.011 $\pm$ 0.004%. Absorption rate profiles for each compound are seen in Figures 15-17. The relative humidity at which the experiments were conducted ranged from 60-80% and did not vary by compound. Reliable hygrometer readings were limited, but there appeared to be a tendency for AUC to

Table 8. IPPSF biochemical parameters[a] before and after dosing with topically applied xenobiotics

| Compound | Before dosing | | After dosing | |
	Glucose Utilization (mg/g/hr)	Flow (ml/min)	Glucose Utilization (mg/g/hr)	Flow (ml/min)
B(6)[b]	0.76 ± 0.14	3.16 ± 0.23	0.89 ± 0.13	3.29 ± 0.24
C(7)	0.61 ± 0.06	1.73 ± 0.31	0.92 ± 0.15	2.42 ± 0.52
D(4)	0.64 ± 0.11	2.42 ± 0.11	0.46 ± 0.05	2.39 ± 0.13
M(5)	0.81 ± 0.03	2.49 ± 0.61	0.81 ± 0.07	3.12 ± 0.62
P(3)	0.40 ± 0.10	2.65 ± 0.15	0.58 ± 0.14	2.80 ± 0.24
R(6)	0.82 ± 0.14	2.27 ± 0.22	0.70 ± 0.10	2.37 ± 0.16
T(4)	0.58 ± 0.09	2.65 ± 0.16	0.67 ± 0.20	3.07 ± 0.34
A(5)	0.80 ± 0.04	1.65 ± 0.09	1.27 ± 0.13[c]	2.17 ± 0.20[c]
All viable IPPSF's (40)	0.70 ± 0.04	2.35 ± 0.13	0.82 ± 0.05[d]	2.70 ± 0.14[d]
Nonviable IPPSF's (9)	0.20 ± 0.04	2.54 ± 0.24		

[a]Mean ± SE.

[b]Number of skin flaps.

[c]Significantly diffferent from predosing value using the two-sided Student's t-statistic ($p < 0.05$).

[d]Significantly greater than predosing value ($p < 0.05$).

Table 9. Radiolabel recovery (% dose) after topical administration of ^{14}C-labeled compounds to the IPPSF[a,b]

Compound	Total Flux	Dosed Skin	Patch Skin[c]	Other Tissues[d]	Patch	Bedding	Total Recovery
B(6)[e]	29.9 ± 9.2	4.3 ± 1.2	2.9 ±1.0	2.8 ±0.5	41.6 ± 7.5	1.4 ± 1.0	83.0 ± 2.3
C(7)	4.3 ± 1.2	39.4 ± 5.5	3.5 ±0.8	4.4 ±2.7	25.0 ± 7.2	0.9 ± 0.5	77.6 ± 3.4
D(4)	5.3 ± 1.8	0.3 ± 0.1	0.6 ±0.2	0.9 ±0.1	2.8 ± 0.7	1.0 ± 0.3	10.9 ± 2.2
M(5)	2.6 ± 0.6	33.4 ± 3.8	6.3 ±2.8	5.8 ±4.7	43.9 ± 7.2	1.2 ± 1.2	93.4 ± 6.4
P(3)	5.2 ± 0.4	33.9 ± 5.6	3.0 ±1.1	5.2 ±0.7	35.6 ± 8.8	11.2 ±10.9	94.6 ± 5.9
R(6)	2.9 ± 0.7	34.4 ± 2.4	8.0 ±1.9	2.6 ±0.3	19.2 ± 1.6	0.9 ± 0.7	67.5 ± 3.0
T(4)	3.8 ± 1.5	30.0 ± 8.4	7.3 ±4.1	1.8 ±0.4	33.8 ± 2.3	13.9 ±13.2	90.8 ± 9.5
A(3)	0.05 ± 0.01	59.3 ± 8.0	5.5 ±2.2	4.0 ±2.1	14.5 ± 6.6	0.1 ± 0.1	83.6 ± 5.2

[a]Total dose = 200 μg; 10 μCi applied to 5 cm^2 (dosed skin).

[b]Mean ± SE.

[c]Skin taken from area immediately adjacent to dosed site out to patch boundaries.

[d]Transverse section through flap remainder which includes subcutaneous fat, vasculature, and fibrous and muscular tissue.

[e]Number of skin flaps.
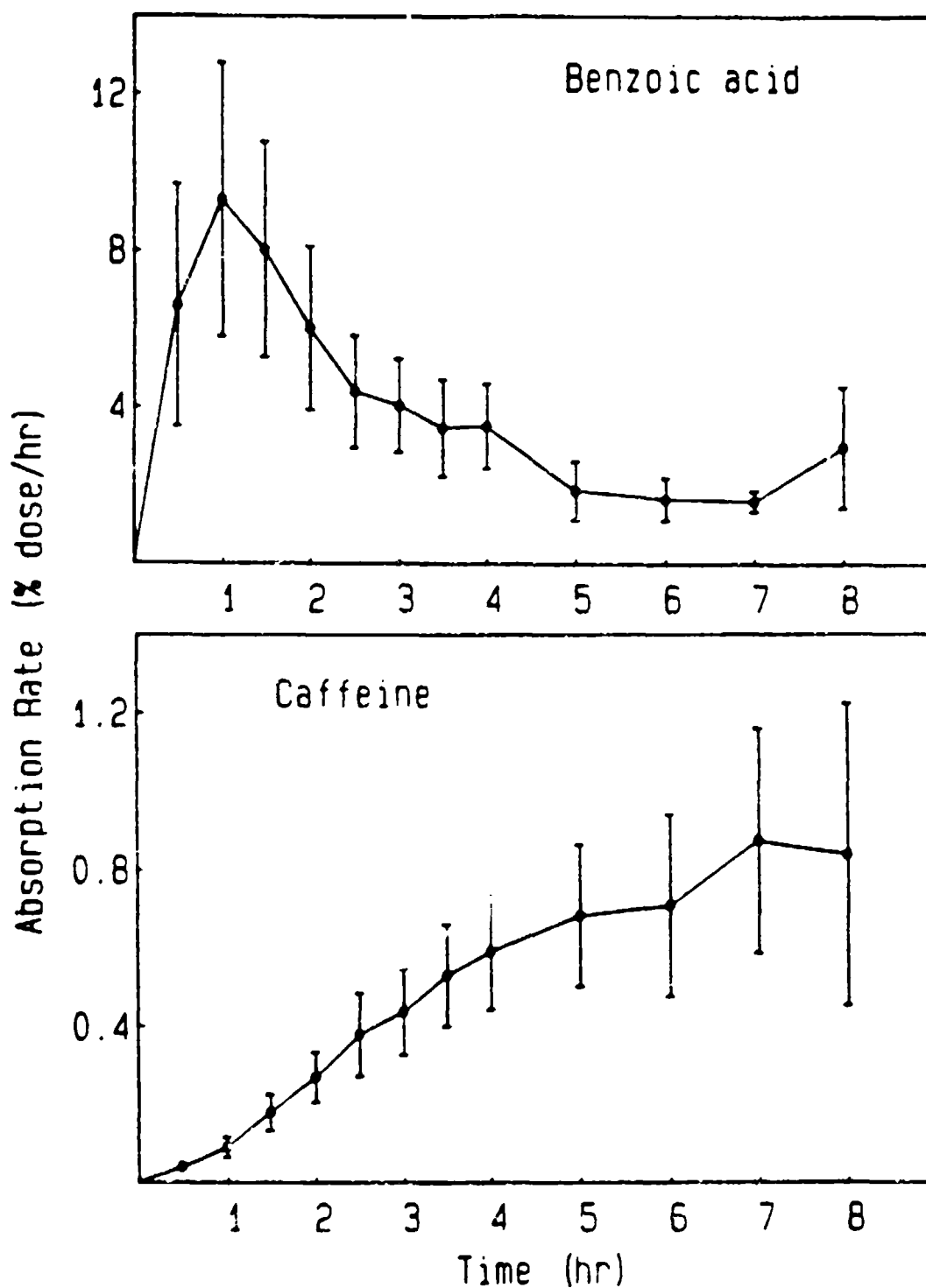
Figure 15. Absorption rate-time curves of benzoic acid (B) and caffeine (C) in the IPPSF. Each point is the mean of six (B) or seven (C) separate experiments and the bars represent ±1 SE.

Figure 16. Absorption rate-time curves of the organophosphates DFP (D),
malathion (M), and parathion (P) in the IPPSF. Each point
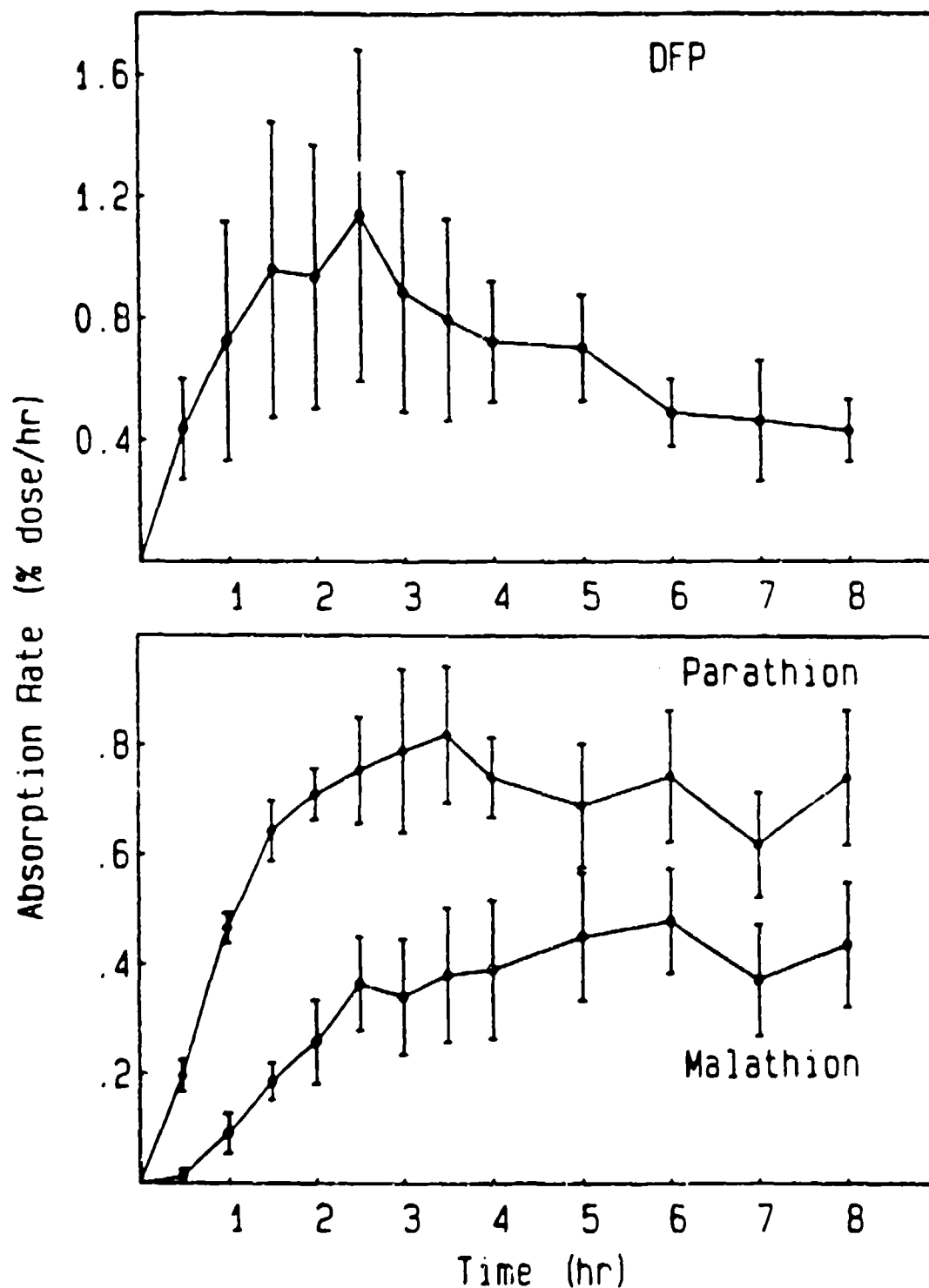is the mean of four (D), five (M), or three (P) separate
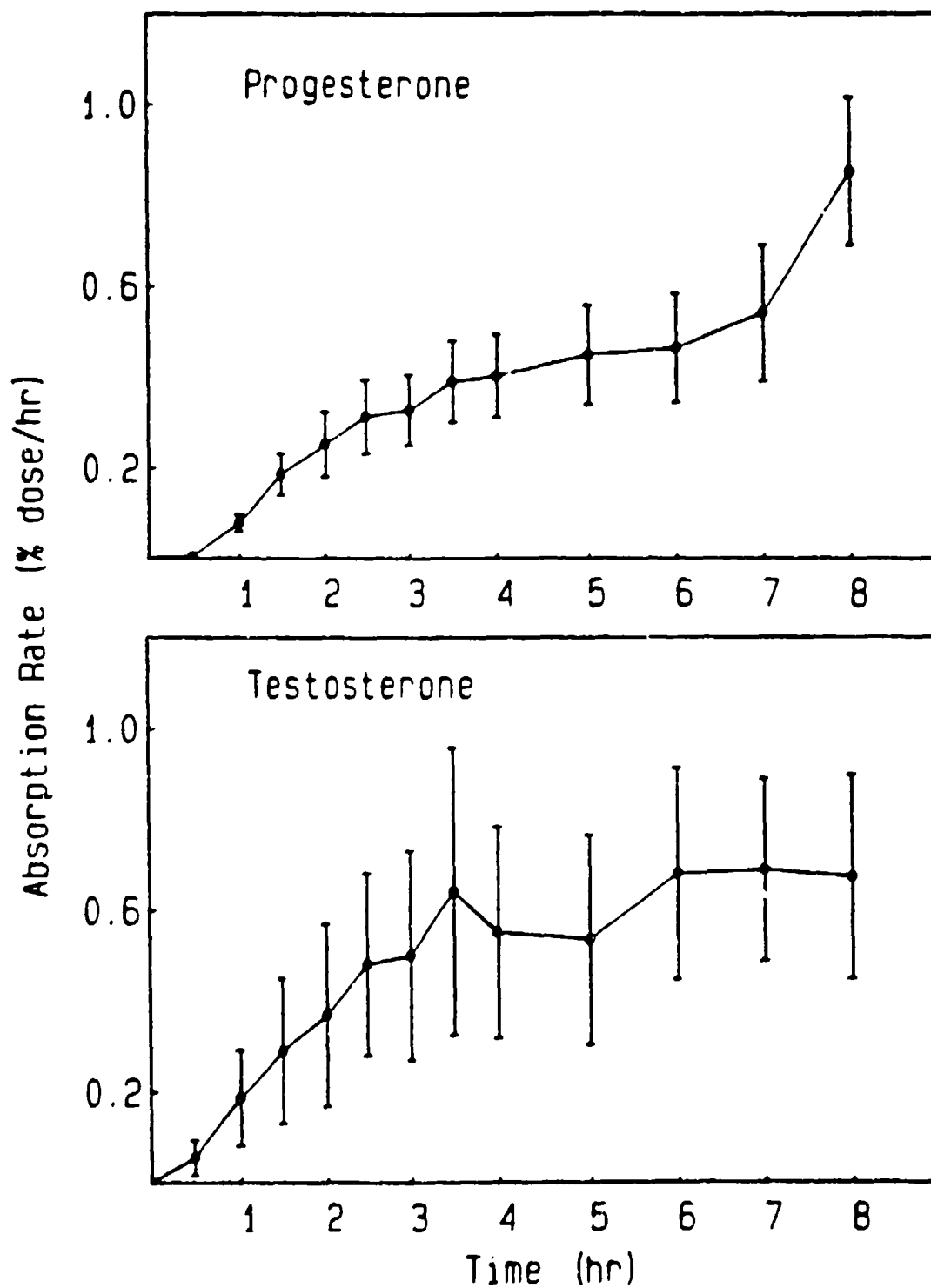experiments. Bars = ±1 SE.

Figure 17. Absorption rate-time curves of steroid hormones progesterone (R) and testosterone (T) in the IPPSF. Each point is the mean of six (R) or four (T) separate experiments and the bars = ±1 SE.

correlate with %RH (p<0.07,n=4 for C; p<0.08, n=4 for B). No correlations between AUC or peak flux and flow were found, probably because flow was kept as constant as possible for all absorption experiments. Similarly, AUC and glucose utilization were not related for viable IPPSF's, however, as mentioned earlier, nonviable skin flaps were not permeable by topical agents.

The absorption rate of B applied to one IPPSF perfused with porcine plasma, instead of the artificially formulated perfusate used for all other experiments, is seen in Figure 18. Although the shape of this curve was comparable to the other B flaps (Figure 15), total flux (AUC) in this IPPSF was 60.7% of dose or about twice as great as the mean B absorption reported in Table 9. Moreover, glucose utilization and flow were normal in this IPPSF, but there was less weight gain during the 10-hr perfusion period (23% vs 37%). B absorption was also evaluated (Figure 19) in two skin flaps that were dosed and sampled entirely _in situ_; i.e., stage 2 surgery (harvest) was not performed. All blood perfusing this skin flap was collected via a catheter placed into one of the paired venae comitantes, while the other vein was permanently clamped. A total of approximately 0.5 L of blood was removed from each pig during the 4 to 4.5-hr course of these experiments, an amount which decreased the PCV by only 10%. Cutaneous blood flow generally averaged between 1.5 and 3 ml/min, similar to the perfusate flows in the IPPSF; however _in situ_ flow was much more variable. Normal blood flow was occasionally interrupted by long periods (20 min or more) of complete cessation of flow. As can be seen in Figure 19, not only was B absorption lower _in situ_, at about 5% and 10% of dose when extrapolated to 8 hr, the rate profile had an entirely different shape and there was more variability between skin flaps. Finally, typical absorption rate profiles in nonviable IPPSF's are shown in Figure 20. These rates were clustered very tightly around 0 and the curves had no predictable shape noted earlier with viable skin flaps.

Due to the difficulties inherent in comparing _in vivo_ with _in vitro_ (IPPSF) percutaneous absorption rates and total fluxes, a pharmacokinetic model based on _in vitro_ rates was constructed using data from seven of the compounds tested. Triamcinolone acetonide was not modeled since these rates were determined from radioactivity levels in the perfusate that were not significantly above background levels, thus these data were considered unreliable. The simplified model developed to describe the absorption profiles for all seven compounds contained four compartments (Figure 21) which were designated: C1 = skin surface, C2 = s.c. + viable epidermis, and C3 = perfusate. C4 is equivalent to systemic circulation and includes all disposition processes which would normally occur after IV injection. Since these rate processes cannot be estimated directly from IPPSF absorption rates, k34 was set equal to 1 in all cases, corresponding to complete washout of C3 during each sampling interval. Thus, C4 was considered to be an infinite sink for all practical purposes. This is a valid approach since arterial
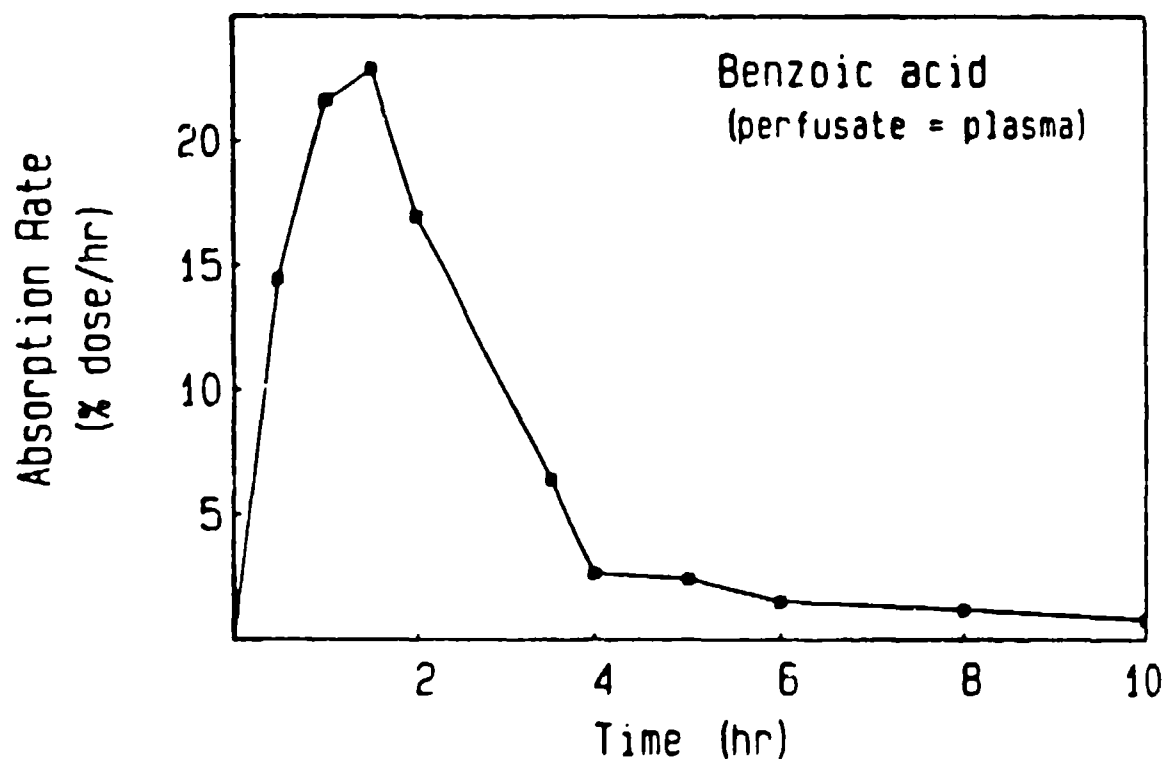
Figure 18. Benzoic acid absorption in a single IPPSF perfused with porcine plasma.
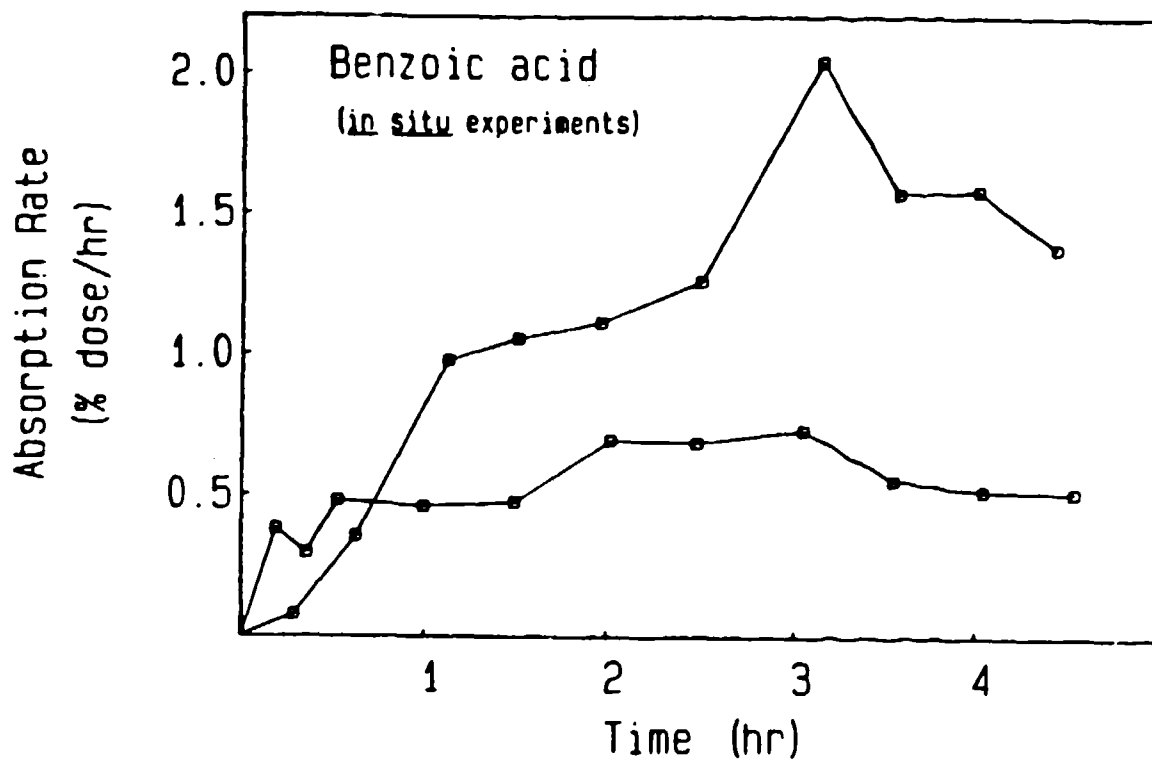
Figure 19. Benzoic acid absorption determined from whole blood collection
after in situ application to the IPPSF. Note the difference in
rates and shapes of these profiles contrasted with those in
Figures 15 and 18.
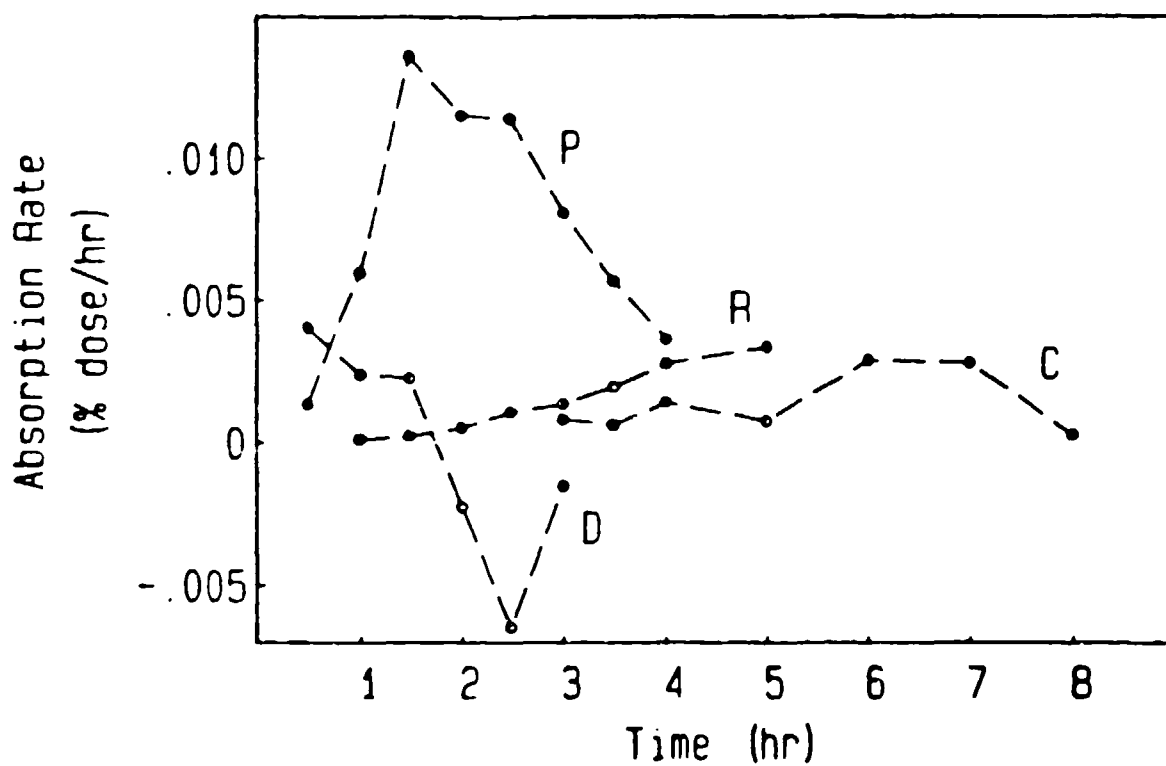
Figure 20. Absorption rate-time curves of several compounds (see text for abbreviations) in nonviable IPPSF's.
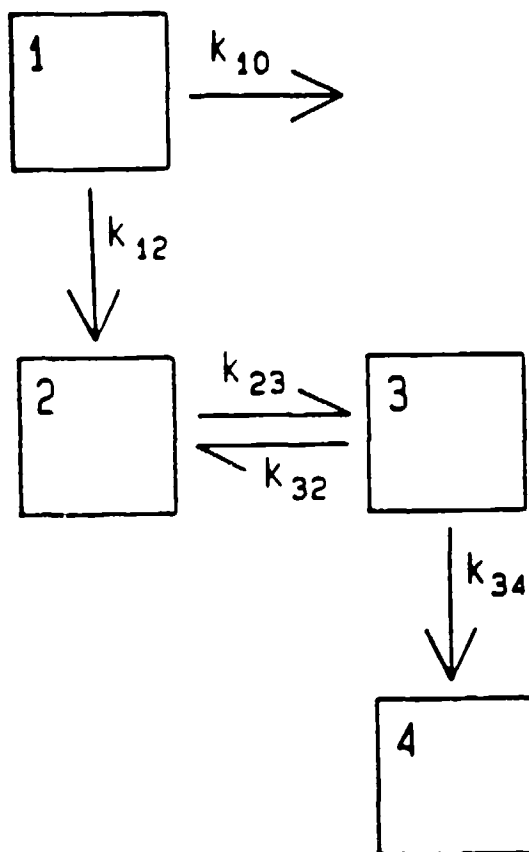
Figure 21. Compartmental model used to describe the pharmacokinetics of percutaneous absorption in the IPPSF. The compartments, rate constants, and their relation to physiological spaces are discussed in the text.

concentrations were subtracted from the venous effluent concentrations when calculating the absorption rates used in this rranalysis. The rate constant $k10$ was used to describe the sum of all rates for processes which permanently restrict dermal penetration, including surface evaporation and adsorption with irreversible binding to both skin components and the patch surrounding the application site. C0 is therefore designated to be the unavailable compartment.

Differential equations describing the model can be written as follows:

$$dA_0/dt = k_{10}A_1 \qquad (1)$$

$$dA_1/dt = -(k_{10} + k_{12})A_1 \qquad (2)$$

$$dA_2/dt = k_{12}A_1 - k_{23}A_2 + k_{32}A_3 \qquad (3)$$

$$dA_3/dt = k_{23}A_2 - (k_{32} + k_{34})A_3 \qquad (4)$$

where A_i = fraction of dose in the i-th compartment, dA_i/dt is the rate of change of this amount with time, and the rate constants (k's) are expressed in reciprocal time units (1/min or 1/hr). Taking the Laplace transform of each equation and solving for A_i gives:

$$A_1 = 1/(s + k_{10} + k_{12}) \qquad (5)$$

$$A_2 = (k_{12}A_1 + k_{32}A_3)/(s + k_{23}) \qquad (6)$$

$$A_3 = k_{23}A_2/(s + k_{32} + k_{34}) \qquad (7)$$

Inserting equations 5 and 6 into equation 7 and rearranging gives the transform for the compartment of interest (C3 = perfusate):

$$A_3 = (k_{12}k_{23})/\{[s^2 + (k_{32} + k_{34} + k_{23})s + k_{23}k_{34}][s + k_{10} + k_{12}]\} \qquad (8)$$

The quadratic equation in the denominator can be solved by substituting and for the roots:

$$A_3 = k_{12}k_{23}/(s + \;)(s + \;)(s + k_{10} + k_{12}) \qquad (9)$$

Finally, expansion of the denominator to partial fractions and inversion to the time domain yield the final, unique solution for C3:

$$A_3 = (k_{12}k_{23}) \cdot \frac{e^{-(k10+k12)t}}{(k_{10}+k_{12}-)(k_{10}+k_{12}-)} + \frac{e^{-t}}{(-k_{10}-k_{12})(-)} +$$

$$\frac{e^{-t}}{(-k_{1(}-k_{12})(-)} \qquad (10)$$

Figures 22-24 show the rate-time curves generated by equation 10, along with the measured absorption rates (data points) from the IPPSF experiments for each compound. In general, the three-compartment model accurately predicted the experimentally determined absorption profiles, from 0-8 hr after dosing. In addition, extrapolation of the model prediction to 24 hr for M and P (bottom half of Figure 23) agreed quite closely with the observed absorption rates from 17-24 hr, obtained from the flaps dosed _in situ_ 17 hr prior to perfusion. For two compounds, B and C (Figure 22), the model predictions deviated somewhat from the measured rates. The fit for C was improved considerably by allowing the normally "fixed" rate constant (k34) to vary as a function of perfusate flow. Two "black-box" shunts, each containing multiple subcompartments, were used to simulate mass transfer via unknown but saturable processes for B, in order to model the prominent deviations from curvilinearity (humps in the rate-time curves) seen in Figures 15 and 18.

All estimates of the rate constants and variables in equation 10 were generated using the CONSAM computer program. The relevant rate constants are listed in Table 10, which also shows the bioavailability (F) of each compound in the IPPSF, calculated from:

$$F_{IPPSF} = k_{12}/(k_{10} + k_{12}) \qquad (11)$$

Equation 11 can be derived directly from the differential equation describing the amount of compound leaving C1 (penetrating through s.c., equation 2), combined with rate of delivery to the unavailable compartment (C0, equation 1). This estimate of _in vitro_ F represents the AUC of the absorption rate-time curve, extrapolated to infinity. Comparison of the F value obtained for each compound in the IPPSF with absorption totals _in vivo_, which are the best experimental estimates of topical bioavailability for any compound, demonstrated a poor correlation ($R = 0.498$, $p > 0.1$). However, removing the two compounds for which the unmodified model did not accurately predict absorption in the IPPSF (B and C), resulted in the following, statistically significant ($R = 0.944$, $p < .02$) relationship between _in vivo_ and _in vitro_ percutaneous absorption:

$$F_{IPPSF} = 1.92 \, F_{in \ vivo} + 0.03 \qquad (12)$$
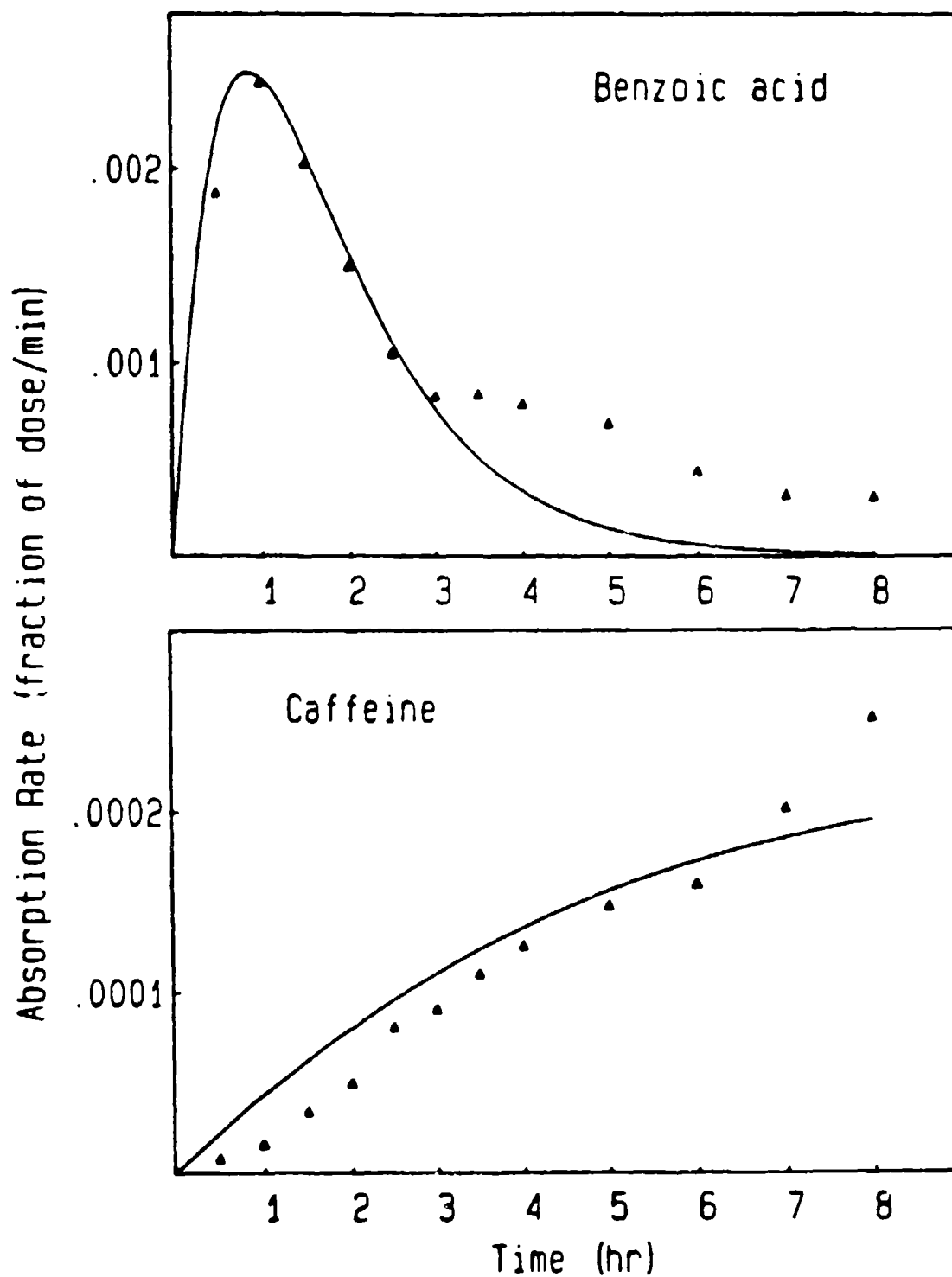
Figure 22. Simulations for B and C derived from the model seen in Figure 21, plotted along with observed absorption rates.
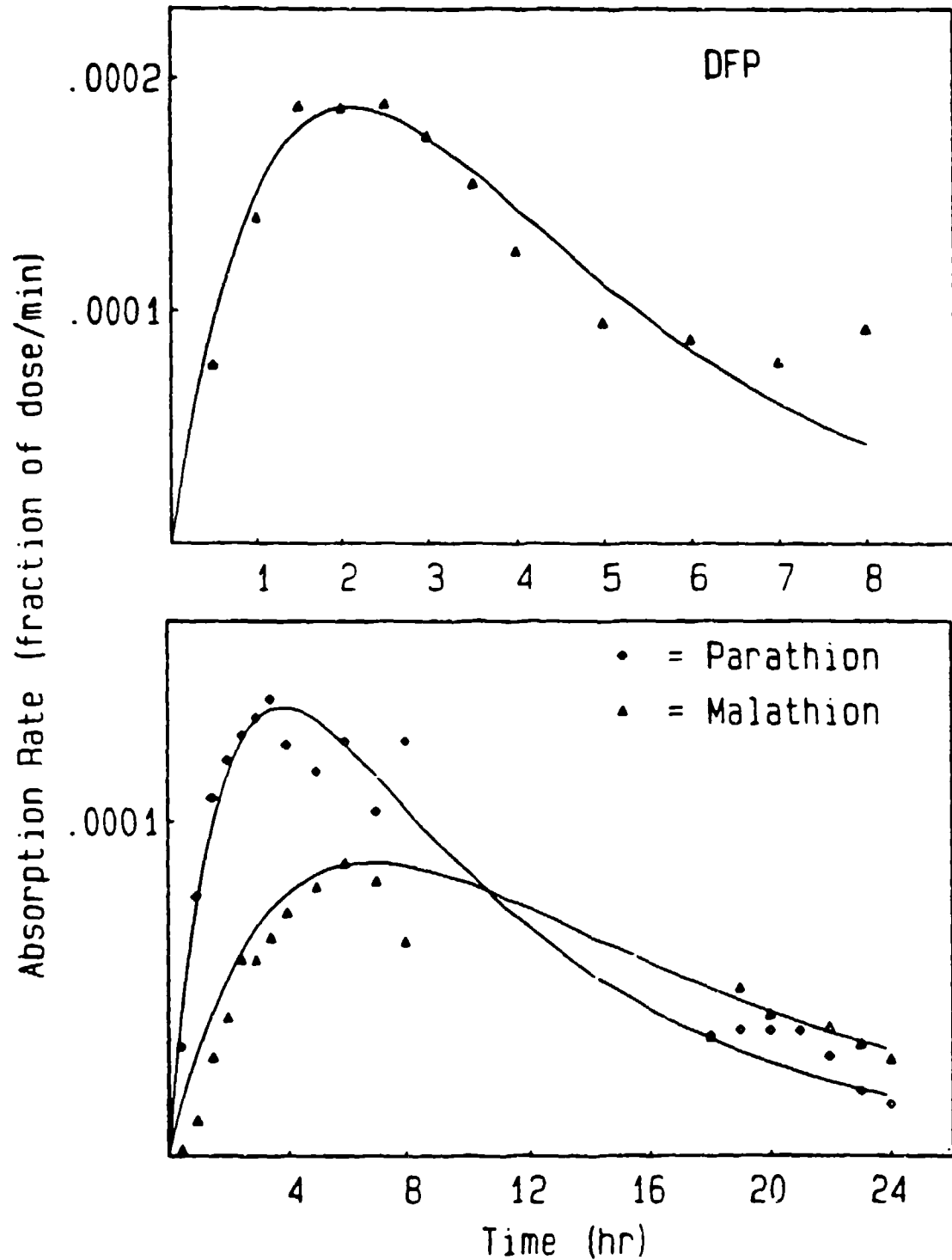
Figure 23. Simulations for the organophosphates from the model in Figure 21, plotted along with observed absorption rates. In the bottom plot, open symbols are rates determined from in situ application 17 hr prior to perfusion.
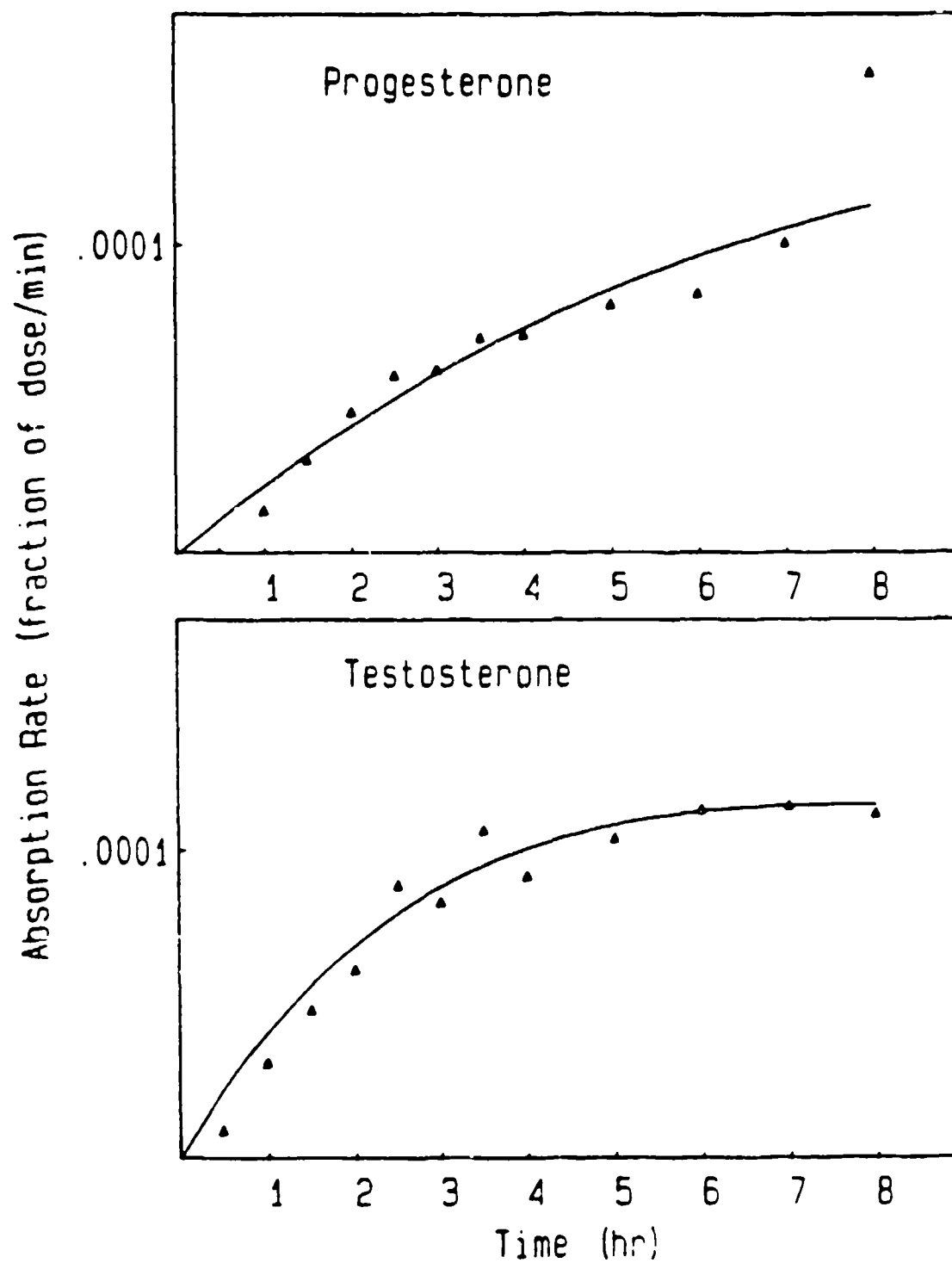
Figure 24. Simulations for the steroids from the model in Figure 21, plotted with observed rates.

Table 10. Mass transfer rate constants obtained from multicompartment pharmacokinetic model[a] describing xenobiotic absorption in the IPPSF

| Compound | Rate Constant (hr^{-1}) | | | | F^{b} |
	k_{10}	k_{12}	k_{23}	k_{32}	
B	0.972	0.540	0.900	0.0048	0.357
C	0.020	0.022	0.132	0.0002	0.526
D	0.499	0.034	0.432	0.057	0.064
M	0.075	0.009	0.270	9.00	0.108
P	0.437	0.055	0.120	3.30	0.111
R	0.026	0.024	0.060	0.003	0.333
T	0.026	0.009	0.360	5.70	0.250

[a]Schematic diagram appears in Figure 21.

[b]Bioavailability (fraction of dose).

Furthermore, replacing the F values for B and C from the standard compartmental model with those obtained from the modified model (0.752, 0.142) yields a similar, statistically significant correlation (Figure 25).

Parathion Metabolism

Flux profiles for the experiments involving P absorption in the IPPSF are presented in Figure 26. Data from only a single skin flap for each treatment group, ABT or occlusion, were available due to a lack of viability in the second occluded flap and a perfusion pump failure in the case of the second ABT flap. Although glucose utilization in the occluded flap was somewhat higher than in control and that for ABT slightly lower, these values were still within normal ranges, established earlier. As can be seen, total P penetration (area under the rate-time curve) was higher with occlusion and lower when pretreated with ABT. Total radiolabel recoveries in the three P control flaps and two treated flaps ranged from 65-105%, consistent with the known moderate volatility of this organophosphate (OP).

Table 11 provides a more detailed description of these flux rates and total P penetration. Values for the control flaps represent the mean of three determinations and are taken from the same experiments shown in the previous section. In vitro P absorption in the skin flap dosed in situ (ISP), obtained during the perfusion studies conducted 17-25 hr after application, is also shown. In vivo percutaneous absorption of P in this flap, based on corrected urinary and fecal excretion of label during the 17-hr period in which the flap remained on the pig, averaged 226 ng/cm^2/hr. As can be seen, the actual flux during the subsequent perfusion studies decreased considerably, to 66 ng/cm^2/hr. Both penetration rate and Ka in all three treatment groups fell outside the range of mean $\pm$ 2 SD obtained in the controls, indicating that P absorption was significantly lower both in the IPPSF dosed in situ and in the ABT-pretreated flap. For the same reasons, P absorption was considered to be significantly greater in the occluded IPPSF.

Metabolite profiles, derived from radiochromatograms similar to the one seen earlier in Figure 4 and expressed as a percentage of perfusate contents at termination of the 8-hr experiment, are shown in the top half of Table 12. From the control experiments (n=2), it can be seen that two thirds of the radiolabel penetrated as the oxygenated derivative of P, or P=O, which is considered to be the active cholinesterase inhibitor in vivo. Occlusion effected complete biotransformation of absorbed P, but did not result in net detoxification of the P=O since it was produced in the same fractional amounts. ABT pretreatment essentially abolished metabolism of the P during absorption, with levels of each metabolite very close to background (no flap), and no metabolites were identified in the perfusate from the flap dosed in situ. The lower half of this table shows approximate rates of product formation, calculated from the flux rates (nanograms/sq.cm/hr) in Table 11 and the percentages listed
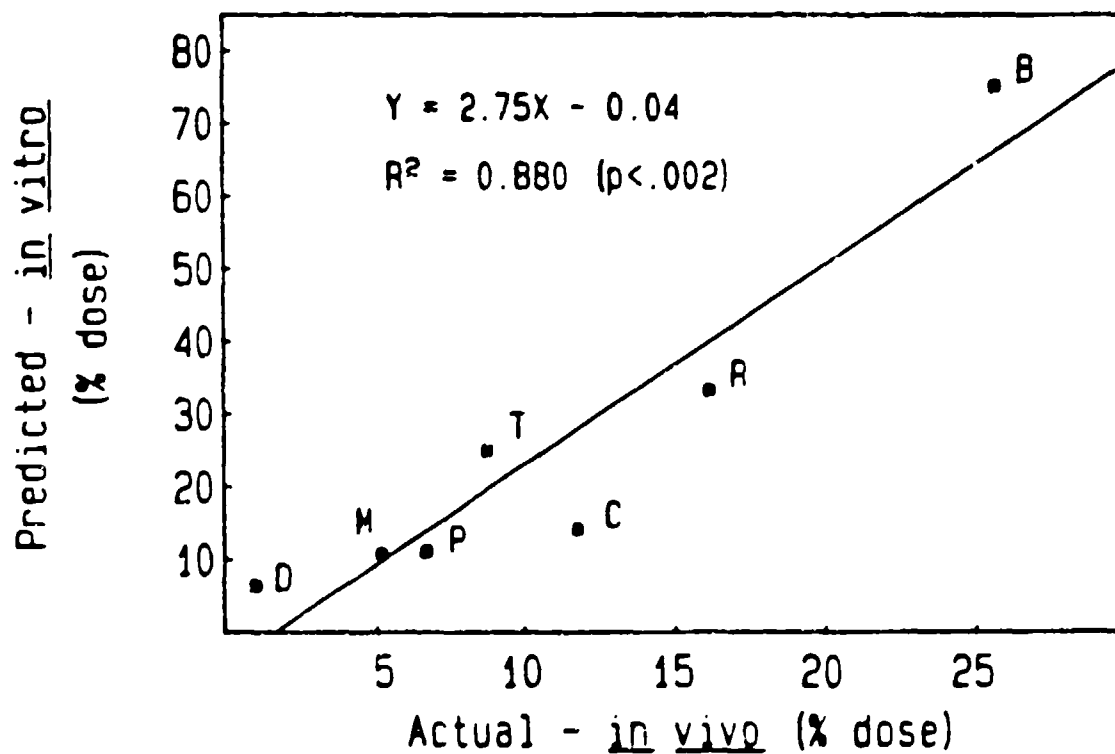
Figure 25. Simple linear regression of predicted absorption (IPPSF) model extrapolations) vs in vivo percutaneous absorption totals obtained in pigs. Compound abbreviations are provided in the text.
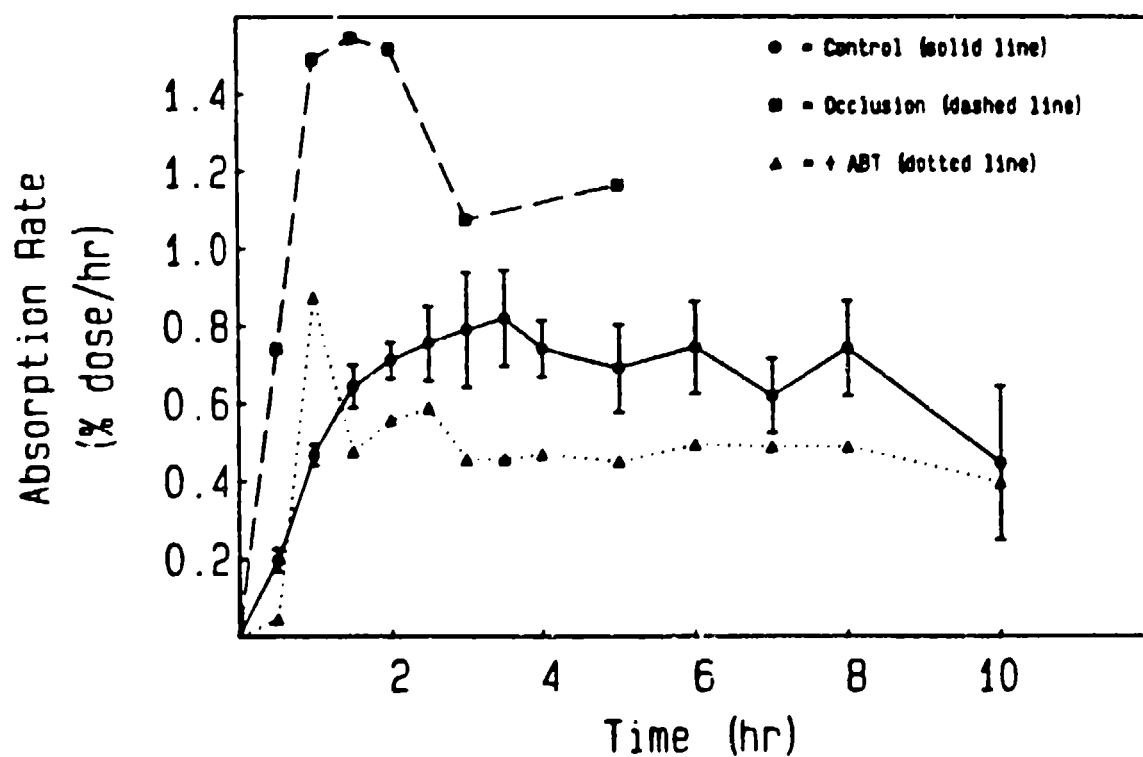
Figure 26. Absorption rate-time curves for parathion in the IPPSF under
different experimental conditions. Control data (mean $\pm$ SE,
n=3) are from Figure 16. ABT and occlusion pretreatments
(n=1) experiments.

Table 11.   Parathion absorption in the IPPSF

Parameter	Treatment or Pretreatment [a]			
	Control	Occlusion	ABT	In situ[b]
Flux (%dose)	5.2	5.2	3.7	⊥.3
(ng/cm^2/hr	265	430	187	66
Ka (10^4 hr^{-1})[c]	66	108	47	17
Peak rate (ng/cm^2/hr)	371	618	349	91

[a]Flaps were dosed topically with 40 $\mu g/cm^2$ (10 μCi) ^{14}C-radiolabeled parathion solution in ethanol.

[b]Dosed in situ 7 hr prior to perfusion. Corrected in vivo absorption during the initial 17-hr period = 19.2 μg or 226 ng/cm^2/hr.

[c]Time-averaged rat constant calculated using the formula:
Ka = -ln[1-(%absorp./100)]/t (Mayer & vandeWaterbeemd, 1985).

Table 12.   Parathion metabolite profiles in the IPPSF

Parameter	Compound	Control	Occluded	ABT	In situ	No flap[b]
			Treatment or Pretreatment[a]			
Perfusate	P[c]	24	0	85	100	86
Contents	P=O	69	69	3	0	9
(%)	PNP	5	31	6	0	5
	Other	2	0	6	0	0
Rate of	P	310	0	780	320	520
product	P=O	890	1450	30	0	50
formation	PNP	70	650	50	0	30
(ng/hr)	Other	30	0	50	0	0

[a]IPPSF's dosed with 200 µg (10 µCi) ^{14}C-parathion applied topically in ethanol.

[b]Injected 40 µL (0.3 µCi, 0.6 µg) of dilute ^{14}C-parathion solution into perfusate.

[c]Abbreviations used are: parathion (P), paraoxon (P=O), and p-nitrophenol (PNP).

above. Because the only samples available for assay were taken at the end of each IPPSF experiment and the enzyme kinetics was unknown, these values represent, at best, rough estimates. Nevertheless, when placed in the proper perspective, the relative bioavailabilities of the particular molecular species penetrating may be useful in dermal risk assessment models of P absorption, pending replication of these experiments.

DISCUSSION

These experiments demonstrate the feasibility of maintaining a viable skin preparation for 10-12 hr in an isolated organ system. The finding of increasing lactate concentrations linearly correlated to glucose utilization over the course of an experiment is consistent with other in vitro studies in skin, demonstrating that anaerobic glycolysis is a primary bioenergetic pathway for skin and that lactate is the primary end product of epidermal glycolysis (87). In this preparation, an overall mean lactate/glucose ratio of 1.7 suggests primarily anaerobic glycolysis and a smaller component due to non-lactate-producing pathways. The linear glucose consumption over time maintained by an extraction ratio inversely proportional to perfusate flow indicates a stable, self-regulating metabolic system. Consistent with previous skin studies (88), glucose extraction was directly proportional to available glucose concentrations in the four flaps in which constant glucose concentrations were not maintained above 80 mg/dl. Sodium fluoride inhibition of glucose utilization, coupled with morphological indications of an anatomically normal epidermis, is further evidence of the viability of this preparation.

Morphological assessments are a valuable tool to differentiate lesions due to various factors in the IPPSF. The results from the LM analysis to assess viability appear to be insufficient for the development of a morphological index because of animal and site-site variability. In contrast, morphological criteria using TEM are essential for the differentiation of changes due to cell death, postoperative procedures, isolated perfusion, and xenobiotic induced toxicity.

The continued accumulation of lactate and other waste products in this closed system probably contributed to decreased function with time in flaps not terminated at 10-12 hr. However, 10 hr of viability is considerably longer than the 4-6 hr generally seen in isolated liver and kidney preparations (89). Perfusate exchange, addition of a membrane dialyzer into the system, or forced utilization of lactate as an energy source by hormonal stimulation may significantly extend the viable period of this preparation. Recent use of a nonrecirculating chamber has also eliminated this problem. Incorporation of amino acids or short-chained fatty acids into the perfusate may also prolong viability. At present, a period of 10-12 hr should be adequate for modeling the initial rapid phase in percutaneous absorption studies, the phase which is critical in cases of acute

intoxication. Finally, based on the biochemical data, there is no difference between IPPSF's harvested 2 or 6 days after stage 1 surgery, except for an increased tendency to gain weight during the experiment in 6-day IPPSF's. Morphologically, by 6 days the epidermis appears to be much thicker than at 2 days and the interflap variability is also greater. Because the IPPSF is intended for percutaneous absorption studies, 2-day flaps appear to be optimal.

Percutaneous absorption totals in vivo in the present study were generally lower than values reported by others in pigs, despite the similarities in overall rank order, both by compound and chemical class (18-20,22,23). The high degree of inter-laboratory variability in excretion of these compounds, given either parenterally or topically to pigs, renders absolute comparisons problematic. However, there are several factors known to affect percutaneous absorption in vivo, which may help explain these conflicting results. Variables such as applied surface concentration, the vehicle used, or the anatomical site onto which topicals are applied have not been evaluated in pigs, although their relative effects on percutaneous absorption are known in other species and should be qualitatively similar in pigs.

A major factor affecting percutaneous absorption in vivo is the applied surface concentration, for which an inverse relationship with fractional (percent) absorption has been demonstrated in both humans and rhesus monkeys (31,90-92). A similar relationship for finite doses applied in vitro has also been documented (93). It is reasonable to assume that the higher topical doses applied in this study contributed to the lower percutaneous absorption totals, expressed as a percent of total dose, reported here, particularly since the overall rank orders were in agreement.

The application site may also be involved, since an area on the dorsum has traditionally been the site of choice for animal studies. Regional variations in percutaneous absorption are reasonably well known in humans (94-98), however, these studies are rare in other mammalian species except for the rhesus monkey, which appears to have similar rank orders as humans for certain compounds (99-101). There is some evidence that the abdominal region in rats is more permeable than the back (95,102). Although the ratio of pig-to-human absorption for some compounds is similar to back-to-forearm ratios in humans (21,22,98), other application sites have not been examined in pigs. Further studies of various anatomic regions and applied doses are clearly warranted if these animal data are to have any relevance in human dermal risk assessment. The ventral abdomen was chosen in the present study because it is the location from which porcine skin flaps, useful for examining cutaneous pharmacology and toxicology in vitro, are surgically removed (7,48,49).

The dependence of the urinary-fecal excretion ratios on route of administration shown in this study for B, C, P, and T

has not been demonstrated previously. Examples of altered excretion profiles are available for both T (47) and polychlorinated biphenyls (46) in guinea pigs, 1,3-diphenylguanidine in rats (44), and dimethylbenzanthracene in mice (43). In this study, the injected dose was systemically bioavailable in amounts 4-20 times greater than the amounts absorbed after topical application, which, when coupled with slower presentation to eliminating organs by the latter route, might explain the route-dependent excretion pattern observed. Moreover, incomplete recovery totals of radiolabel from IV doses of organophosphates suggest that volatile metabolites and expired $^{14}CO_2$ are eliminated by different mechanisms than after topical administration. However, a complete explanation for our finding of altered urine-fecal excretion ratios must lie elsewhere, since parenteral doses several orders of magnitude higher than the topical doses had little effect on radiolabel excretion in a previous study in pigs (20).

An intriguing possibility is that first-pass cutaneous biotransformation during percutaneous absorption could have occurred, followed by preferential excretion of some metabolites in the feces. Although there is no information in the literature concerning metabolism of either B or C in skin, T has been shown to be metabolized _in vitro_ by human skin, in addition to skin from five other species--rat, rabbit, guinea pig, mouse, and marmoset (103-105). No evidence of the bioactivation of P to its more toxic oxygenated derivative, paraoxon, was seen when rabbit, rat, cat, or human skin slices were incubated _in vitro_ (106). However, poor P solubility in the reaction mixture, low tissue viability, or species differences in cutaneous metabolic capacity could explain why this reaction did not occur. The preliminary results using the IPPSF have demonstrated a substantial capacity for P metabolism during percutaneous absorption in pig skin.

The failure of others using similar _in vivo_ methods to detect corresponding shifts in the excretion of radiolabel (20) may be a consequence of low substrate concentrations in viable cutaneous tissues, produced by the lower topical doses used. Although Michaelis-Menten enzyme kinetics has not been determined for any of the biotransformation pathways occurring in skin, substrate concentrations near the km for P in liver may result in protein binding by paraoxon, thereby preventing its release from the liver (75). Relative amounts of P (nanograms or nanomoles cm^{-2}) permeating the epidermis in this study would be 3-5 times greater than provided by the dose (4 g cm^{-2}) used in previous investigations. Whether similar kinetic and protein binding phenomena occur in skin is presently unknown. It is difficult to examine cutaneous biotransformation _in vivo_; however, these results imply that future investigations of percutaneous absorption should focus more carefully on the metabolic fate of compounds applied topically.

In summary, percutaneous absorption of several compounds, representing three chemical classes, has been examined _in vivo_ in

pigs. Total penetration, expressed as a percentage of topical dose, was lower than in previous reports (18-20,22,23) due to differences in concentration applied and the application site. The approximate rank order penetration by chemical class was: organic acids/bases > steroids > organophosphates, which was similar to that found by others in both pigs and humans. Excretion of these compounds was dependent on the route of administration, which, at the very least, violates inherent assumptions in established correction factors for using urine alone to assess percutaneous absorption. The altered excretion after topical administration may also be indicative of cutaneous biotransformation; however, further study is required to determine the metabolic capacity of skin and what effect it has on the disposition of compounds applied topically.

The IPPSF has been shown to be accepted as a versatile experimental model, providing information pertaining to cutaneous physiology (7,49,107), biochemical and histological markers of cutaneous toxicology (7,48), and for studying the biotransformation of chemicals during percutaneous absorption (108,109). The flap also appears to be significantly more viable than a human groin flap preparation (107,110). Although several preliminary reports have demonstrated that the IPPSF is permeable to a variety of xenobiotics (109,111-113), the pharmacokinetics of percutaneous absorption has not yet been fully characterized using this model. In this study, a three-compartment pharmacokinetic model which describes the relevant mass transfer processes, was developed from the absorption rates obtained in the IPPSF for compounds representing three chemical classes: organic acid/base chemicals, organophosphate insecticides, and steroid hormones.

The model is similar to one based on both _in vivo_ and _in vitro_ absorption rates, reported previously by others (83,84,86,114). There are two major differences between our approach and previous attempts to provide detailed models of percutaneous absorption pharmacokinetics. First, no assumptions about partitioning phenomena or the interrelationships between mass transfer, diffusion rates through various skin structures, or the molecular weight of the penetrant are made _a priori_, because models developed using IPPSF absorption rate data provide all the relevant parameters. Second, the IPPSF is the only experimental model currently available capable of providing absorption rate-time profiles in viable, fully functional skin, which can be used to resolve subtle differences in the mechanisms of dermal penetration. This feature was illustrated by the modification of the B model and the discovery of more than one saturable diffusion process, which may prove to represent multiple penetration pathways for this lipophilic weak acid. B absorption profiles have strikingly consistent shapes in many systems studied, including diffusion chambers (115), other skin flaps (116,117), and _in vivo_ (83). The combination of good lipid and aqueous solubilities in any one compound, which may be ideal for promoting dermal absorption, has been termed "chameleonic" by Roberts and Horlock (118), and may be one underlying mechanism

for the saturable processes identified using the IPPSF to determine percutaneous absorption rates. Regardless of the nature of these mechanisms, the pharmacokinetics of B absorption is obviously more complicated than past studies have shown.

The reason why C deviated from the standard model, which adequately predicted the in vivo absorption of organophosphates and steroids, is less readily apparent. An intriguing possibility is that C influenced its own penetration by pharmacological manipulation of the cutaneous microcirculation. In isolated arterial preparations C is a vasodilator (119,120) in addition to modulating smooth muscle response to other vasoactive substances (121). The correlation of C penetration rates in the IPPSF and increases in perfusate flow, particularly near the end of the 8-hr perfusion period when epidermal concentrations would be expected to be greatest, was not observed for any other compound tested. Cutaneous blood flow is an important factor in the absorption of compounds that are capable of very rapid penetration to the cutaneous vasculature (117,122-124); however, C was not well absorbed in this study in vitro or in vivo, which probably rules out the simplistic interpretation that C penetration depends on flow and not vice versa. Moreover, incorporation of a perfusate flow function for k34 into the basic compartmental model, driven by the amounts of C available in the perfusate compartment (C3), improved the fit considerably. Further work will be necessary to elucidate the mechanisms of C-induced vasodilation in the cutaneous microcirculation, including determining the concentrations of C needed to produce increased perfusate flow (dose-response studies) and whether or not this effect can be blocked, perhaps by co-administration of other vasoactive substances to the skin flap.

Correlations between IPPSF absorption totals, rank orders, or peak rates with in vivo percutaneous absorption totals or ranks could not be demonstrated, primarily because of large differences in the time frames over which these experiments take place: 8 hr vs 6 days. On the other hand, the pharmacokinetic models were highly predictive of in vivo percutaneous absorption. The fitted regression line had a slope of about three and passed through the origin (equations 12 and 13). This latter finding is important, since it suggests that there are few, if any, fundamental differences between the IPPSF and intact skin with regard to permeability to various chemicals. In contrast, comparison of human and pig skin grafted-athymic nude mouse permeability and in vivo absorption totals in man and pigs revealed a strong regression line which did not pass through the origin (19,20), suggesting that the underlying mechanisms of percutaneous absorption in grafted skin models are not the same. Whether or not other recently developed skin flap models are capable of reliably predicting in vivo absorption rates, elucidating the mechanisms of percutaneous absorption, or determining the disposition of topical agents has not been satisfactorily established (110,116,117).

The slope of the regression line from equations 12 and 13

suggests that total _in vitro_ penetration was approximately 2-3 times that found _in vivo_. The relative humidity at which the corresponding experiments were conducted differed by a factor of two (60-80% _in vitro_ vs 30-35% _in vivo_). Although the relationship between water-binding capacity of the s.c. and %RH has been well characterized (125-127), the impact of humidity on percutaneous absorption is less well understood. Ambient temperature differences ($37^{\circ}C$ vs $25^{\circ}C$) may have been involved as well, since ambient temperature is believed to have a direct effect on dermal absorption _in vivo_ (128-132). However, in past studies temperature effects could not be distinguished from temperature-induced cutaneous blood flow increases. As discussed earlier, blood flow may be the determining factor _in vivo_. Clearly, more studies in the IPPSF, in which these variables are controlled and varied independently, will help resolve the individual effects of cutaneous blood flow, ambient temperature, and humidity. Finally, differences between the perfusate contents and the normal composition of serum may also be involved, since the estimate of B bioavailability in the single IPPSF perfused with porcine plasma (60%) was closer to the value obtained from the regression line seen in Figure 25.

The demonstration that P is metabolized by pig skin to such a significant extent during percutaneous absorption is unique, since an earlier report indicated that skin slices of rabbit, cat, rat, and human origin were incapable of P bioactivation (106). One factor which could explain this discrepancy is species differences in the metabolic capacity of skin, noted in the earlier study when the P=O hydrolysis rates were compared using similar methods. Although species effects have also been demonstrated recently for cutaneous BaP (benzo(a)pyrene) and T metabolism in organ culture, they were primarily quantitative. No species was completely devoid of a particular enzyme or reaction pathway (104). Sex differences may be even more important than species for P metabolism in other organs (74,133,134) and may have been a factor in the present study; however, sex of the animals from which skin slices were taken in the earlier work was not mentioned.

Substrate (P) concentrations in the reaction mixture used by Fredriksson et al. (106) were well above km values established for liver (75,135-137) and extrahepatic tissues (133,137); however, delivery to active sites in the skin slices may have been a problem due to the observed poor solubility of P in the reaction mixture. Consequently, protein binding of the resulting low product (P=O) concentrations could have prevented its detection in the reaction mixture, consistent with similar phenomena which have been described in the liver (64,138). Extrapolations using either the peak absorption rate or the average rate (nanograms/sq.cm/hr) in the present study, assuming that 1 cm^2 of skin contains approximately 10 mg of epidermis (139), and that the P is distributed equally throughout the epidermis just prior to vascular uptake, show substrate concentrations in the vicinity of the viable epidermis in the 100 M range, which should be sufficient to allow P metabolism to

occur in the IPPSF.

Cutaneous viability may also be a factor when skin is studied _in_ _vitro_. The influence of viability on both percutaneous absorption and biotransformation has been well docur?nted for skin maintained in organ culture (104,140,141). In fact, there is evidence of a direct correlation between viability and flux, at least for a few compounds that are metabolized by skin (104,142). As reported above, viability in both control and occluded or ABT-pretreated skin flaps was within established normal ranges (7,48,107). Viability of the skin slices was not addressed in the earlier study of P metabolism and there is no evidence that the skin was supplied with even minimally sufficient nutrients in the reaction mixture described. A mitigating factor is the short time frame of the incubation experiments (90 min) and the ability of skin to survive relatively long periods of anoxia and/or ischemia. On the other hand, this may also have precluded detection of any P oxidation products, given the time it takes some substances to penetrate and diffuse within the various layers of the skin, because these "permeation" processes would have to occur first.

The demonstration that suicide substrates such as ABT (78) can modulate the activity of cutaneous mixed-function oxidases is also unique, since previous work with skin focussed on the effects of various inducing agents (41,104,142,143). ABT is relatively nontoxic when administered _in_ _vivo_ to rats (79), and in this study direct cutaneous toxicity, i.e., signiïicant reductions in glucose utilization or the release of intracellular LDH, was not observed. Nevertheless, ABT completely abolished the biotransformation of P in skin. The resulting metabolite concentrations in the perfusate were near background levels, as determined in the "no-flap" recirculation experiments (Table 12). Penetration of P (187 vs control = 265 $\pm$ 38 ng/cm^2/hr, n=3) was lower in this skin flap as well, which may indicate a direct relationship between percutaneous absorption and metabolism in the IPPSF, one which is opposite that seen in PCB-induced skin (104,142). Despite the lower rate of absorption, the aforementioned Michaelis-Menten enzyme kinetics cannot explain the total lack of P metabolism because substrate concentrations in the viable epidermis were still above reported km values for other organs. ABT is a novel suicide substrate in that it is very nonspecific, believed to inhibit most of the known cytochrome-dependent monooxygenase isozymes to a similar degree (78), which makes it a useful probe for cutaneous metabolism since the inducible enzyme in skin is probably not cytochrome P-450 (41,104,142-144).

The experiment in which P was applied _in_ _situ_ 17 hr prior to perfusion of the skin flap, also resulting in complete abrogation of cutaneous metabolic activity, is somewhat more difficult to interpret without further research. The most likely mechanism, involving suicide enzyme inhibition by the P itself, which penetrated at an average rate of 226 ng/cm^2/hr during the first 17 hr (_in_ _situ_), is well documented in isolated hepatocytes and

perfused livers (66,67,145). One way to test this hypothesis is to apply a second, nonsuicidal substrate to the flap just prior to the perfusion experiment to see whether the cutaneous enzymes have actually been blocked. The other contributing factor may be the low penetration rate of P during the course of the _in vitro_ perfusion study, 17-24 hr after application, which relates to the previous discussion of Michaelis-Menten considerations. A second application of P prior to the _in vitro_ portion of the experiment might independently verify this hypothesis.

The manipulation of cutaneous metabolism by physical means, i.e., the complete degradation of P in the occluded skin flap, is also novel and could have implications in dermal risk assessment. There are several possible mechanisms by which occlusion could increase P metabolism, the most obvious being that the hydration state of the epidermis favors P=O partitioning, resulting in greater substrate concentrations for hydrolysis to PNP. Although the esterase reaction is undoubtedly facilitated by high substrate (P=O) concentrations whenever P is directly metabolized to PNP, studies of intrinsic liver clearance have shown that P=O is generated faster than it is hydrolyzed (135), in apparent contradiction of this hypothesis. Alternatively, the greater cutaneous hydration may have produced more favorable thermodynamic conditions for water attack on the phosphooxythirane intermediate (see reaction pathway 4, Figure 3). Direct metabolism to PNP + DEP is not a preferential pathway in the liver because, in addition to unfavorable thermodynamic conditions, water has limited access to the P-450 active sites (66).

A final consideration, again relating back to the kinetics of the initial oxygenation of P to P=O, is the fact that epidermal P concentrations themselves are likely to be higher due to the greater penetration which resulted from occlusion. As expected, occlusion of the application site increased the rate of P absorption in the IPPSF (430 ng/cm^2/hr), although not quite to the extent reported _in vivo_ (96,146). This may be due to the rather high temperature (37°C) and relative humidity (60-90 %RH) at which the perfusion chambers were maintained. Better methods for controlling the environment within the perfusion apparatus will be implemented, which should allow the IPPSF to be examined under more normal conditions. Furthermore, bioactivation of P to P=O in the IPPSF may not represent "first-pass" metabolism by classical definition, since the perfusate was recirculated. Results of the ABT study indicate that substances are delivered to, and can be metabolized by, the viable epidermis without resorting to topical application. However, the concentrations of ABT in the perfusate were several orders of magnitude higher than amounts of P taken up from topical doses. In addition, preliminary results from IPPSF experiments in which P was added to the perfusate (data not shown) suggest that less than 20% of the P=O formation and almost none of the PNP was due to dermal uptake from the recirculating perfusate.

Regardless of these methodological concerns, first-pass

cutaneous bioactivation of P, which is strongly suggested by the IPPSF studies reported here, could have an impact on dermal risk assessment of this important agricultural poison. Production of P and methylparathion (MeP), which probably peaked in the early 1970's, has been estimated at approximately 60-80 million s/year during that period of time and the population at risk was thought to include most of the 8-9 million agricultural workers in the United States alone, along with a small number of workers at manufacturing plants (147,148). The proportion of accidental worker poisonings attributable to either OP use in general, or to P and MeP in particular, appears to have stabilized in industrialized nations (148-151). However, these and other compounds representing the so-called "first-generation" organophosphates are both cheaper to use and more toxic than second-generation OP's (malathion is the prototype) or carbamates (carbaryl, etc.), in addition to being less well regulated in third world nations, where thousands of deaths associated with their use are continually reported (149).

Dermal absorption appears to be the main route of exposure for both applicators and fieldworkers (re-entry), contributing 100-1000 times greater amounts than respiratory exposure (131,132,152-157). Oral lethal doses have been estimated at 0.2-0.3 mg/kg for P, with correction factors for lower systemic bioavailability from dermal exposure ranging from 3-10 (69,156,158). However, it is usually assumed that P penetrates the skin intact when making these comparisons and that rat exposures can be extrapolated to humans. If the doses of each of the penetrating species were determined experimentally, in an animal model comparable to humans, dermal dosimetry estimates could provide more relevant information for toxicological assessment of this pesticide. The bottom half of Table 12 lists estimated rates of absorption for the products and parent compound in the IPPSF, which could be used to calculate actual doses of each chemical which are systemically available. Occupational exposure to P, when predicted for the larger surface areas and high concentrations normally encountered by man, could easily give rise to systemic doses of P=O (0.1-1 mg/kg) which are near the limits established for lethality in humans.

As presently configured, the IPPSF may be useful for a number of investigations. The ability to place drugs or chemicals on the surface of viable skin maintained in a controlled environment, combined with the measurement of arterial and venous drug concentrations, makes this preparation well suited for investigating the percutaneous absorption of drugs and chemicals. If first-pass cutaneous metabolism of the compound occurs, the IPPSF should allow for the identification of metabolites produced by epidermal processes and be useful for quantitating the rate of these processes for incorporation into recently proposed pharmacokinetic models (86,114,159). Present in vivo studies are confounded by the biotransformation of absorbed agent in the liver and kidney, while in vitro techniques using cadaver skin are not applicable because of limited viability (32,160). The

IPPSF would also allow quantitation of the effects of temperature, altered cutaneous microcirculation, disease, bioenerge᠁ profile, and decontamination strategies on percutare᠁s absorption. The IPPSF preparation appears well suited f᠁ studying the normal biochemistry of the skin. If IPPSF's were raised in swine breeds which possess spontaneous cutaneous melanomas (161), an isolated perfused vascular bed containing normal and cancerous tissue would be available for various studies in cancer biology. Finally, the IPPSF is an alternative animal model which should allow cutaneous toxicology studies to be conducted in a humane manner.

The IPPSF would have a number of uses relevant to military needs. T᠁ pharmacokinetics and cutaneous biotransformation of topically exposed chemical warfare agent could be studied independent of systemic toxic effects. Decontamination protocols for cutaneous agent exposure could be assessed. The design of transdermal drug delivery system᠁ for chemical warfare nerve agent prophylaxis would be great᠁ facilitated since the data collected in the IPPSF would be appropriate for direct incorporat᠁on into existing pharmaco-kinetic models. Finally, the IPPSF ᠁ight be ideally suited for studying the mechanisms of cutaneous toxicity induced by the vesicant chemical warfare agents mustard and lewisite, since early biochemical and morphological changes could be assessed in an isolated viable skin preparation with a responsive microcirculation. Decontamination and protection strategies against vesicant agents could then be humanely evaluated in the IPPSF.

PERTINENT PUBLICATIONS ON THE IPPSF

MANUSCRIPTS:

Riviere, J.E., Bowman, K.F., Monteiro-Riviere, N.A., Carver, M.P., and Dix, L.P. (1986). I. A novel in vitro model for percutaneous absorption and cutaneous toxicology studies. Fundam. Appl. Toxicol. 7, 444-453.

Monteiro-Riviere, N.A., Bowman, K.F., Scheidt, V.J., and Riviere, J.E. (1987). The isolated perfused porcine skin flap (IPPSF). II. Ultrastructural and histological characterization of epidermal viability. In Vitro Toxicol. 1, 241-252.

Riviere, J.E., Bc man, K.F., and Monteiro-Riviere, N.A. (1987). On the definition of viability in isolated perfused skin preparations. Brit. J. Dermatol. 116, 739-741.

Carver, M.P., Williams, P.L., and Riviere, J.E. (1989). The isolated perfused skin flap. III. Percutaneous absorption pharmacokinetics of organophosphates, steroids, benzoic acid, and caffeine. Toxicol. Appl. Pharmacol.
(In press)

(5 additional full-length manuscripts submitted or in preparation)

BOOK CHAPTERS, REPORTS, PROCEEDINGS:

Riviere, J.E., Bowman, K.F., Monteiro-Riviere, N.A. (1985). The Isolated Perfused Porcine Skin Flap: a novel in-vitro animal model system for drug and xenobiotic percutaneous absorption studies. Fifth Medical Chemical Defence Bioscience Review. USAMRICD Report SP85-051, Appendix III, pp. A911-A926.

Bowman, K.F., Monteiro-Riviere, N.A., and Riviere, J.E. (1985). Development of surgical techniques for preparation of in-Vitro isolated perfused porcine skin flaps for study of percutaneous absorption of xenobiotics. Fifth Medical Chemical Defence Bioscience Review. USAMRICD Report SP85-051, Appendix III, pp. A927-A939.

Riviere, J.E., Bowman, K.F., and Monteiro-Riviere, N.A. (1986). The isolated perfused porcine skin flap: A novel animal model for cutaneous toxicologic research. In: Swine in Biomedical Research (M.E. Tumbleson, ed.), pp. 657-666, New York: Plenum Press.

Riviere, J.E., Carver, M.P., Monteiro, N.A., and Bowman, K.F. (1987). Percutaneous absorption of organophosphates, steroids, caffeine, and benzoic acid In Vivo and In Vitro using the isolated perfused porc'ne skin flap (IPPSF). Sixth Medical Chemical Defence Bioscience Review, pp. 763-766.

Riviere, J.E., The isolated perfuse porcine skin flap. In: Humane Innovations and Alternatives in Animal Experimentation: A Notebook (E. M. Bernstein), Saranac Lake, New York: Currier Press.

Monteiro-Riviere, N.A., and Manning, T.D. (1987). The effects of different fixatives on the porcine integument. In: Proceedings of the 45th Annual Meeting of the Electron Microscopy Society of America (G.W. Bailey, ed.), pp. 948-949, San Francisco Press.

Riviere, J.E. and Carver, M.P., Isolated perfused skin flap and skin grafting technniques. In: Fundamentals and Methods of Dermal and Ocular Toxicology (D.W. Dobson, ed.), Caldwell, New Jersey, The Telford Press.
(In press)

ABSTRACTS:

Riviere, J.E., Bowman, K.F., and Monteiro-Riviere, N.A.(1985). The isolated perfused porcine flap: A novel In-Vitro animal model system for drug and xenobiotic percutaneous absorption studies. Fifth Annual Chemical Defense Bioscience Review, p. 94.

Bowman, K.F.,and Monteiro-Riviere, N.A. (1985). Development of surgical techniques for preparation of IN Vitro isolated perfused porcine skin flaps for study of percutaneous absorption of xenobiotics. Fifth Annual Chemical Defense Bioscience Review, p. 95.

Riviere, J.E., Bowman, K.F., and Monteiro-Riviere, N.A. (1985). The isolated perfused porcine skin flap: A novel animal model for cutaneous toxicologic research. Conference on Swine in Biomedical Research, p. 64.

Monteiro-Riviere, N.A., Bowman, K.F., and Riviere, J.E. (1985). Acute toxicity of sodium fluoride in an isolated perfused porcine skin flap. Pharmacologist 27, 158.

Bowman, K.F., Monteiro, N.A., and Riviere, J.E. (1986). The isolated perfused porcine skin flap: A novel model for skin biology. Veterinary Surgery 15, 114.

Riviere, J.E., Bowman, K.F., Monteiro-Riviere, N.A., Carver, M.P., and Dix, L.P. (1986). A novel model for cutaneous toxicologic research: The isolated perfused porcine skin flap (IPPSF). Toxicologist 6, 242.

Monteiro-Riviere, N.A., Bowman, K.F., Scheidt, V.J., Dix, L.P., and Riviere, J.E. (1986). Morphologic assessment of viability and toxicity in the isolated perfused porcine skin flap. Toxicologist 6, 242.

Riviere, J.E., Monteiro, N.A., Bowman, K.F., Carver, M.P., Scheidt, V.J., and Manning, T.O. (1986). Research methods in percutaneous absorption. JAVMA 189, 355.

Bowman, K.F., Riviere, J.E., Monteiro-Riviere, N.A., Crane, S.W., Klitzman, B., and Serafin, D. (1987). Preliminary studies on the in vitro isolated perfused porcine skin flap for physiological modeling in surgical research. Veterinary Surgery 16, 84.

Carver, M.P., Monteiro-Riviere, N.A., Bowman, K.F., and Riviere, J.E. (1987). Percutaneous absorption kinetics of organophosphates, steroids, caffeine, and benzoic acid in the isolated perfused porcine skin flap (IPPSF). Toxicologist 7, 244.

Carver, M.P., Levi, P.E., and Riviere, J.E. (1988). Significant first-pass bioactivation of parathion (P) during percutaneous absorption in the isolated perfused porcine skin flap (IPPSF). Toxicologist 8, 125.

Riviere, J.E., and Williams, P.L. (1988). Interaction of regional nyperthermia with antineoplastic drug delivery pharmacokinetics. Studies in an isolated perfused skin flap system. Proceedings of the Radiation Research Society 36, 16.

REFERENCES

1. Yardley, H.J. (1983). Isolation and lipid compositions of fractions from the superficial stratum corneum of the pig. In: Stratum Corneum (R. Marks and G. Plewig, eds.), pp. 73-78, Berlin: Springer-Verlag.

2. Bronaugh, R.L., Stewart, R.F., and Congdon, E.R. (1982a). Methods for in vitro percutaneous absorption studies. II. Animal models for human skin. Toxicol. Appl. Pharmacol. 62, 481-488.

3. Kligman, A.M. (1964). The biology of the stratum corneum. In: The Epidermis (W. Montagna and W.C. Lobitz, eds.), pp. 387-433, New York: Academic Press.

4. Pavletic, M.M. (1980). Vascular supply to the skin of the dog: A review. Vet. Surg. 9, 77-80.

5. Ingram, D.L., and Weaver, M.E. (1969). A quantitative study of the blood vessels of the pig's skin and the influence of environmental temperature. Anat. Rec. 163, 517-524.

6. Forbes, P.D. (1967). Vascular supply of the skin and hair in swine. In: Advances in Biology of Skin, Vol. 9 (W. Montagna and R. Dobson, eds.), pp. 419-423, Oxford, New York: Pergamon Press.

7. Riviere, J.E., Bowman, K.F., and Monteiro-Riviere, N.A. (1986a). The isolated perfused porcine skin flap: A novel model for cutaneous toxicological research. In: Swine in Biomedical Research (M.E. Tumbelson, ed.), pp. 657-666, New York: Plenum Press.

8. Klain, G.J., Bonner, S.J., and Bell, W.G. (1986). The distribution of selected metabolic processes in the pig and human skin. In: Swine in Biomedical Research (M.E. Tumbleson, ed.), pp. 667-671, New York: Plenum Press.

9. Weinstein, G.D. (1966). Comparison of turnover time and of keratinous protein fractions in swine and human epidermis. In: Swine in Biomedical Research (L.K. Bustad, R.O. McClellan, and M.P. Burns, eds.), pp. 287-297, Richland, Washington: Battelle Memorial Institute, Pacific Northwest Laboratory.

10. Meyer, W., Schwarz, R., and Neurand, K. (1978). The skin of domestic mammals as a model for the human skin, with special reference to the domestic pig. Curr. Prob. Dermatol. 7, 39-52.

11. Meyer, W., and Neurand, K. (1976). The distribution of enzymes in the skin of the domestic pig. Lab. An. 10, 237-247.

12. Elias, P.M. (1981). Epidermal lipids, membranes, and keratinization. Int. J. Dermatol. 20, 1-19.

13. Elias, P.M. (1983). Epidermal lipids, barrier function, and desquamation. J. Invest. Dermatol. Suppl. 80, 44-49.

14. Gray, G.M., White, R.J., and Majer, J.R. (1978). 1-(3'-O'acyl)-B-glucosyl-N-dihydroxypentatriacontadienoylsphin-gosine, a major component of the glucosylceramides of pig and human epidermis. Biochem. Biophys. Acta 528, 127-137.

15. Nicolaides, N., Fu, H.C., and Rice, G.R. (1968). The skin surface lipids of man compared with those of eighteen species of animals. J. Invest. Dermatol. 51, 83-89.

16. Monteiro-Riviere, N.A. (1986). Ultrastructural evaluation of the porcine integument. In: Swine in Biomedical Research (M.E. Tumbleson, ed.), pp. 641-655, New York: Plenum Press.

17. Monteiro-Riviere, N.A., and Stromberg, M.W. (1985). Ultrastructure of the integument of the domestic pig (Sus scrofa) from one through fourteen weeks of age. Zbl. Vet. Med. C. Anat. Histol. Embryol. 14, 97-115.

18. Reifenrath, W.G., and Hawkins, G.S. (1986). The weanling yorkshire pig as an animal model for measuring percutaneous penetration. In: Swine in Biomedical Research (M.E. Tumbelson, ed.), pp. 673-680, New York: Plenum Press.

19. Reifenrath, W.G., Chellquist, E.M., Shipwash, E.A., and Jederberg, W.W. (1984a). Evaluation of animal models for predicting skin penetration in man. Fund. Appl. Toxicol. Suppl. 4, S224-S230.

20. Reifenrath, W.G., Chellquist, E.M., Shipwash, E.A., Jederberg, W.W., and Krueger, G.G. (1984b). Percutaneous penetration in the hairless dog, weanling pig, and grafted athymic nude mouse: Evaluation of models for predicting skin penetration in man. Br. J. Dermatol. 111 (Suppl. 27), 123-135.

21. Chow, C., Chow, A.Y.K., Downie, R.H., and Buttar, H.S. (1978). Percutaneous absorption of hexachlorophene in rats, guinea pigs and pigs. Toxicology 9, 147-154.

22. Bartek, M.J., and LaBudde, J.A. (1975). Percutaneous absorption, in vitro. In: Animal Models in Dermatology (H.I. Maibach, ed.), pp. 103-120, New York: Churchill Livingstone.

23. Bartek, M.J., LaBudde, J.A., and Maibach, H.I. (1972). Skin permeability in vivo: Comparison in rat, rabbit, pig and man. J. Invest. Dermatol. 58, 114-123.

24. Hawkins, G.S., and Reifenrath, W.G. (1984). Development of an in vitro model for determining the fate of chemicals applied to skin. Fundam. Appl. Toxicol. Suppl. 4, 133-144.

25. Hawkins, G.S., and Reifenrath, W.G. (1986). Influence of skin source, penetration fluid, and partition coefficient on in vitro skin penetration. J. Pharm. Sci. 75, 378-381.

26. Marzulli, F.N., Brown, D.W.C., and Maibach, H.I. (1969). Techniques for studying skin penetration. Toxicol. Appl. Pharmacol. Suppl. 3, 76-83.

27. Bronaugh, R.L., and Maibach, H.I. (1985). Percutaneous absorption of nitroaromatic compounds: In vivo and in vitro studies in the human and monkey. J. Invest. Dermatol. 84, 180-183.

28. Maibach, H.I., and Wolfram, L.J. (1981). Percutaneous penetration of hair dyes. J. Soc. Cosmet. Chem. 32, 223-229.

29. Wester, R.C., and Maibach, H.I. (1975a). Percutaneous absorption in the rhesus monkey compared to man. Toxicol. Appl. Pharmacol. 32, 394-398.

30. Wester, R.C., and Maibach, H.I. (1975b). Rhesus monkey as an animal model for percutaneous absorption. In: Animal Models in Dermatology (H.I. Maibach, ed.), pp. 133-137, New York: Churchill Livingstone.

31. Wester, R.C., and Maibach, H.I. (1976). Relationship of topical dose and percutaneous absorption in rhesus monkey and man. J. Invest. Dermatol. 67, 518-520.

32. Wester, R.C., and Maibach, H.I. (1983). Cutaneous pharmacokinetics: 10 steps to percutaneous absorption. Drug Metab. Rev. 14, 169-205.

33. Montagna, W., and Yun, J. (1964). The skin of the domestic pig. J. Invest. Dermatol. 43, 11-21.

34. Bartek, M.J., LaBudde, J.A., and Maibach, H.I. (1972). Skin permeability in vivo: Comparison in rat, rabbit, pig and man. J. Invest. Dermatol. 58, 114-123.

35. Millikan, L.E., Smith, L.L., and Ochsner, J.C. (1985). Arimal models in melanoma. In: Models in Dermatology I (H.I. Maibach and N.J. Lowe, eds.), pp. 23-33, Basel: Karger.

36. Bissett, D.L., and McBride, J.F. (1985). Use of the domestic pig as an animal model of human dry skin. In: Models in Dermatology I (H.I. Maibach and N.J. Lowe, eds.), pp. 159-168, Basel: Karger.

37. Kjaersgaard, A.R. (1954). Perfusion of isolated dog skin. J. Invest. Dermatol. 22, 135-141.

38. Bell, R.L., Lundquist, R., and Halprin, K.M. (1958). Oxidative metabolism in perfused and surviving dog skin. J. Invest. Dermatol. 31, 13-14.

39. Feldmann, R.J., and Maibach, H.I. (1965). Penetration of 14C-hydrocortisone through normal skin. The effect of stripping and occlusion. Arch. Dermatol. 91, 661-666.

40. Guy, R.H., Guy A.H., Maibach, H.I., and Shah, V.P. (1986). The bioavailability of dermatological and other topically applied drugs. Pharm. Res. 3, 253-262.

41. Bickers, D.R. (1983). Drug, carcinogen, and steroid hormone metabolism in the skin. In: Biochemistry and Physiology of the Skin, Vol. II (L.A. Goldsmith, ed.), pp. 1169-1186, New York: Oxford University Press.

42. Pannatier, A., Jenner, P., Testa, B., and Etter, J.C. (1978). The skin as a drug-metabolizing organ. Drug Metab. Rev. 8, 319-343.

43. Sanders, C.L., Skinner, C., and Gelman, R.A. (1986). Percutaneous absorption of 7,10 14C-benzo[a]pyrene and 7,12 14C-dimethylbenz[a]anthracene in mice. J. Environ. Pathol. Toxicol. Oncol. 7, 25-34.

44. Shah, P.V., Sumler, M.R., Ioannou, Y.M., Fisher, H.L., and Hall, L.L. (1985). Dermal absorption and disposition of 1,3-diphenylguanidine in rats. J. Toxicol. Environ. Health 15, 623-633.

45. Rougier, A., Dupuis, D., Lotte, C., and Roguet, R. (1985). The measurement of the stratum corneum reservoir. A predictive method for in vivo percutaneous absorption studies: Influence of application time. J. invest. Dermatol. 84, 66-68.

46. Wester, R.C., Bucks, D.A.W., Maibach, H.I., and Anderson, J. (1983). Polychlorinated biphenyls (PCBs): Dermal absorption, systemic elimination, and dermal wash efficiency. J. Toxicol. Environ. Health 12, 511-519.

47. Andersen, K.E., Maibach, H.I., and Anjo, M.D. (1980). The guinea pig: An animal model for human skin absorption of hydrocortisone, testosterone and benzoic acid? Br. J. Dermatol. 102, 447-453.

48. Monteiro-Riviere, N.A., Bowman, K.F., Scheidt, V.J. and Riviere, J.E. (1987). The isolated perfused porcine skin flap. II. Ultrastructural and histological characterization of epidermal viability. In Vitro Toxicol. 1, 241-252.

49. Riviere, J.E., Bowman, K.F., Monteiro-Riviere, N.A., Dix, L.P., and Carver, M.P. (1986b). The isolated perfused porcine skin flap (IPPSF). I. A novel in vitro model for percutaneous absorption and cutaneous toxicology studies. Fund. Appl. Toxicol. 7, 444-453.

50. Hansch, C., and Leo, A.J. (1979). Substituent Constants for Correlation Analysis in Chemistry and Biology, pp. 179-319, New York: John Wiley & Sons.

51. Milton, S.H. (1971). Experimental studies on island flaps. I. The surviving length. Plast. Reconstr. Surg. 48, 574-578.

52. Milton, S.H. (1972). Experimental studies on island flaps. II. Ischemia and delay. Plast. Reconstr. Surg. 49, 444-447.

53. Prather, A., Blackburn, J.P., Willams, T.R., and Lynn, J.A. (1979). Evaluation of tests for predicting viability of axial pattern skin flaps in the pig. Plast. Reconstr. Surg. 63, 250-257.

54. Daniel, R.K., and Kerrigan, C.L. (1982). The omnipotential pig buttock flap. Plast. Reconstr. Surg. 70, 11-15.

55. Kerrigan, C.L., Zelt, R.G., Thompson, J.C., and Diano, E. (1986). The pig as an experimental animal in plastic surgery research for the study of skin flaps, myocutaneous flaps, and fasciocutaneous flaps. Lab. Anim. Sci. 36, 408-412.

56. Newton, J.F., and Hook, J.B. (1981). Isolated perfused rat kidney. Methods Enzymol. 77, 94-105.

57. Van Genderen, J., Mol, M.A.E., and Wolthius, O.L. (1985). On the development of skin models for toxicity testing. Fundam. Appl. Toxicol 45, 71-83.

58. Pearce, P.J. (1944). Concerning the stability of pyruvate and citrate in fluorided shed blood. Vet. Rec. 38, 447.

59. Troyer, H. (1980). Standard method for demonstrating soluble dehydrogenases. In: Principles and Techniques of Histochemistry, pp. 300-301, Boston: Little Brown and Co..

60. Waters, S.E., and Butcher, R.C. (1980). Studies on the Gomori acid phosphate reaction: The preparation of the incubation medium. Histochem. J. 12, 191-200.

61. Barka, T., and Anderson, P. (1962). Histochemical methods for acid phosphates using hexazonium pararosanilin as coupler. J. Histochem. Cytochem. 10, 741-753.

62. Juhlin, L., and Shelley, W.B. (1977). New staining techniques for the Langerhans cell. Acta. Dermatovener 57, 289-296.

63. Noble, L.W. (1982). Histochemistry workshop manual. Ninth North Carolina Society of Histopathology Technologists.

64. McMeekan, C.P. (1940). Growth and development in the pig, with special reference to carcass quality characters. J. Agr. Sci. 30, 276-343.

65. Gibaldi, M., and Perrier, D. (1982). Pharmacokinetics, 2nd Ed., pp. 45-59, 211-215, 321, 435-439, New York: Marcel Dekker.

66. Neal, R.A., (1985). Thiono-sulfur compounds. I. Mechanisms of metabolism of parathion, carbon disulfide, and thioacetamide. In: Bioactivation of Foreign Compounds (M.W. Anders, ed.), pp. 523-540, New York: Academic Press.

67. Sultatos, L.G., Minor, L.D., and Murphy, S.D. (1985). Metabolic activation of phosphorothioate pesticides: Role of the liver. J. Pharmacol. Exp. Ther. 232, 624-628.

68. Nabb, D.P., Stein, W.J., and Hayes, W.J. (1966). Rate of absorption of parathion and paraoxon. Arch. Environ. Health 12, 501-505.

69. Negherbon, W.O. (1959). Handbook of Toxicology, Vol. III - Insecticides, pp. 580-597, Philadelphia: W.B. Saunders.

70. Frawley, J.P., Cook, J.W., Blake, J.R., and Fitzhugh, O.G. (1958). Effect of light on chemical and biological properties of parathion. J. Ag. Food Chem. 6, 28-30.

71. Cage, J.C. (1953). A cholinesterase inhibitor derived from O-O-diethyl-p-nitrophenyl thiophosphate in vivo. Biochemistry 54, 426-430.

72. Diggle, W.M., and Cage, J.C. (1951). Cholinesterase inhibition by parathion in vivo. Nature 168, 998.

73. Norman, B.J., Poore, R.E., and Neal, R.A. (1974). Studies on the binding of sulfur released in the mixed-function oxidase-catalyzed metabolism of diethyl-p-nitrophenyl phosphorothionate (parathion) to diethyl-p-nitrophenyl phosphate (paraoxon). Biochem. Pharmacol. 23, 1733-1744.

74. Neal, R.A. (1967). Studies on the metabolism of diethyl 4-nitrophenyl phosphorothionate (parathion) in vitro. Biochem. J. 103, 183-191.

75. Sultatos, L.G., and Minor, L.D. (1986). Factors affecting the biotransformation of the pesticide parathion by the isolated perfused mouse liver. Drug Metab. Dispos. 14, 214-220.

76. Dauterman, W.C. (1971). Biological and nonbiological modifications of organophosphorus compounds. Bull. WHO 44, 133-150.

77. Main, A.R. (1960). The purification of the enzyme hydrolysing diethyl p-nitrophenyl phosphate (paraoxon) in sheep serum. Biochem. J. 74, 10-20.

78. Ortiz de Montellano, P.R., and Correia, M.A. (1983). Suicidal destruction of cytochrome P-450 during oxidative drug metabolism. Annu. Rev. Pharmacol. Toxicol. 23, 481-503.

79. Mico, B.A., Federowicz, D.A., Burak, E., and Swagzdis, J.E. (1987). In vivo inhibition of phenacetin by suicide substrate 1-aminobenzotriazole. Drug Metab. Dispos. 15, 274-276.

80. Foster, D.H., and Boston, R.C. (1983). The use of computers in compartmental analysis: The SAAM and CONSAM programs. In: Compartmental Distribution of Radiotracers (J. Robertson, ed.), pp. 73-142, Cleveland: CRC Press.

81. Berman, M., Beltz, W.F., Greif, P.C., Chabay, R., and Boston, R.C. (1983). CONSAM User's Guide (U.S. Dept. of Health and Human Services, Public Health Service, and National Institutes of Health), Washington: U.S. Government Printing Office.

82. Berman, M., and Weiss, M.F. (1983). SAAM Manual (Simulation, Analysis and Modelling) Dept. of Health, Education and Welfare Publication No. (NIH) 78-180, Washington: U.S. Government Printing Office.

83. Guy, R.H., Hadgraft, J., and Maibach, H.I. (1985). Percutaneous absorption in man: A kinetic approach. Toxicol. Appl. Pharmacol. 78, 123-129.

84. Guy, R.H., and Hadgraft, J. (1985). Pharmacokinetic interpretation of the plasma levels of clonidine following transdermal delivery. J. Pharm. Sci. 74, 1016-1018.

85. Guy, R.H., and Hardgraft, J. (1984a). Prediction of drug disposition kinetics in skin and plasma following topical administration. J. Pharm. Sci. 73, 883-887.

86. Guy, R.H., Hadgraft, J., and Maibach, H.I. (1982a). A pharmacokinetic model for percutaneous absorption. Int. J. Pharmaceut. 11, 119-129.

87. Freinkel, R.K. (1983). Carbohydrate metabolism of the epidermis. In: Biochemistry and Physiology of the Skin I (L.A. Goldsmith, ed.), pp. 328-337, New York: Oxford University Press.

88. Freinkel, R.K., and Traczyk, T.N. (1976). Patterns of glucose catabolism during differentiation of fetal rat epidermis. J. Invest. Dermatol. 67, 577-581.

89. Mehendale, M.H. (1982). Isolated organ techniques in toxicology. In: Principles and Methods of Toxicology (A.W. Hayes, ed.), pp. 509-557, New York: Raven Press.

90. Wester, R.C., Noonan, P.K., Cole, M.P., and Maibach, H.I. (1977a). Percutaneous absorption of testosterone in the newborn rhesus monkey: Comparison to the adult. Ped. Res. 11, 737-739.

91. Wester, R.C., Noonan, P.K., and Maibach, H.I. (1977b). Frequency of application on percutaneous absorption of hydrocortisone. Arch. Dermatol. 113, 620-622.

92. Maibach, H.I., and Feldmann, R.J. (1969). Effect of applied concentration on percutaneous absorption in man. J. Invest. Dermatol. 52, 382.

93. Scheuplein, R.J. and Ross, L.W. (1974). Mechanism of percutaneous absorption. V. Percutaneous absorption of solvent deposited solids. J. Invest. Dermatol. 62, 353-360

94. Rougier, A., Dupuis, D., Lotte, C., Roguet, R., Wester, R.C., and Maibach, H.I. (1986). Regional variation in percutaneous absorption in man: Measurement by the stripping method. Arch. Dermatol. Res. 278, 465-469.

95. Rougier, A., Lotte, C., and Maibach, H.I. (1987). The hairless rat: A relevant animal model to predict in vivo percutaneous absorption in humans? J. Invest. Dermatol. 88, 577-581.

96. Wester, R.C., and Maibach, H.I. (1985). In vivo percutaneous absorption and decontamination of pesticides in humans. J. Toxicol. Environ. Health 16, 25-37.

97. Maibach, H.I., Feldmann, R.J., Milby, T.H., and Serat, W.F. (1971). Regional variation in percutaneous penetration in man. Arch. Environ. Health 23, 208-211.

98. Feldmann, R.J., and Maibach, H.I. (1967). Regional variation in percutaneous penetration of 14C-cortisol in man. J. Invest. Dermatol. 48, 181-183.

99. Wester, R.C., Noonan, P.K., and Maibach, H.I. (1980). Variations in percutaneous absorption of testosterone in the rhesus monkey due to anatomic site of application and frequency of application. Arch. Dermatol. Res. 267, 229-235.

100. Britz, M.B., Maibach, H.I., and Anjo, D.M. (1980). Human percutaneous penetration of hydrocortisone: The vulva. Arch. Dermatol. Res. 267, 313-316.

101. Noonan, P.K. and Wester, R.C. (1980). Percutaneous absorption of nitroglycerin. J. Pharm. Sci. 69, 365-366.

102. Horhota, S.T., and Fung, H.-L. (1978). Site dependence for topical absorption of nitroglycerin in rats. J. Pharm. Sci. 67, 1345-1346.

103. Kao, J., and Hall J. (1987). Skin absorption and cutaneous first pass metabolism of topical steroids: In vitro studies with mouse skin in organ culture. J. Pharmacol. Exp. Ther. 241, 482-487.

104. Kao, J., Patterson, F.K. and Hall, J. (1985). Skin penetration and metabolism of topically applied chemicals in six mammalian species, including man: An in vitro study with benzo[a]pyrene and testosterone. Toxicol. Appl. Pharmacol. 81, 502-516.

105. Gomez, E.C., and Hsia, S.L. (1968). In vitro metabolism of testosterone-4-^{14}C and 4-androstene-3,17-dione-4-^{14}C in human skin. Biochemistry 7, 24-32.

106. Fredriksson, T., Farrior, W.L., and Witter, R.F. (1961). Studies on the percutaneous absorption of parathion and paraoxon. I. Hydrolysis and metabolism within the skin. Acta Dermato-Venereol. 41, 335-343.

107. Riviere, J.E., Bowman, K.F., and Monteiro-Riviere, N.A. (1987a). On the definition of viability in isolated perfused skin preparations. Br. J. Dermatol. 116, 739-741.

108. Carver, M.P., Levi, P.E., and Riviere, J.E. (1988). Significant first-pass bioactivation of parathion (P) during percutaneous absorption in the isolated perfused porcine skin flap (IPPSF). The Toxicologist 8, 125.

109. Riviere, J.E., Carver, M.P., Monteiro, N.A., and Bowman, K.I. (1987b). Percutaneous absorption of organophosphates, steroids, caffeine, and benzoic acid in vivo and in vitro using the isolated perfused porcine skin flap (IPPSF). In: Proceedings of the Sixth Medical Chemical Defense Bioscience Review, pp. 763-766, Columbia, Maryland: Johns Hopkins Applied Physics Laboratory.

110. Hiernickel, H. (1985). An improved method for in vitro perfusion of human skin. Br. J. Dermatol. 112, 299-305.

111. Carver, M.P., Monteiro-Riviere, N.A., Rogers, R.A., Bowman, K.F., and Riviere, J.E. (1987). Percutaneous absorption kinetics of organophosphates, steroids, caffeine, and benzoic acid in the isolated perfused porcine skin flap (IPPSF). The Toxicologist 7, 244.

112. Carver, M.P., Bowman, K.F., Monteiro-Riviere, N.A., Rogers, R.A., and Riviere, J.E. (1986). Percutaneous absorption of caffeine and malathion in the isolated perfused porcine skin flap (IPPSF). The Toxicologist 6, 243.

113. Riviere, J.E., Monteiro, N.A., Bowman, K.F., Carver, M.P., Scheidt, V.J., and Manning, T.O. (1986c). Research methods for percutaneous absorption. JAVMA 189, 355.

114. Guy, R.H., and Hadgraft, J. (1984b). Pharmacokinetics of percutaneous absorption with concurrent metabolism. Int. J. Pharmaceut. 20, 43-51.

115. Franz, T.J. (1975). Percutaneous absorption. On the relevance of in vitro data. J. Invest. Dermatol. 64, 190-195.

116. Wojciechowski, Z., Pershing, L.K., Huether, S., Leonard, L., Burton, S.A., Higuchi, W.I., and Krueger, G.G. (1987). An experimental skin sandwich flap on an independent vascular supply for the study of percutaneous absorption. J. Invest. Dermatol. 88, 439-446.

117. Krueger, G.G., Wojceichowski, Z.J., Burton, S.A., Gilhar, A., Huether, S.E., Leonard, L.G., Rohr, U.D., Petelenz, T.J., Higuchi, I., and Pershing, L.K. (1985). The development of a rat/human skin flap served by a defined and accessible vasculature on a congenitally athymic (nude) rat. Fund. Appl. Toxicol. 5, S112-121.

118. Roberts, M.S., and Horlock, E. (1978). Effect of repeated skin application on percutaneous absorption of salicylic acid. J. Phar. Sci. 67, 1685-1687.

119. Chytkowski, A., Panczenko, B., Krupinska, J., Bieron, K., and Zmuda, A. (1970). Circulatory actionof 7(beta-methyl, thio-ethyl)- theophylline. Diss. Pharm. Pharmacol. 22, 199-207.

120. Anrep, G.V., and Stacey, R.F. (1927). Comparative effect of various drugs upon the coronary circulation. J. Physiol. 64, 187-192.

121. Kalsner, S. (1971). Mechanism of potentiation of contractor responses to catecholamines by methylxanthines in aortic strips. Br. J. Pharmacol. 43, 379-388.

122. Pershing, L.K., Conklin, R.L., and Krueger, G.G. (1986a). Effects of reduced body temperature on blood flow and percutaneous absorption of 14C benzoic acid across grafted nude rat skin. Clin. Res. 34, 418A.

123. Wojciechowski, Z.J., Burton, S.A., Petelenz, T.J., and Krueger, G.G. (1985). Role of microcirculation in percutaneous absorption. Clin.Res. 33, 696A.

124. Scheuplein, R.J., and Blank, I.H. (1971). Permeability ofthe skin. Physiol. Rev. 51, 702-747.

125. Spencer, T.S., Linamen, C.E., Akers, W.A., and Jones, H.E. (1975). Temperature dependence of water content of stratum corneum. Br. J. Dermatol. 93, 159-164.

126. Middleton, J.D. (1968). The mechanism of water binding in stratum corneum. Brit. J. Dermatol. 80, 437-450.

127. Vinson, L.J., Singer, E.J., Koehler, W.R., Lehman, M.D., and Masurat, T. (1965). The nature of the epidermal barrier and some factors influencing skin permeability. Toxicol. Appl. Pharmacol. 7 (Suppl.2), 7-19.

128. Danon, A., BenoShimon, S., and Ben-Zvi, Z. (1986). Effect of exercise and heat exposure on percutaneous absorption of methyl salicylate. Eur. J. Clin. Pharmacol. 31, 49-52.

129. Barkve, T.F., Langseth-Manrique, K., Bredesen, J.E., and Gjesdal, K. (1986). Increased uptake of transdermal glyceryl trinitrate during physical exercise and during high ambient temperature. Am. Heart J. 112, 537-541.

130. Craig, F.M., Cummings, E.G., and Sim, V.M. (1977). Environmental temperature and the percutaneous absorption of a cholinesterase inhibitor, VX. J. Invest, Dermatol. 68, 357-361.

131. Spear, R.C., Popendorf, W.J., Leffingwell, J.T., Milby, T.H., Davies, J.E., and Spencer, W.F. (1977a). Fieldworkers' response to weathered residues of parathion. J. Occup. Med. 19, 406-410.

132. Spear, R.C., Popendorf, W.J., Spencer,W.F., and Milby, T.H. (1977b). Worker poisonings due to paraoxon residues. J. Occup. Med 19, 411-414.

133. Neal, R.A., and Dubois, K.P. (1965). Studies on the mechanism of detoxification of cholinergic phosphorothioates. J. Pharmacol. Exp. Ther. 148, 185-192.

134. Davison, A.N. (1955). The conversion of Schradan (OMPA) and parathion into inhibitors of cholinesterase by mammalian liver. Biochem. J. 61, 203-209.

135. Wallace, K.B., and Dargan, J.E. (1987). Intrinsic metabolic clearance of parathion and paraoxon by livers from fish and rodents. Toxicol. Appl. Pharmacol. 90, 235-242.

136. Wolcott, R.M., Vaughr, W.K., and Neal, R.A. (1972). Comparison of the mixed function oxidase-catalyzed metabolism of a series of dialkyl p-nitrophenyl phosphorothionates. Toxicol. Appl. Pharmacol. 22, 213-220.

137. Neal, R.A. (1972). A comparison of the in vitro metabolism of parathion in the lung and liver of the rabbit. Toxicol. Appl. Pharmacol. 23, 123-130.

138. Lauwerys, R.R., and Murphy, S.D. (1969). Interaction between paraoxon and tri-o-tolyl phosphate in the rats. Toxicol. Appl. Pharmacol 14, 348-357.

139. Schaefer, H., Stuttgen, G. Zesch, A., Schalla, W., and Gazith, J. (1978). Quantitative determination of percutaneous absorption of radiolabelled drugs in vitro and in vivo by human skin. Curr. Prob. Dermatol 7, 80-94.

140. Holland, J.M., Kao, J.Y. and Whitaker, M.J. (1984). A multisample apparatus for kinetic evaluation of skin penetration in vitro: The influence of viability and metabolic status of the skin. Toxicol. Appl. Pharmacol. 72, 272-280.

141. Smith, L.H., and Holland, J.M. (1981). Interaction between benzo[a]-pyrene and mouse skin in organ culture. Toxicology 21, 47-57.

142. Kao, J., Hall, J. Shugart, L.R., and Holland, J.M. (1984). An _in vitro_ approach to studying cutaneous metabolism and disposition of topically applied xenobiotics. _Toxicol. Appl. Pharmacol._ **75**, 289-293.

143. Pohl, R.J., Philpot, R.M., and Fouts, J.R. (1976). Cytochrome P-450 content and mixed-function oxidase activity in microsomes isolated from mouse skin. _Drug Metab. Dispos._ **4**, 442-450.

144. Merk, H., Rumpf, M., Bolsen, K., Wirth, G., and Goerz, G. (1884). Inductibility of arylhydrocarbon-hydroxylase activity in human hair follicles by topical application of liquor carbonis detergens (coal tar). _Br. J. Dermatol._ **111**, 279-284.

145. Sulatos, L.G. (1987). The role of the liver in mediating the acute toxicity of the pesticide methyl parathion in the mouse. _Drug Metab. Dispos._ **15**, 613-617.

146. Maibach, H.I., and Feldman, R. (1974). Systemic absorption of pesticides through skin of man. In: _Occupational Exposure to Pesticides_, Appendix B, pp. 120-127, Washington: U.S. Government Printing Office.

147. NIOSH report (1976). _Criteria for a Recommended Standard... Occupational Exposure to Parathion_. Washington: U.S. Government Printing Office.

148. Milby, T.F., Bailey, J.B., Davies, J.E., Guthrie, F.E., Hays, H.W., Long, K.R., May, J., and Wymer, W.H. (1974). _Occupational Exposure to Pesticides. Report to the Federal Working Group from the Task Force on Occupational Exposure to Pesticides_. pp.1-144 Washington: U.S. Government Printing Office.

149. Guthrie, F.E. (1980). Pesticides and humans. In: _Introduction to Environmental Toxicology_ (F.E. Guthrie and J.J. Perry, eds.), pp. 299-312, New York: Elsevier North Holland.

150. Stevenson, D.E. (1966). The assessment of possible health hazards associated with the use of pesticides. _Chem. Indus._ **No. 17**, 690-694.

151. Abrams, H.K., Hamblin, D.O., and Marchan, J.F. (1950). Pharmacology and toxicology of certain phosphorus insecticides. Clinical experience. _JAVMA_ **144**, 107-108.

152. Wolfe, H.R., Armstrong, J.F., Staiff, D.C., Comer, S.W., and Durham, W.F. (1975). Exposure of apple thinners to parathion residues. _Arch. Environ. Health_ **14**, 622-633.

153. Durham, W.F., Wolfe, H.R., and Elliot, J.W. (1972). Absorption and excretion of parathion by spraymen. Arch. Environ. Health **24**, 381-387.

154. Wolfe, H.R., Durham, W.F., and Armstrong, J.F. (1967). Exposure of workers to pesticides. Arch. Environ. Health **14**, 622-633.

155. Wolfe, H.R., Armstrong, J.F., and Durham, W.F. (1966). Pesticide exposure from concentrate spraying. Arch. Environ. Health **13**, 340-344.

156. Durham, W.F. (1965). Pesticide exposure levels in man and animals. Arch. Environ. Health **10**, 884-885.

157. Sompson, G.R. (1965). Exposure to orchard pesticides. Arch. Environ. Health **10**, 884-885.

158. Winteringham, F.P.W. (1969). Mechanisms of selectiove insecticidal action. Annu. Rev. Entomol. **14**, 409-442.

159. Andersen, M.E., and Keller, W.C. (1984). Toxicokinetic principles in relation to percutaneous absorption and cutaneous toxicology. IN: Cutaneous Toxicity (V.A. Drill and P. Lazer, eds.), pp. 9-28, New York: Raven Press.

160. Wester, R.C., and Maibach, H.I. (1984). Advances in percutaneous absorption. In: Cutaneous Toxicity (V.A. Drill and P. Lazar, eds.), pp. 29-40. New York: Raven Press.

161. Manning, P.J., Millikan, L.E., Cox, V.A., Carey, K.D., and Hook, R.R. (1974). Congenital cutaneous and visceral melanomas of sinclair miniature swine. J. Nat. Cancer Inst. **52**, 1559-1565.

CONTRACT NO. DAMD 17-84-C-4103
U. S. ARMY MEDICAL RESEARCH AND DEVELOPMENT COMMAND

STANDARD OPERATING PROCEDURE FOR PREPARATION OF
IN VITRO ISOLATED PERFUSED PORCINE SKIN FLAPS
(IPPSF) FOR PERCUTANEOUS ABSORPTION STUDIES

K. F. Bowman, DVM, MSc, Diplomate ACVS, Diplomate ABVP
N. A. Monteiro-Riviere, PhD
J. E. Riviere, DVM, PhD

From the Laboratory of Surgical Research (Bowman), Department of
Food Animal and Equine Medicine, the Laboratory of Comparative
Dermatology (Monteiro-Riviere), and the Laboratory of
Toxicokinetics (Riviere), Department of Anatomy, Physiological
Sciences, and Radiology, School of Veterinary Medicine, North
Carolina State University, 4700 Hillsborough Street, Raleigh, NC
27606

The surgical techniques for preparation of a novel in vitro alternative animal model, the isolated perfused porcine skin flap (IPPSF), for percutaneous absorption studies are described in this paper. Specifically, a single-pedicle, axial pattern tubed skin flap will be raised in operation (stage 1 procedure), it will survive to its entire length, and it will be harvested 2 days later (stage 2 procedure) for transfer to the in vitro isolated organ perfusion chamber[1-4, a-d].

Method

Pigs weighing 18 to 32 kg are premedicated with atropine sulfate (0.04 mg/kg i.m.) and xylazine hydrochloride[e] (0.2 mg/kg i.m.). Anesthesia is induced with ketamine hydrochloride (11 mg/kg i.m.) and maintained with halothane delivered by endotracheal tube. Each pig is prepared for routine aseptic surgery in the caudal abdominal and inguinal regions. The proposed skin incisions and reference marks for wound margin alignment and skin flap retraction/expansion studies[4] are outlined in the caudolateral epigastic region using a sterile marking pen (Figure 1). The skin incisions are made in order (medial, cranial, lateral, and caudal) and extended to the level of the muscular fascia. Craniomedial branches of the caudal superficial epigastric artery (CSEa) that supply the caudal mammae are ligated and divided. Using skin hooks, the wound margins of the medial incision are retracted for direct visualization of the CSEa (Figure 2), allowing scalpel dissection of the subcutaneous tissue and skin flap elevation without vascular damage (Figure 3). The caudal incision is apposed and sutured with size 3-0 polypropylene suture, using modified 3-point sutures to anchor the corners and simple continuous pattern for the included wound margins (Figure 4). The tubed skin flap is formed and trimmed minimally of fat at its edges, if necessary. Tubed flap skin edges are closed using size 3-0 polypropylene in a simple continuous pattern (Figure 5). Starting 2.5 cm cranial to the base of the tubed skin flap, the deep subcutaneous tissues are apposed with 5-7 interrupted sutures using size 2-0 chromic gut. The superficial subcutaneous tissue is closed with size 2-0 chromic gut in a simple continuous pattern (Figure 6). The remaining skin incisions are closed routinely using size 2-0 nylon. (Figure 7).

Using previously described photographic methods[5] fluorescein angiograms are evaluated 12 minutes after infusion of 5 ml of 10% fluorescein[f] for prediction of surviving length of the tubed skin flaps (Figure 8). Thereafter, the surgical site and tubed skin flap are bandaged with a self-adherent wound dressing[g] reinforced with size 2-0 nylon in a continuous cruciate pattern. Each pig is reinforced with size 2-0 nylon in a continuous cruciate pattern. Each pig is recovered from anesthesia and housed individually.

Healing of the single pedicle, axial pattern tubed skin flap is evaluated by visual inspection, fluorescein angiography, and determination of tissue surface area change during the postoperative period.

Routine cannulation of the CSEa and harvest of a single-pedicle, axial pattern tube flap is done in the second surgical procedure. Each pig is premedicated, induced, and maintained on anesthesia as described above. Visual inspection is performed to ascertain that each single pedicle, axial pattern tubed skin flap raised during stage 1 procedure has survived to its entire length. The caudal abdominal and inguinal regions of each pig is prepared for routine aseptic surgery. A skin incision measuring 6 cm is made in the inguinal region that extends caudally from the base of the tubed flap (Figure 9). Using blunt dissection, the incision is deepened to the level of the superficial inguinal lymph node, thereby exposing the CSEa, which emerges from its deep surface. Each pig is heparinized (3,000 IU i.v.) and the exposed vasculature is bathed with 1-2 ml of 2% lidocaine hydrochloride to minimize vasospasm during subsequent manipulations. The surgeon, aided visually by 2.3x microsurgical lenses[h], isolates the CSEa between two stay sutures of size 3-0 polypropylene. An opening in the wall of the CSEa is established and extended, using Potts cardiovascular scissors[i] (Figure 10a). The CSEa is cannulated with size PE20 polyethylene tubing, which is secured by stay sutures (Figure 10b). The venae commitantes may be cannulated using a commercially-available microcatheter[j]. The patient side of the pedicle containing the caudal superficial epigastric vasculature is cross-clamped and the tubed skin flap is resected (Figure 11a). Heparinized, 0.9% normal saline solution (approximately 20 ml) is infused via the arterial cannula to clear the tubed skin flap of blood and establish that patency of the venae commitantes remains. The tubed skin flap is transferred to an assistant for transport to the isolated organ perfusion laboratory. The vascular pedicle is double ligated with size 0 chromic gut. The wound is flushed and inspected to assure adequate hemostasis and ventral drainage (Figure 11b). Each pig is recovered from anesthesia and the wound is allowed to heal by granulation and contraction. Any remaining skin sutures are removed 7-10 days following the stage 1 procedure.

Comments:

Following harvest, tubed skin flaps are transferred to a computer-controlled, temperature-regulated perfusion chamber for 10-12 hr. studies (Figure 12). Perfusate consists of Krebs-Ringer bicarbonate buffer (pH 7.4) containing albumin and glucose. Media is gassed with a mixture of 95% oxygen and 5% carbon dioxide using a silastic tube oxygenator. Viability of IPPSF is assessed by glucose utilization, lactate production, an absence of significant concentrations of the intracellular enzyme lactate dehydrogenase in the perfusate, and light and electron

microscopy. An overall mean lactate to glucose ratio of 1.7 for harvested flaps suggests that anaerobic glycolysis is the primary metabolic pathway for IPPSF.

At present, it has been found that a 10 - 12 hr. period is adequate for percutaneous absorption studies, and preliminary experiments involving caffeine and malathion indicate that these compounds are capable of penetrating into the perfusate following topical application to the IPPSF[1 - 4, a - d].

Moderate edema of the tubed skin flap for 24 - 48 hours following stage 1 procedure does not affect its ability to survive to its entire length, nor its suitability for use in percutaneous absorption studies. The presence of edema indicates that variable degrees of venous compromise, most likely due to altered venous circulation and the dependent position of the tubed skin flap are occurring. The relative contributions of these factors or others to edema formation are not known and fortunately, this information has not been needed, especially since correction factors for skin surface area are available (Table 1). However, some degree of epidermal necrosis, followed by second intention healing will occur, if excessive subcutaneous tissue is included within the tubed skin flap. It has been found that pigs weighing in excess of 35 kg are not suitable for preparation of single-pedicle, axial-pattern tubed skin flaps, because their subcutaneous fat deposits makes closure of the tubed skin flap difficult, even with maximal subcutaneous tissue debulking. Recently, we have begun to raise, harvest, and perfuse two IPPSF from the same pig simultaneously, a procedure that decreases inter-IPPSF variability and reduces further the costs with each experiment.

All stages of development of the surgical procedures for preparation of IPPSF have used fluorescein angiography to assess viability. Previously reported rapid photographic methods [5] have been modified successfully for use in our protocols. We have found no difference visually between fluorescein angiograms obtained at 12 versus 20 minutes postinfusion; therefore, we have standardized our fluorescein angiography protocol by obtaining baseline and 12-minute postinfusion photographs. It is likely that other fluorescein angiography protocols, especially those performed to obtain serial data during a short period, would require adjustment of the standardized photographic procedure.[6] Interestingly, subtle differences in skin fluorescence between individual preparations may be observed when fluorescein angiography is performed immediately following stage 1 procedure, eg, bright yellow versus muted yellow versus uneven distal staining[7] Similar to reports on axial pattern skin flaps in humans [7] our experience indicates that these flaps will survive to their entire length. Presently, fluorescein angiography is used only to assess viability immediately following stage 1 procedure. Subsequent studies are not done because survival of the tubed skin flap is evident visually and presence of residual fluorescein in the IPPSF vasculature may confound percutaneous absorption studies.

Selection of the 2-day interoperative period confers 2 technical advantages on the harvest of island tubed skin flaps. Since island tubed skin flaps are prepared by division of the skin bridge and extensive dissection of the subcutaneous pedicle, the stage 2 procedure proceeds quickly, because the skin incision may be done by finger dissection (see Figure 9b), and there is minimal subcutaneous dissection to be done prior to vascular cannulation. Obviously, longer periods between preparation and harvest of tubed skin flaps, which may be important for other skin biology studies, would allow healing of the skin and subcutaneous tissue bridge and invalidate, all or in part, the reasons for selection of the island configuration for the stage 1 procedure. The vascular dissection and cannulation are technically demanding procedures. Since the vessels to be cannulated are 0.5 - 2 mm in diameter, it is recommended strongly that the surgeon uses either magnifying lenses or a surgical microscope to aid visualization of the operative field. Initially, the stage 2 procedure was performed aseptically, and the wound was closed primarily. Since we have begun percutaneous absorption studies, tubed skin flaps are harvested following sterile water cleansings only, and the would is allowed to heal by granulation and contraction. It has been reasoned that use of topical antiseptics during (sterile) preparation of the operative site may affect adversely the percutaneous absorption studies. Stage 1 procedure has been and will continue to be performed aseptically.

Footnotes

[a] Monteiro-Riviere NA, Bowman KF, Riviere JE. Acute toxicity of sodium fluoride in an isolated perfused porcine skin flap (abstr). Pharmacologist 1985; 27:158.

[b] Bowman KF, Monteiro-Riviere NA, Riviere JE. The isolated perfused porcine skin flap: a novel model for skin biology (abstr). Vet Surg 1986; 15:114.

[c] Monteiro-Riviere NA, Bowman KF, Scheidt VJ, Dix LP, Riviere JE. Morphologic assessment of viability and toxicity in the isolated perfused porcine skin flap (abstr). Toxicologist 1986; 6:242.

[d] Carver MP, Bowman KF, Monteiro-Riviere NA, Rogers RA, Riviere JE. Percutaneous absorption of caffeine and malathion in the isolated perfused porcine skin flap (abstr). Toxicologist 1986; 6:242.

[e] Rompun[R], Bayvet Division, Miles Laboratories Inc, Shawnee, Kansas.

[f] Fluorescite Injection[R], Alcon Laboratories Inc, Fort Worth, Texas.

[g] Telfa [R] Adhesive Dressing, 4x8 in, catalog no. 5111, The Kendall Co, Boston, Mass.

[h] Gullstrand Binocular Loupe, catalog no. 17-1100, Scanlan Instruments, Englewood, Colo.

[i] Potts scissor, delicate, 45°, 7.0 in, catalog no. 640212, Edward Weck and Co, Research Triangle Park, NC.

[j] Microcath[R], 24 gauge x 3/4 in, Burron Medical Inc, Bethlehem, Penn.

References

1. Riviere JE, Bowman KF, Monteiro-Riviere NA. The isolated perfused porcine skin flap: a novel model for cutaneous toxicologic research. In: Tumbleson ME, ed. Swine in Biomedical research, ed. 2 New York: Plenum Publishing Corp 1986; 657-666.

2. Riviere JE, Bowman KF, Monteiro-Riviere NA, Dix LP, Carver MP. The isolated perfused porcine skin flap (IPPSF). I. a novel in vitro model for percutaneous absorption and cutaneous toxicology studies. Fundam Appl Toxicol 1986; 7:444-453.

3. Monteiro-Riviere NA, Bowman KF, Scheidt VJ, Riviere JE. The isolated perfused porcine skin flap (IPPSF). II. Ultrastructural and histological characterization of epidermal viability. In Vitro Toxicology 1987; 1:241-252.

4. Bowman KF, Monteiro-Riviere NA, Riviere JE. Development of surgical techniques for in vitro isolated perfused porcine skin flaps for percutaneous studies. Am J Vet Res 1986; acceppted.

5. Lanzafame RJ, Naim JO, Blackman JR, Welch E, Hinshaw JR. A method for documentation of tissue perfusion using instant photography. Surg Gynecol Obstetr 1983; 156:749-752.

6. Myers MB, Donovan W. An evaluation of eight methods of using fluorescein to predict the viability of skin flaps in the pig. Plast Reconstr Surg 1985; 75:245-250.

7. McGregor IA, Morgan G. Axial and random pattern flaps. Brit J Plast Surg 1973; 26:202-213.

Figures

Fig 1 - Stage 1 procedure. Proposed skin incisions and reference marks for wound margin alignment (A-A^1 and B-B^1) and skin flap surface area change studies are outlined in the caudolateral epigastric region. Notice the locations of the superficial inguinal lymph node, the caudal superficial epigastric artery, the caudal border of the cutaneous trunci muscle, and the anastomotic branch of the deep circumflex iliac vein. Following surgery, measurements of tip diameter (A-A$_1$), base diameter (B-B$_1$), and tube length (distance between A-A$_1$ and B-B$_1$) are recorded (See Table 1)

Fig 2 - Stage 1 procedure. Using skin hooks, the wound margins of the medial incision have been retracted for direct visualization of the caudal superficial epigastric artery (arrows). Notice the craniomedial branches of the caudal superficial epigastric artery supplying the caudal mammae that have been ligated and divided.

Fig 3 - Stage 1 procedure.

    a - Scalpel dissection of the subcutaneous tissue and skin flap elevation without damage to the direct cutaneous vasculature is done.

    b - Division of the skin bridge and extensive dissection of the subcutaneous tissue is done to create an island skin flap.

Fig 4 - Stage 1 procedure. The caudal incision is apposed and sutured, using modified 3-point sutures (inset) to anchor the corners.

Fig 5 - Stage 1 procedure. The tubed skin flap is formed, trimmed minimally of fat at its edges, if necessary, and closed.

Fig 6 - Stage 1 procedure.

    a,b - Starting 2.5 cm cranial to the base of the tubed skin flap (reference marks B-B^1), the subcutaneous tissues are closed with vertically-oriented, interrupted sutures.

    c - The superficial subcutaneous tissue is closed.

Fig 7 - Stage 1 procedure. The remaining skin incisions are closed. Notice the mattress-type suture used to appose the incision where the wound margins of the tubed skin flap and donor site meet (inset).

Fig 8 - Fluorescein angiography of island tubed skin flap (stage 1 procedure) immediately following surgery. Notice the variation in skin fluorescence, ie, bright yellow (Fig 8a), muted yellow (Fig 8b), and uneven distal staining (Fig 8c). All preparations survived to their entire length.

Fig 9 - Stage 2 procedure.

    a - A skin incision is made in the inguinal region that extends caudally from the base of the tubed skin flap. Using blunt dissection, the incision is deepened to the level of the superficial inguinal lymph node, thereby exposing the caudal superficial epigastric artery that emerges from its deep surface.

    b - Alternate method of skin incision and subcutaneous tissue dissection using gentle traction and finger dissection in day 2 island tubed skin flaps (See Comments)

Fig 10 - Stage 2 procedure.

    a - The caudal superficial epigastric artery is isolated between 2 stay sutures and an opening in the arterial wall is made.

    b - The artery is cannulated with polyethylene tubing and secured by stay sutures.

Fig 11 - Stage 2 procedure.

    a - The patient side of the vascular pedicle is cross clamped and the tubed skin flap is resected.

    b - The wound is flushed, inspected for hemorrhage, and allowed to heal by granulation and contraction.

Fig 12 - Schematic diagram of the isolated perfused porcine skin flap apparatus.
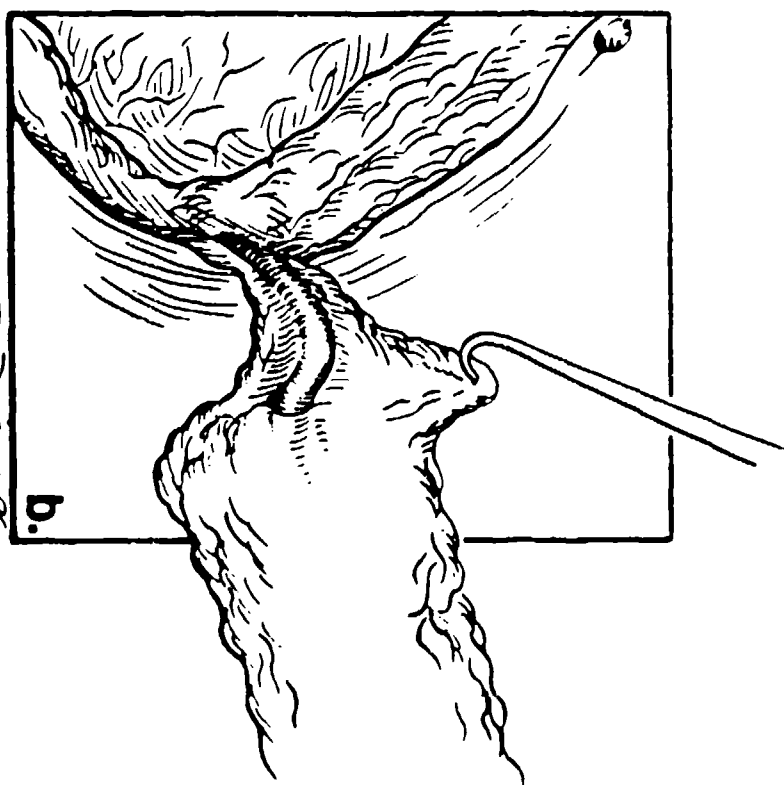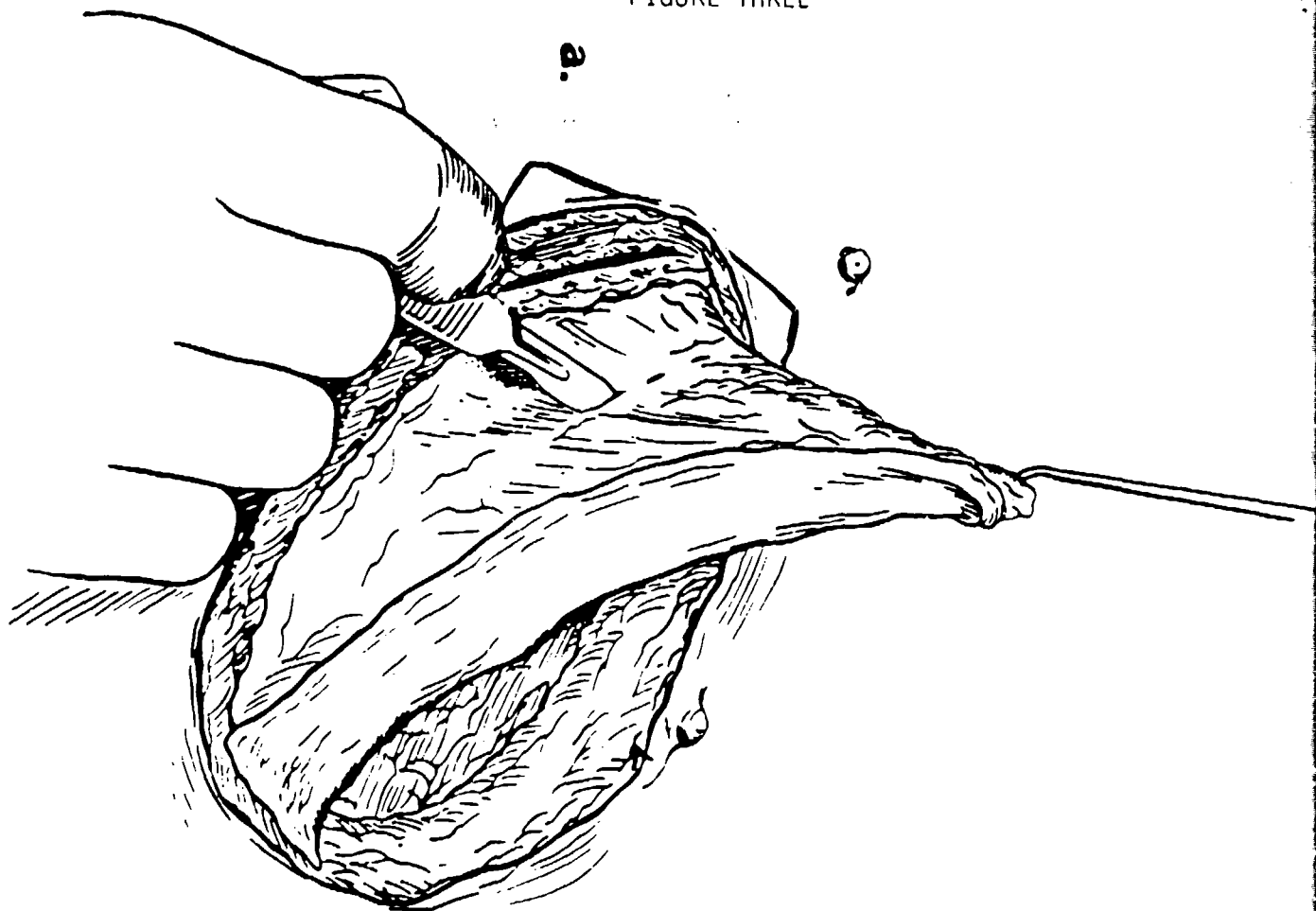
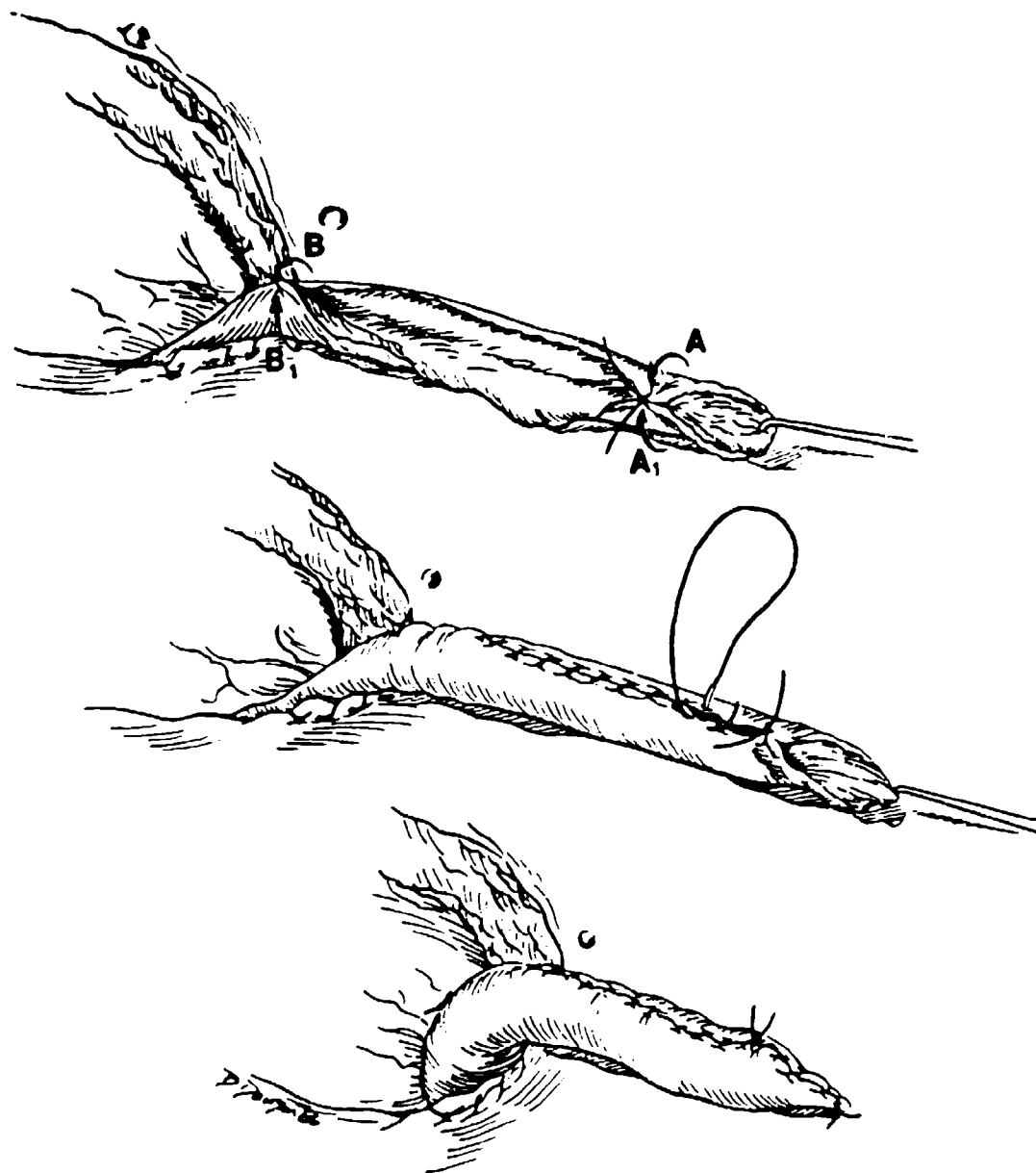FIGURE ONE
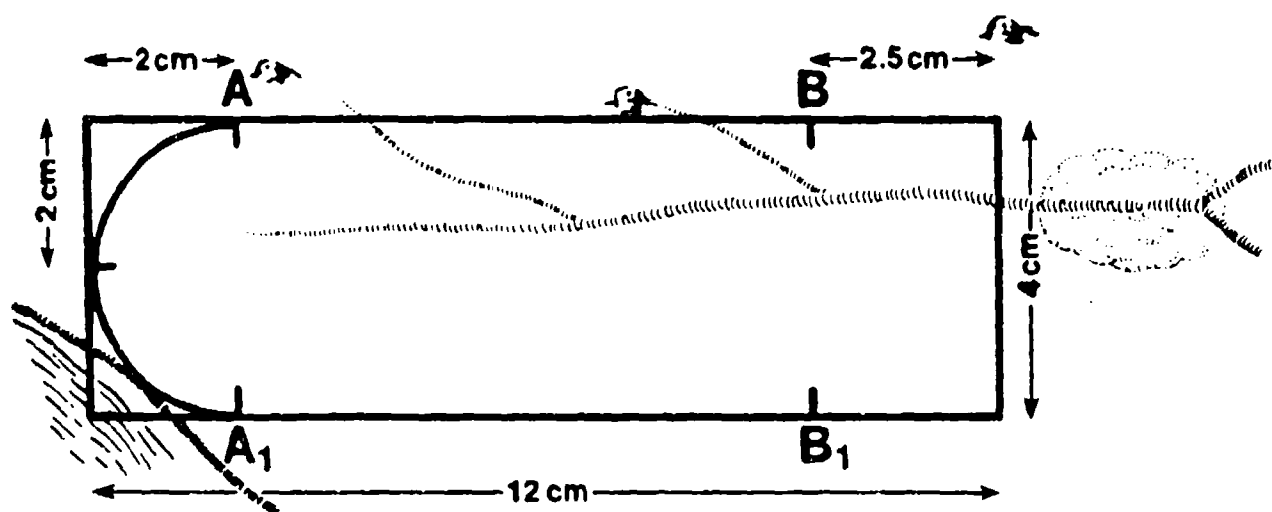
FIGURE TWO

FIGURE THREE
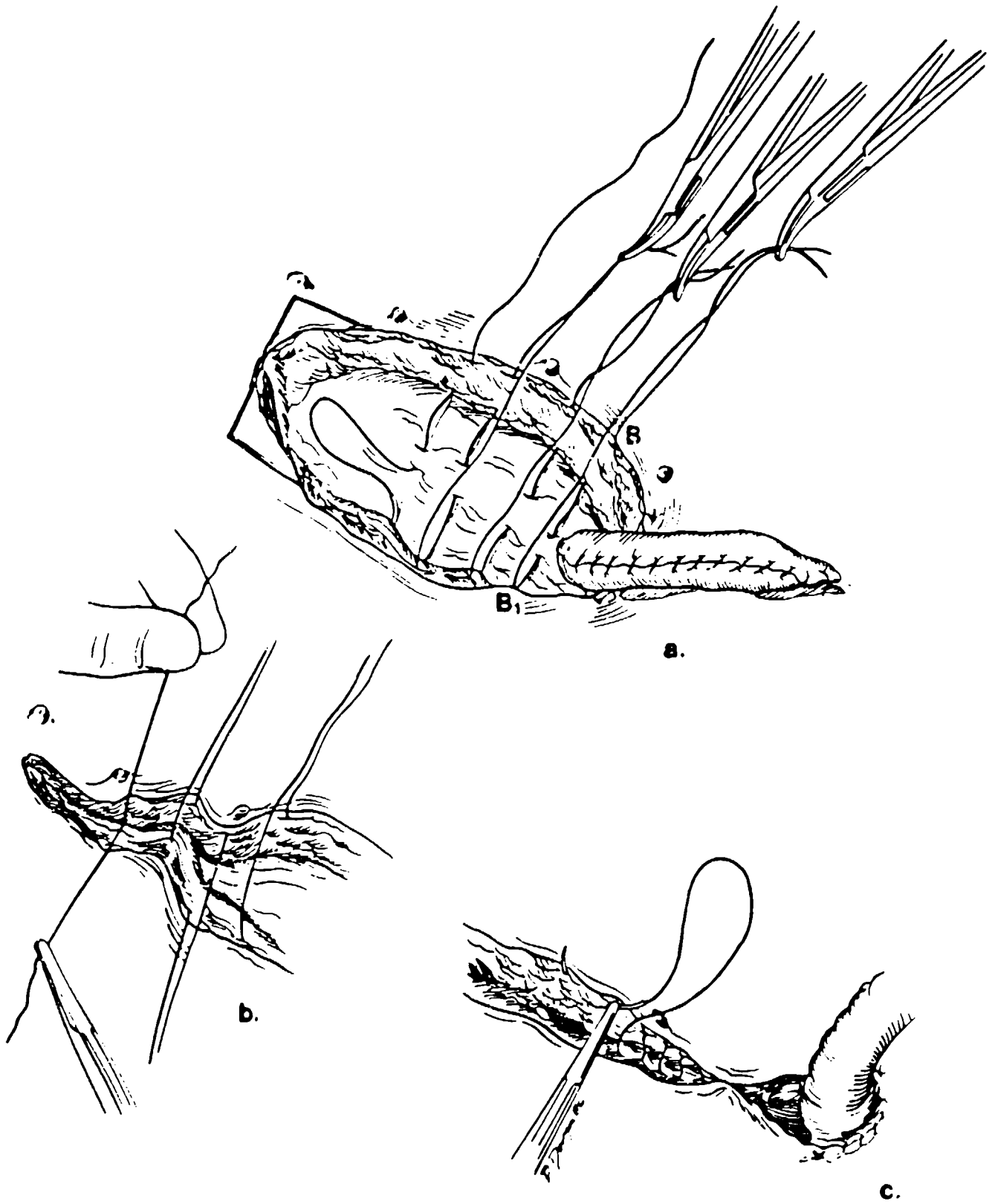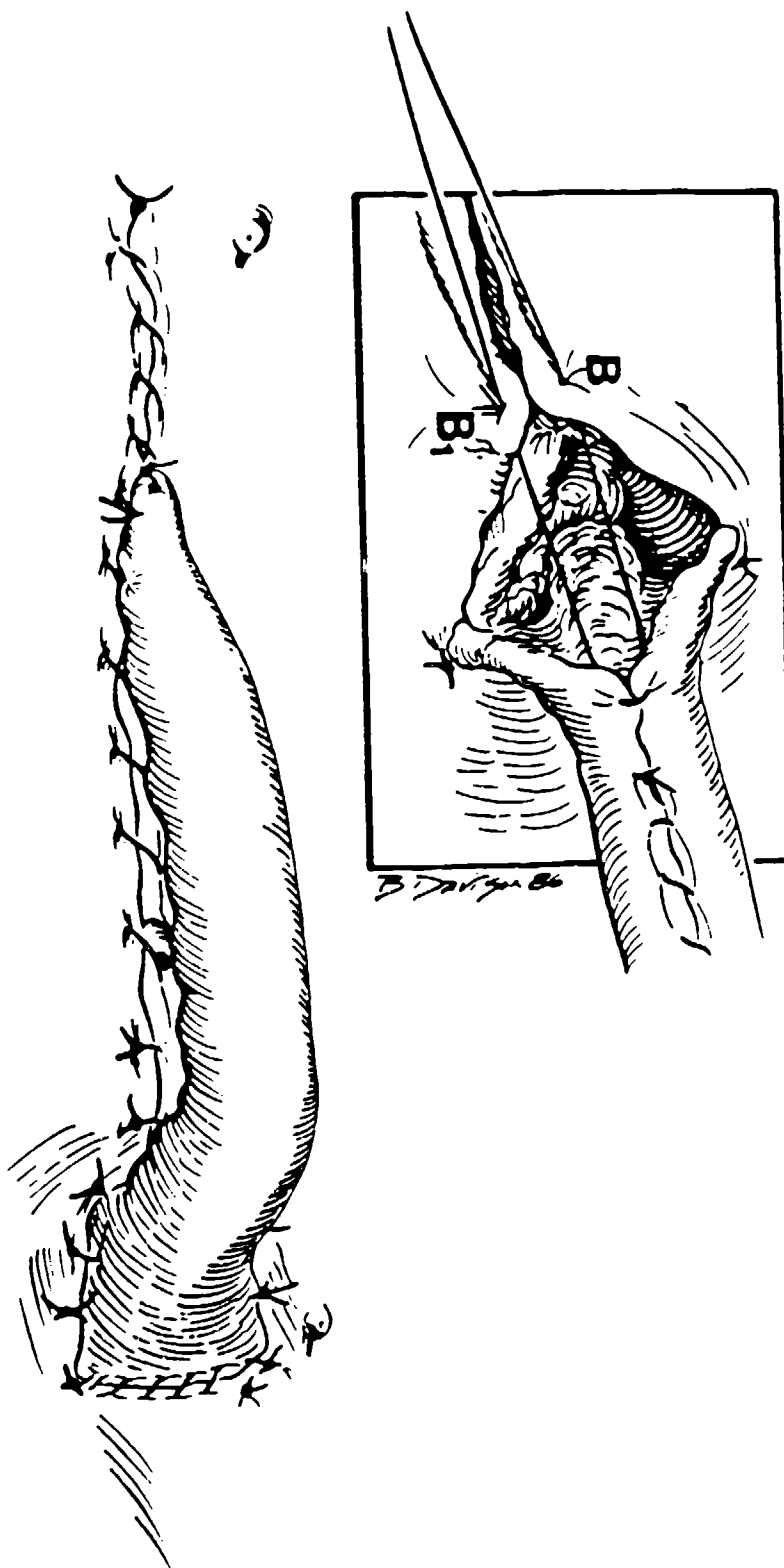
FIGURE FOUR

B Davign 86
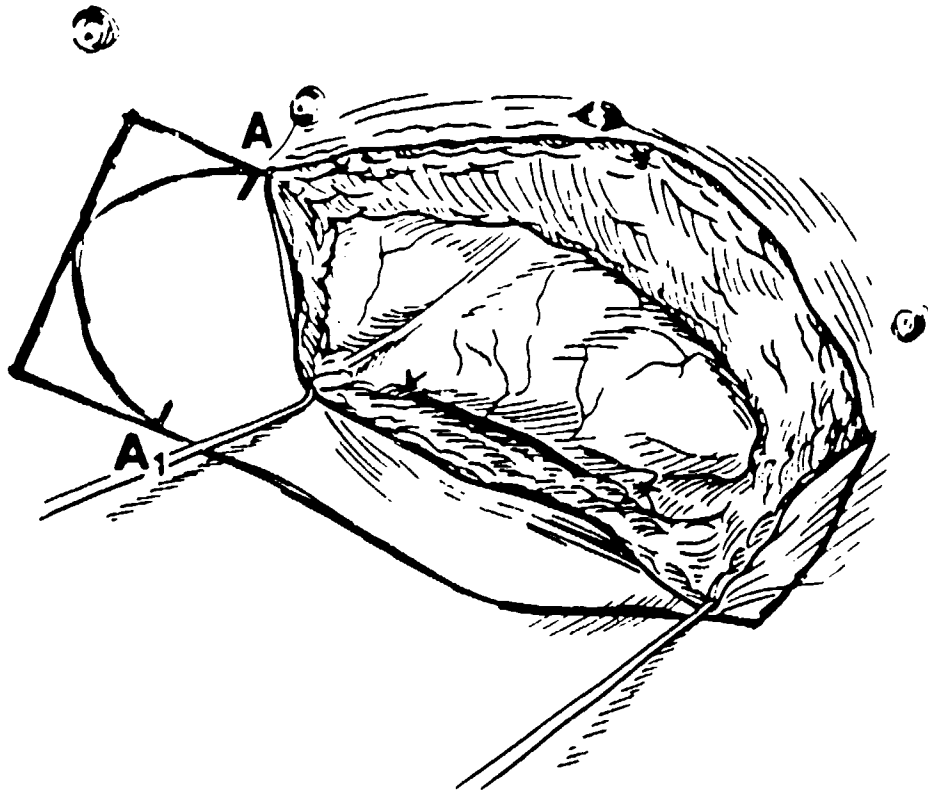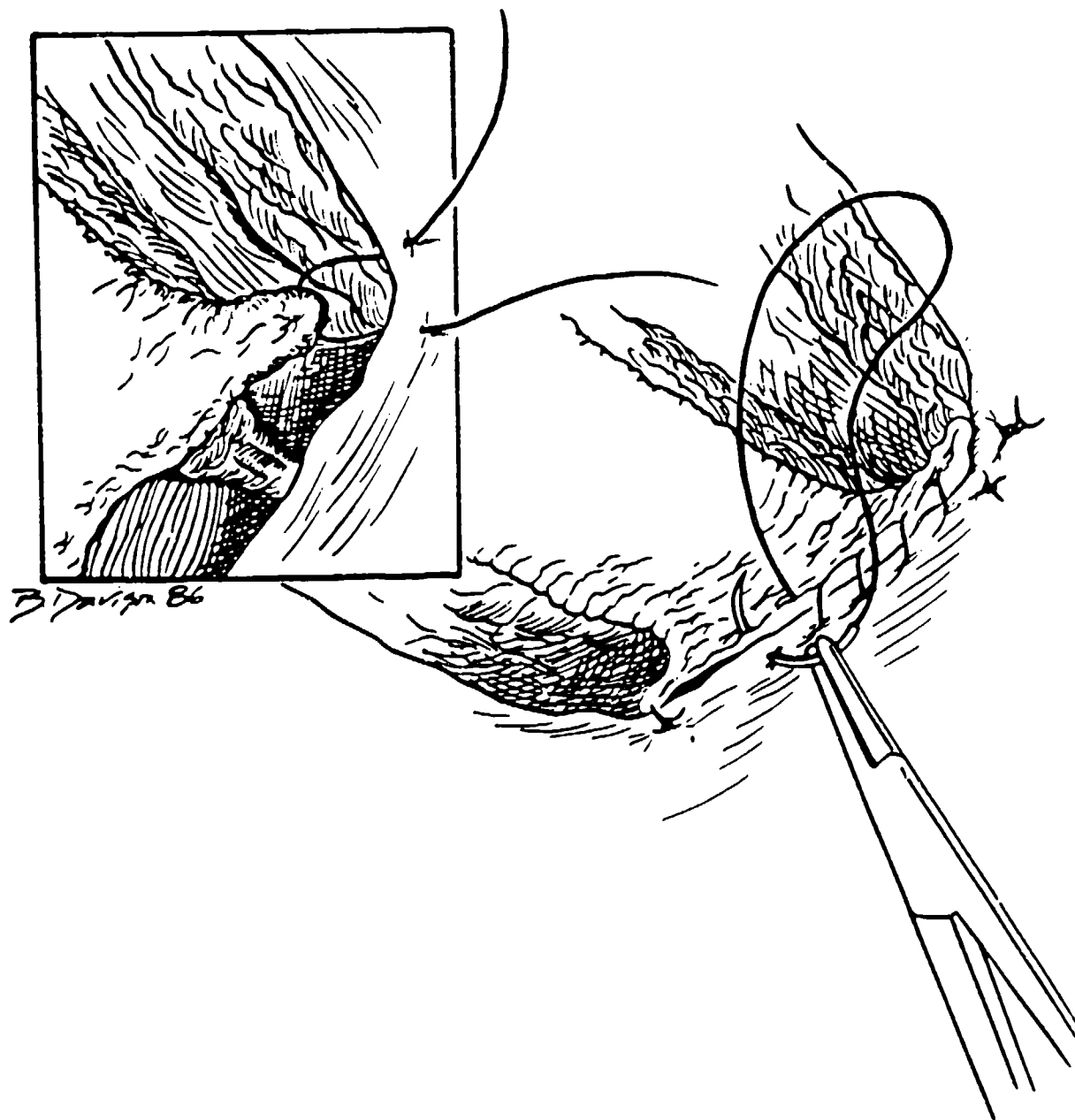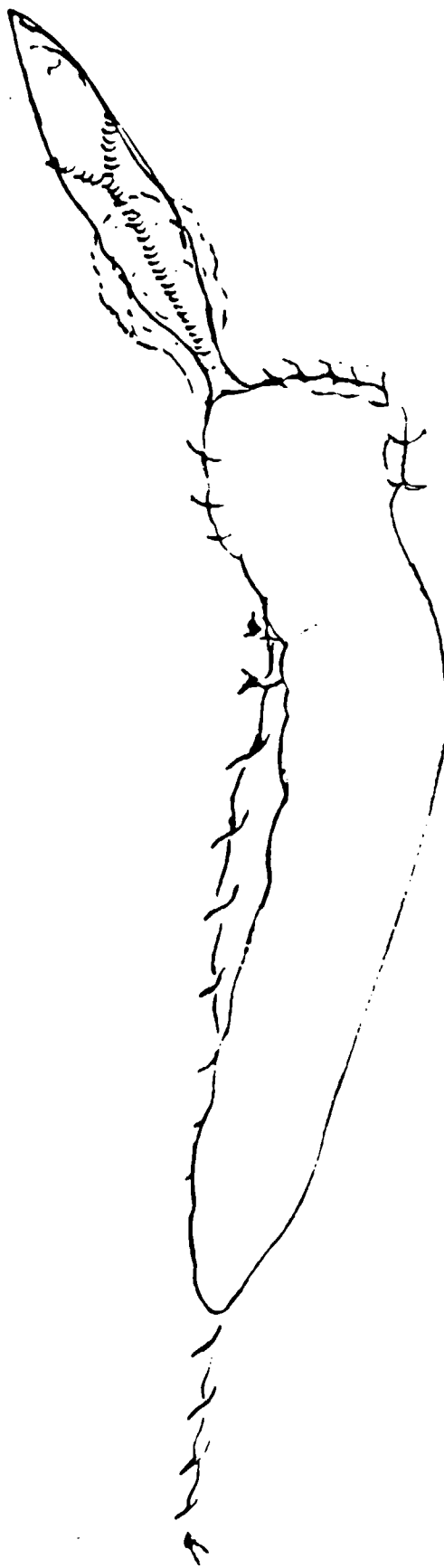
FIGURE FIVE

FIGURE SIX

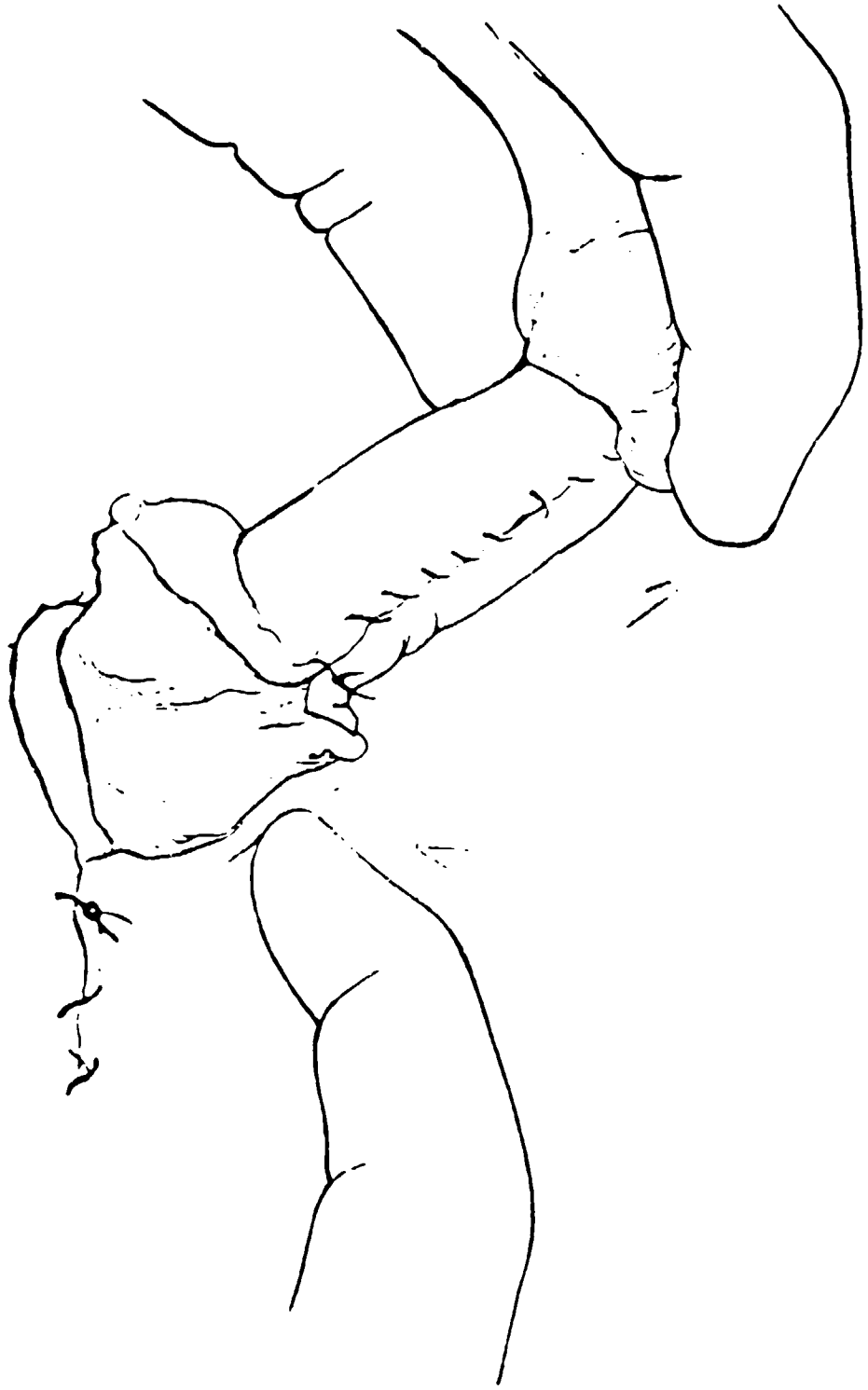

a.

b.

c.

FIGURE SEVEN

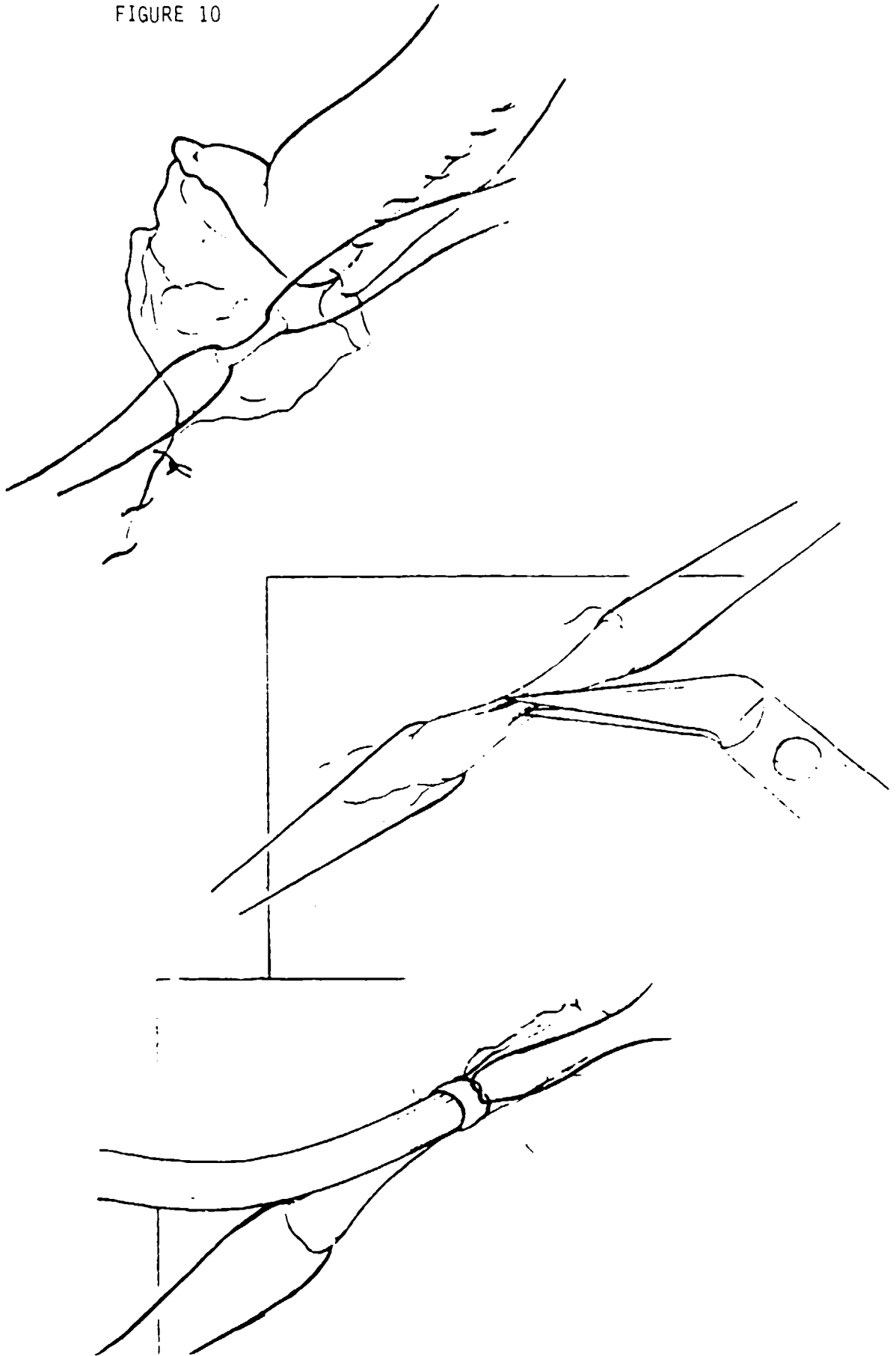FIGURE 9a

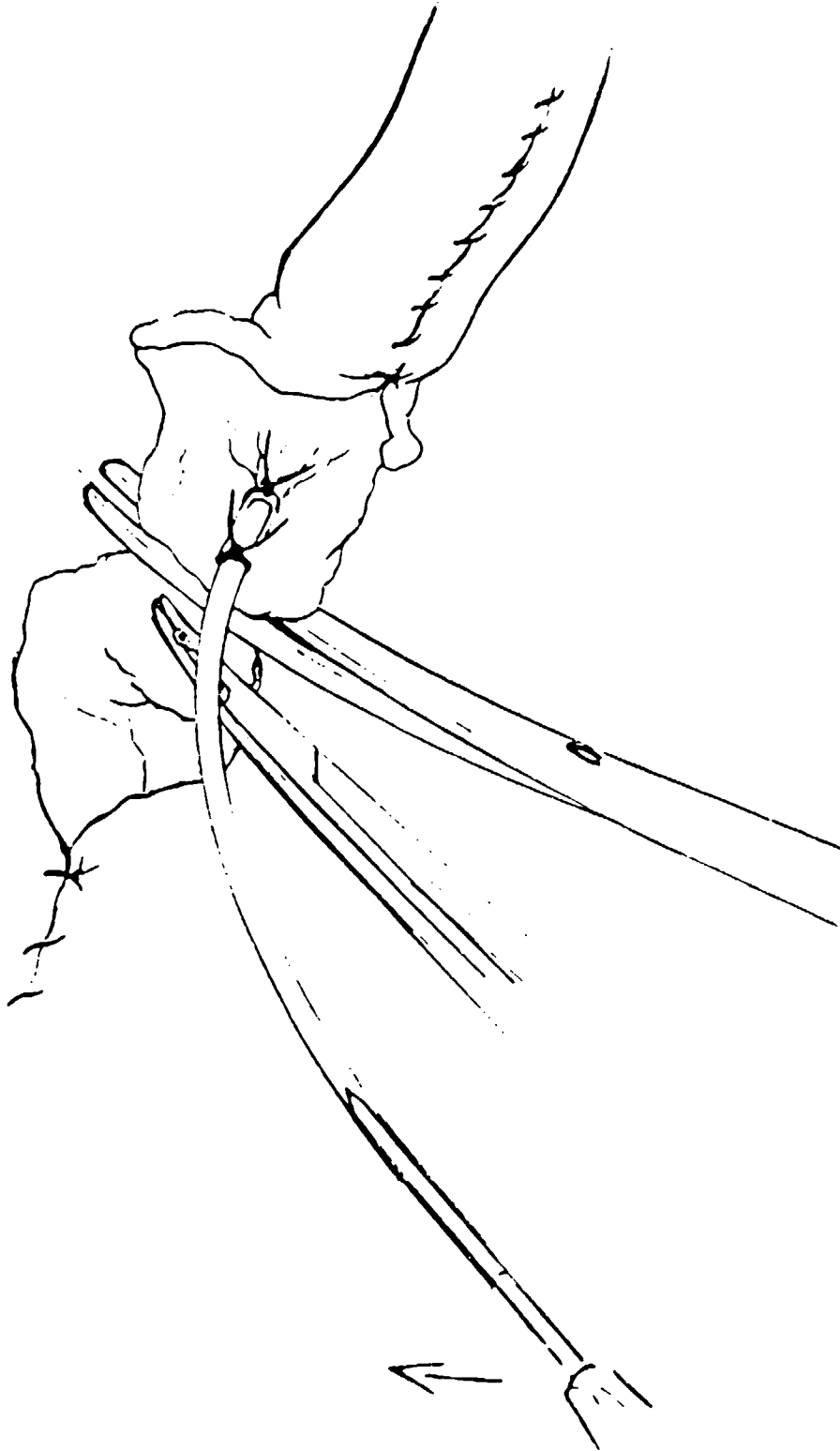FIGURE 9b

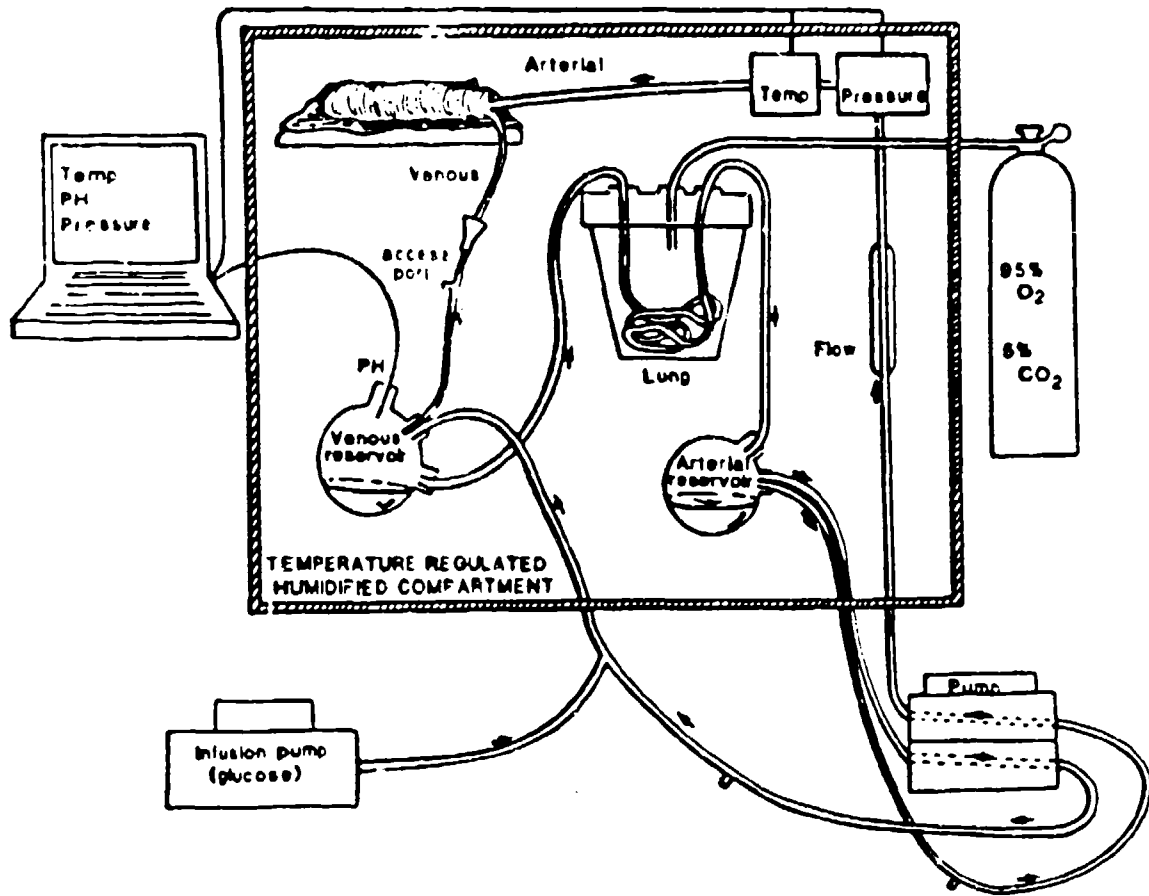FIGURE 10

FIGURE ELEVEN

FIGURE TWELVE

Table : Measurements of stage 1 tubed skin flaps for determination of skin surface area changes.

Parameter	In situ dimensions	Day 2 tubed skin flaps (n=5)		Day 6 tubed skin flaps (n=6)	
		Postoperative	Day 2 harvest	Postoperative	Day 6 harvest
Length*	7.5	7.89 ± 0.11	7.86 ± 0.11	7.15 ± 0.35	7.50 ± 0.23
Diameter*					
Base:	1.27§	1.46 ± 0.03	1.68 ± 0.03	1.32 ± 0.03	1.61 ± 0.09
Tip:	1.27§	1.41 ± 0.03	1.78 ± 0.04	1.42 ± 0.10	1.70 ± 0.09
Calculated area†	30.0	35.61 ± 0.79	42.85 ± 0.92	30.83 ± 2.24	39.06 ± 2.17
Percentage of original area‡	100	118.71 ± 2.66‖	142.85 ± 3.07‖	102.76 ± 7.48	130.19 ± 7.24‖

*Dimensions in cm ($\bar{x} \pm SE$).

†Based on formula: $\dfrac{(Diameter_{base} + Diameter_{tip})}{2} \pi \times length$ = calculated area in cm^2.

‡Percentage of original in situ dimensions.

§Based on formula: diameter = circumference (4.0 cm)/π

‖Significantly different from original, in situ dimensions (p<0.0001).

"Significantly different from original, in situ dimensions (p<0.01)

DISTRIBUTION LIST

1 copy   Commander
US Army Medical Research and Development Command
ATTN: SGRD-RMI-S
Fort Detrick, Frederick, Maryland 21701-5012

5 copies   Commander
US Army Medical Research and Development Command
ATTN: SGRD-PLE
Fort Detrick, Frederick, Maryland 21701-5012

1 original Defense Technical Information Center (DTIC)
1 copy   ATTN: DTIC-DDAC
Cameron Station
Alexandria, VA 22304-6145

1 copy   Dean
School of Medicine
Uniformed Services University of the
  Health Sciences
4301 Jones Bridge Road
Bethesda, MD 20814-4799

1 copy   Commandant
Academy of Health Sciences, US Army
ATTN: AHS-CDM
Fort Sam Houston, TX 78234-6100